Characterizing the Endoribonuclease Activity of APE1

Wan Cheol Kim

BSc., Simon Fraser University, 2007

Thesis Submitted in Partial Fulfillment of

The Requirements for the Degree of

Master of Science

In

Mathematical, Computer, and Physical Sciences

(Chemistry)

The University of Northern British Columbia

June 2009

Your file Votre référence
ISBN: 978-0-494-60814-2
Our file Notre référence
ISBN: 978-0-494-60814-2

Abstract

Recent evidence shows that mRNA degradation is a major control point in the regulation of gene expression. APE1, apurinic/apyrimidinic DNA endonuclease 1, has recently been discovered to possess an endoribonuclease activity against c-*myc* messenger RNA (mRNA) *in vitro*. We showed that APE1 shares catalytic residues to cleave both RNA and AP-DNA. Our results also suggested that the roles of active site residues in each reaction are not entirely identical. A consensus RNA secondary structures and sequences that are preferentially cleaved by APE1 were determined. Our results revealed that APE1 has a preference for cleaving the single stranded regions or weakly base paired regions of the RNA. Also, preferred sequences of cleavage were determined to be UA, UG, and CA. When APE1 was knocked down in HeLa cells, an increased level of *c-myc* mRNA and half-life was detected. This demonstrated that APE1 is involved in the regulation of *c-myc* mRNA turnover.

TABLE OF CONTENTS

CHAPTER 2 – Identifying the critical amino acid residues for endoribonuclease activity of APE1 and characterizing its biochemical properties

CHAPTER 3 – Establishing the RNA structure and sequence cleaved by APE1

CHAPTER 4 – Assessing the endoribonuclease activity of APE1 in biological systems

CHAPTER 5 – General discussion

List of Tables

List of Figures

Acknowledgements

I would like to thank my MSc. Theis supervisor, Dr. Chow H. Lee for his absolute support and guidance in completing this thesis. Also, I would like to thank the members of my MSc. supervisory committee, Drs. Andrea Gorrell and Dezene Huber, for their helpful suggestions and insights in carrying out this research. I would like to extend my thanks to the members of the Lee lab, Sang-Eun (Eunice) Kim, Chris Uy, Navkarndeep Bal, Dustin King, Dana Thomsen, Conan Ma, Mavis Ye, and Maggie Li for their friendship, encouragement, and technical support. Finally, I would like to say special thanks to my parents and friends in Prince George who have supported me during my time here at UNBC.

Candidate's Publications Relevant to this Thesis

Articles

Kim, W-C., Li, W-M., Wilson Jr III, D. M., Lee, C. H. (2009) Endoribonuclease activity of apurinic/apyrimidinic endonuclease 1 (APE1) variants identified in human population. (Manuscript in preparation)

Kim, W-C., Kim, S-E., Li, W-M., Wilson Jr III, D. M., Lee, C. H. (2009) Endoribonuclease active site of human apurinic/apyrimidinic endonuclease 1 (APE1). To be submitted to J. Biol. Chem. (Manuscript in preparation)

Kim, W-C., King, D., Lee, C. H. (2009) RNA-Cleaving Properties of Human Apurinic/Apyrimidinic Endonuclease 1 (APE1). Submitted to RNA (ID: RNA/2009/017327)

Kim, W-C., and Lee, C. H. (2009) The role of mammalian ribonucleases in cancer. Biochim. Biophys. Acta. - Reviews on Cancer doi:10.1016/j.bbcan.2009.05.002 *In press*

Barnes, T., **Kim, W-C.**, Mantha, A., Kim, S-E., Izumi, T., Sankar, M., Lee, C. H. (2009) Identification of apurinic/apyrimidinic endonuclease (APE1) as the endoribonuclease that cleaves c-myc mRNA. Nucleic Acids Res. doi: 10.1093/nar/gkp275 *In press*

Abstracts

Kim, W-C., and Lee, C. H. Understanding endoribonuclease activity of APE1. (2009). Cell & Molecular Biology Interest Group Seminar, Prince George, BC, Jan. 23, Speaker

Kim, W-C., and Lee, C. H. Structure and ribonuclease function of apurinic/apyrimidinic DNA endonuclease 1 (APE1). (2008). RiboClub 2008, Mont Orford, QC, Sep.22, Poster

Kim, W-C., and Lee, C. H. Biochemical characterization of apurinic/apyrimidinic DNA endonuclease 1 (APE1) *in vitro*. (2008). RiboWest 2008, Lethbridge, AB, Jun. 15, Speaker

Patents

U.S. Patent Application No. 83152-9, Title: APE1 AND USES THEREOF, Inventor: LEE, Chow ; BARNES, Tavish; and **KIM, Wan-Cheol**: Filed November 29, 2008.

CHAPTER 1

Introduction

The processes conferring mRNA stability, translational inhibition, and transcript degradation are all intricately related to one another and can be influenced by *cis*-acting elements such as the poly (A) tail and AU-rich elements (AREs) and *trans*-acting factors such as non-coding RNAs (ncRNAs), RNA-binding proteins (RBPs), and ribonucleases (RNases). Alterations of these factors are reported to be implicated in cellular abnormalities and such link has highlighted the significance of studying these factors. Since RNases play a significant role in mRNA metabolism and gene expression, further studies are required to identify and characterize unknown RNases in mammalian cells. Recently, apurinic/apyrimidinic endonuclease 1 (APE1) was identified to possess an endoribonuclease (endoRNase) activity against *c-myc* mRNA and this have led to the formulation of the three major research questions.

1.1 Mechanism of messenger RNA (mRNA) degradation

In eukaryotes, literature emphasizes that mRNA stability and turn-over is an integral control point in the regulation of gene expression (Parker and Song 2004; Garneau *et al.* 2007). The stability of various mRNAs within a cell can differ and this results in a magnitude of difference in mRNA abundance (Ross 1995). Moreover, the stability of individual mRNAs can be controlled in response to a variety of stimuli, allowing for rapid changes in gene expression to take place, and this has been viewed to be a critical component in development and pathogenesis (Wilusz and Wilusz 2004; Audic and Hartley 2004; Steinman 2007). Therefore, previous studies have focused on discovering major mRNA decay pathways and

their players: cis-regulatory elements, protein factors, and enzymes. However, in the last several years, significant efforts have been put to identifying and studying the enzyme involved in mRNA degradation.

From studies in yeast and mammals, major pathways of exoribonucleolytic mRNA decay have been identified. mRNA deadenylases such as Poly A Ribonuclease (PARN) and CCR4b-NOT can initiate mRNA decay by removing the poly (A) tail from the 3' end of the mRNA (Figure 1). Also, mRNA degradation can begin by the removal of the 7'-methylguanosine cap (m^7G) at the 5' end of the mRNA mediated by a complex of decapping enzymes, Dcp1p and Dcp2p (Figure 1). Following these processes, vulnerable transcripts are subjected to further cleavage and clearance by a 5'-3' exoribonuclease (ExoRNase), Xrn1p, and a complex of 3'-5' exosome and other 3'-5' exoribonucleases (Garneau *et al.* 2007; Schaeffer *et al.* 2009). In addition, endoribonucleolytic cleavage can also initiate mRNA degradation pathways. Endoribonucleases (EndoRNases) can cleave in the middle of the mRNA sequence. This way, the decay and the clearance of the transcript can by-pass the requirements of deadenylation and decapping step, allowing for a higher efficiency.

Apart from regular mRNA decay, cellular mechanisms can destroy faulty transcripts and mRNAs undergoing aberrant translation. This mechanism is called an mRNA surveillance control, which includes three distinct categories of mRNA decay: non-stop decay, non-sense mediated decay, and no-go decay. The non-stop decay mechanism recognizes and degrades transcripts without stop codons.

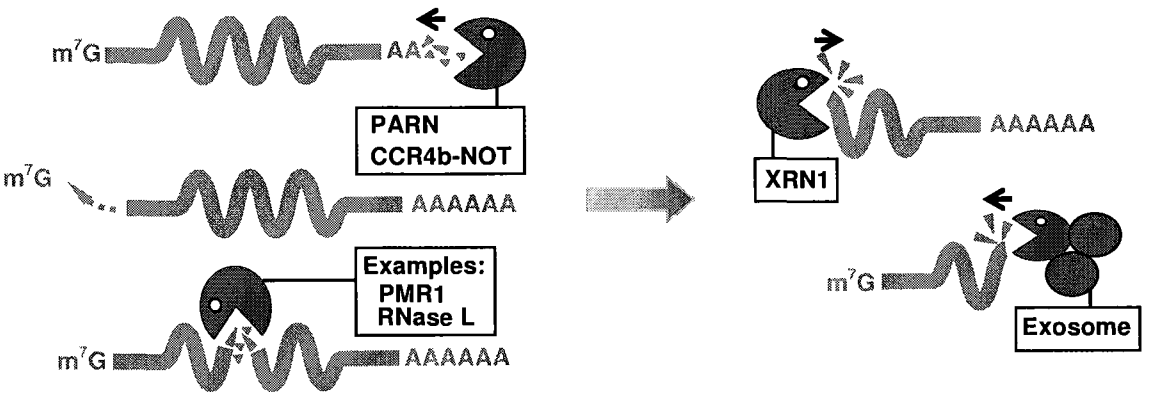

Figure 1: A schematic view of mRNA decay. mRNA decay can be initiated by any of the three processes shown on the left side of the arrow. Deadenylases such as Poly A Ribonuclease (PARN) and CCR4b-NOT remove the Poly A tail of the target mRNA, while decapping enzymes remove the 5'-m^7G mRNA cap. EndoRNases such as PMR1 and RNase L can cleave mRNA in the middle of the sequence. The combinations of these three processes make mRNA available for ExoRNases to further degrade and clear the transcript in 5'-3' (XRN1) or in 3'-5' direction (Exosome complex) as shown on the right side of the arrow.

This is mediated by different factors converging on a stalled ribosome at the 3' end of the mRNA and allows for a recruitment of exosome (Garneau *et al.* 2007). During non-sense mediated decay, stalling of the ribosome near the premature termination codon (PTC) allows for a stable binding of associated factors (UPF1 and SMG1) to the mRNA near the PTC. These factors interact and further recruit SMG5, SMG6, and SMG7 to promote mRNA decay via ExoRNases. In addition, EndoRNase activity of SMG6 can directly degrade the aberrant transcript (Eberle *et al.* 2009). Finally, in no go mRNA decay, stalling of ribosomes caused by a stem–loop RNA structure leads to the destruction of the transcript facilitated by Dom34 and Hbs1 proteins. Here, *in vitro* studies have identified dom34 as the responsible endoRNase (Lee *et al.* 2007). It was found that dom34 is highly conserved from fruitflies to mammals, and it plays an important role in the stem cell self-renewal in fruitflies and cell divisions in mice (Tollervey 2006).

1.2 Role of trans-acting factors in mRNA stability and turnover

Having described the pathways of mRNA degradation, it is now important to understand the roles of trans-acting factors that are notably involved in this process. Hence, the intricate balance between the actions of mRNA stabilizers which enhance the half-life of mRNAs and those of destabilizers which exert opposite effects will be further explained.

1.2.1 Non-coding RNA (miRNA)

Micro RNAs (miRNAs) are a class of non coding RNAs (ncRNAs) that have been revealed to exert an enormous effect on gene expression. This type of RNA (20-25 nucleotides in length) is generated from an endonucleolytic processing of longer transcripts as in the example of H19 RNA, a ncRNA, which can act as a miRNA precursor acting on mRNA degradation and repression (Cai and Cullen 2007). In general, long precursor RNAs, such as H19, can form multiple stem-loop structures and an EndoRNase, Drosha, part of RNase III group, can cleave such RNAs in the nucleus, releasing the pre-miRNA product into the cytoplasm. Once this RNA has reached cytosol, it is subsequently processed again by a yet another RNase III type endoRNase called DICER (Großhans and Filipowicz 2008). Such processed miRNAs are now deemed mature, and these mature miRNAs can bind to their target mRNAs by base pairing and recruit proteins of the Argonaute (Ago) family to form a miRNA ribonucleoprotein (miRNP) complex (Figure 2A). The miRNP complex can influence the stabilities of their target mRNAs mainly through inhibiting translation while promoting degradation (Zhang *et al.* 2007; To *et al.* 2008). The mRNA decay here can be mediated by a deadenylation-dependent or -independent exonucleolytic pathway or via other unidentified decay factors. Reviews on the interplay between miRNA and ExoRNase decay have been published (Jackson and Standart 2007; Garneau *et al.* 2007). In some cases, near

perfect base-pairing between the miRNA and the target mRNA allows Ago2, one of the four Ago family members, to endonucleolytically cleave the mRNA and send the fragments for further degradation as reviewed (Valencia-Sanchez *et al.* 2006).

1.2.2 RNA-binding proteins (RBPs)

RNA-binding proteins (RBPs) can also dramatically influence the longevity of mRNAs (Paschoud *et al.* 2006; Pulcrano *et al.* 2007). This mechanism not only allows the half-life of mRNA to vary, but is also capable of regulating the decay rates of individual mRNA in response to different stimuli, as is the case for transcripts encoding cytokines or proto-oncogenes bearing AU-rich elements in their 3' untranslated region (UTR) (Chen and Shyu 1995; Barreau *et al.* 2006). RBPs can bind to the 3' UTRs as well as to the coding region of mRNAs and shield them from mRNA degradation machineries (Figure 2B). One study has reported in breast cancer cell lines that HuR, an RBP, critically mediates the over-expression of oncogenic biomarker by enhancing its mRNA half-life (Guo and Hartley 2006). Similarly, CRD-BP, an RBP that shields mRNA from degradation, has been found to be elevated not only in the primary samples of melanoma (Elcheva *et al.* 2008), but also in a variety of tumor samples including colon (Dimitriadis *et al.* 2007), colorectal (Ross *et al.* 2001), mesenchymal (Ioannidis *et al.* 2001), breast (Ioannidis *et al.* 2003), Ewing's sarcoma, brain and non-small cell lung (NSCL) (Ioannidis *et al.* 2004). Further, it was reported that ~ 30% of human breast cancer cases exhibited amplification of the CRD-BP gene (Doyle *et al.* 2000), and its ectopic expression in transgenic mice induced the development of mammary tumors (Tessier *et al.* 2004). Other RBPs such as KSRP can stimulate the degradation of several cellular mRNAs that contain AU-rich elements (AREs) by recruiting endoribonucleases and deadenylation factors to regulate their expression (Gherzi *et al.* 2004;

Chou *et al.* 2006; Mazan-Mamczarz *et al.* 2007). The interactions between mRNAs and RBPs and their subsequent effects on cells seem complex and vary between studied cell lines. Recent report shows overexpression of HuR is directly responsible for the increase of kinase mRNA in fibroblasts (Sobue *et al.* 2008) while another study reports HuR can stabilize tumor suppressor mRNA in prostate cancer cell lines and in anti-cancer therapeutics (Quann *et al.* 2007; Bandyopadhyay *et al.* 2008).

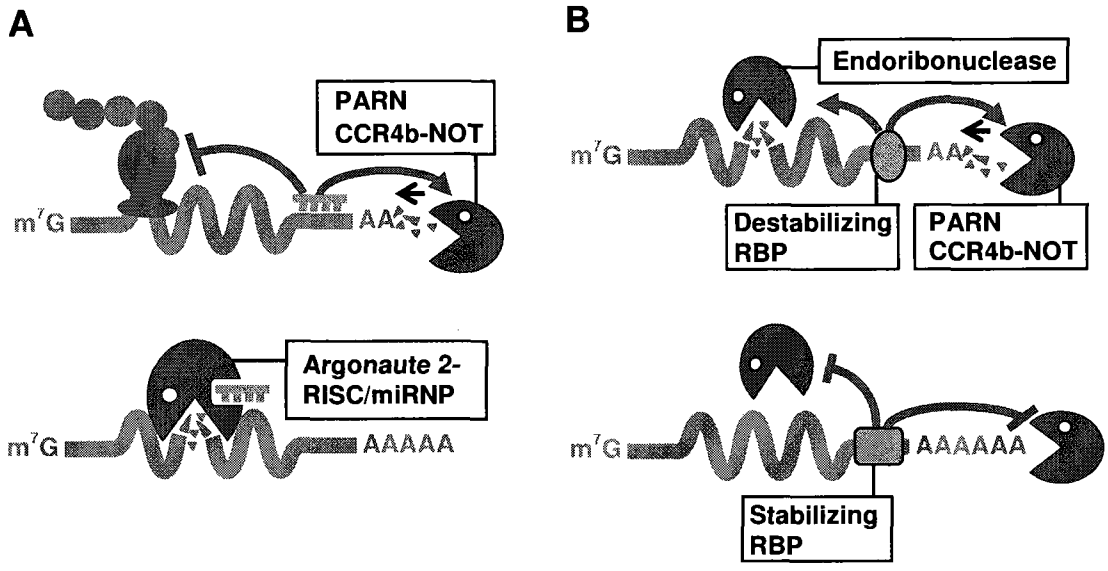

Figure 2: A schematic representation on the modes of action for trans-acting factors. (**A**) Non-coding RNAs can regulate mRNA translation and degradation. Top: miRNAs, a subclass of non-coding RNA, can inhibit the translational process while recruiting the RNA decaying machineries such as deadenylase and decapping enzymes. Bottom: Argonaute 2 can be induced to cleave mRNAs with externally introduced short interfering RNAs (siRNAs). However, a near to perfect complementary hybridization of miRNAs to mRNAs can also induce Argonaute 2, complexed with other gene silencing machineries, to cleave the target mRNA. (**B**) RNA binding protein (RBP) controls the stability of mRNAs. Top: Destabilizing RBP can recruit deadenylase machineries or has implications to recruit endoribonucleases to accelerate the decay of target mRNA. Bottom: Stabilizing RBP can attenuate mRNA decay by binding either to the coding regions or the 3' untranslated regions of the target mRNA.

Nonetheless, these demonstrate how important these molecules can come into play in controlling gene expression and tip the balance between decay and survival of diverse range

of mRNAs. Articles that provide a complete review on the role of RBPs and how they can influence gene expression are available (Audic and Hartley 2004; Garneau *et al.* 2007).

1.2.3 Ribonucleases (RNases)

An efficient interplay between various ribonucleases (RNases) has a major impact on mammalian mRNA turnover (Wilusz and Wilusz 2004). In mammalian cells, mRNAs are degraded upon shortening of their poly A tail (deadenylation) or removal of their 5'-m^7G cap (decapping). Exoribonucleases can clear these 'exposed' mRNAs either from its 5' or 3' end and several of these enzymes are actually involved in the deadenylation step. On the other hand, endoribonucleases can efficiently by-pass these requirements (decapping and deadenylation) and internally cleave mRNAs to generate products that are eventually cleared by exoribonucleases. In the absence of regulatory mechanism, these RNases can have profound impact on gene expression since a single cleavage on a transcript can result in its inactivation. Cells have employed mechanisms to prevent potential aberrant degradation of mRNAs by these endoribonucleases. Some of these (RNase L, IRE1, and PMR1) are tightly controlled through cellular signaling cascades (Garneau *et al.* 2007). The role of ribonucleases (RNases) will be discussed more in depth in the following section.

1.3 Ribonucleases (RNases) associated with cancer

It is noteworthy that some of these aforementioned RNases have been found to influence or shown potential to affect the turnovers of oncogenic and tumor-suppressive mRNAs in relation to cancer (Krüger *et al.* 2005; Oikawa *et al.*2007). Deregulation of RNases involved in RNAi machinery and miRNA processing also have significant impact on cell proliferation and tumorigenesis. Some RNases can be turned on by cellular responses

that are often observed in cancers such as in misfolded protein response and aberrant tyrosine kinase signaling.

Suppression of RNases can contribute to the reduction in mRNA decay. mRNA coding for P-glycoprotein (Pgp) was found to have a prolonged half-life in subcutaneously grown liver tumors compared to normal tissues (Lee *et al.* 1998). Pgp is a transport protein found in plasma membranes that is well associated with multi-drug resistance in many cancer cell lines and its expression increases during carcinogenesis in rats. In normal liver cells, Pgp mRNA is thought to be degraded by endonucleases and/or exonucleases because its mRNA decay intermediates were detected in normal liver cells (Lee *et al.* 2005). But, significant decrease in RNase activity in hepatomas (Roth 1963; Sidransky *et al.* 1978) is considered to be the reason for the prolonged Pgp mRNA half-life (Lee *et al.* 1998) and little or absence of Pgp mRNA decay intermediates in liver tumors (Lee *et al.* 2005). On the contrary, there are examples where elevation of RNases can promote tumorigenesis. Angiogenin, an RNase A family enzyme, can process 28S and 18S rRNAs (Adams and Subramanian 1999) and its RNase activity is essential for angiogenesis (Crabtree *et al.* 2007). This activity has been investigated as the source for inducing angiogenesis and small inhibitors have been tested to inhibit its RNase activity as an anti-tumor therapeutic (Kao *et al.* 2002). Studies have found Angiogenin to be highly over-expressed in numerous tumor samples and its expression correlated with cancer progression and poor prognosis. Its role in cancer progression is supported through induction of cell proliferation in melanoma cell lines while having no effects on normal cells (Crabtree *et al.* 2007). Finally, in pancreatic cancer cell lines, increased levels of RNase 1 in patient serums have been reported and the detection of its elevation is being explored as a distinguishable tumor marker (Fernandez-Salas *et al.* 2000).

As well, different glycosylation states for this RNase have been reported between normal and tumor tissues though it has not been tested whether different states of glycosylation results in difference in RNase activity and mRNA levels in cells (Peracaula *et al.* 2003).

1.3.1 RNases from conventional mRNA decay pathway: CCR4b, PARN, XRN1

The conventional pathway for mRNA decay plays a critical role in gene expression. Apart from the actions of endoribonucleases, much of the mRNA decay in mammalian cells begins with deadenylation. There are diverse sets of enzymes that carry out this important process (Zheng *et al.* 2008; Goldstrohm and Wickens 2008) and it is reported that these enzymes such as, PAN2-PAN3, CCR4-CAF1, and Poly A Ribonuclease (PARN) initiate mRNA degradation and act on a critical step of determining mRNA turnover rates and gene expression levels (Parker and Song 2004; Schwede *et al.* 2008). In mammalian cells, these complexes carry out exonucleolytic degradation of poly (A) tails on various mRNAs and making way for 3'-5' exosome complexes to clear off the transcript (Fig. 1C). They can act ubiquitously on any mRNAs that have poly (A) tails and do not seem to have peculiar specificity. Genetic and RNAi experiments have demonstrated their broad roles in biological functions such as fertility and cell growth (Goldstrohm and Wickens 2008). Subsequently, relatively few reports suggest their implications in cancer.

i) CCR4b

CCR4b, part of CCR4-CAF1 complex, induces growth in fibroblast cell lines by its activity and is speculated to be a proto-oncogene (Morita *et al.* 2007). In normal conditions, this enzyme was reported to regulate the level of p27Kip1 mRNA, a tumor suppressor that inhibits cyclin dependent kinases, and promoted cell growth. Moreover, when the cells were

depleted of it, p27Kip1 levels were increased and there was growth impairment. CCR4b can also be suppressed *in vitro* by a recognized anti-proliferative protein, Tob, supporting previous findings that its activity promotes cell growth (Miyasaka *et al.* 2008). Thus far, there are no reports showing the changes of CCR4b levels from various types of tumors. Similarly, no association study has been done in primary tumors or its derived cell lines to assess the levels of CCR4b and its effect on tumor suppressive mRNA turnover.

ii) PARN

RNases have been shown to control the level of mRNAs by interacting with RBPs. PARN is an example. Its deadenylase activity coupled with destabilizing actions of RBPs can potentially act as a tumor suppressor, decaying mRNAs coding for growth factors such as IL-8 and VEGF. This was seen from a report investigating the role of defective RBP called TTP that could not recruit PARN in malignant glioma cells (Lai *et al.* 2003; Suswam *et al.* 2008). Also, PARN and exosome complex are shown to be recruited by KSRP and/or DHAU and account for the destabilization of various mRNAs including c-jun and uPA, of which their elevation are implicated in cancers (Gherzi *et al.* 2004; Tran *et al.* 2004). Another study looked at the interaction between PARN and CUG-BP in which the RBP recruits the enzyme to destabilize c-fos and TNF-alpha mRNAs (Moraes *et al.* 2006).

iii) XRN1

Besides deadenylation, 5'-3' exonucleases can also initiate mRNA decay once their target transcript is decapped. XRN1 is an example enzyme that is implicated in cancer as a dysregulated TSG. In primary samples of osteogenic sarcoma (OGS) and its derived cell lines, there was a reduction and/or depletion of XRN1 mRNA (Zhang *et al.* 2002). Also, in one of these cell lines, there was a homozygous loss of function mutation for XRN1

suggesting its role as a TSG. From these, we can conclude that such RNases in conventional mRNA decay pathway have the potential to influence the expression of genes that are implicated in cancers.

1.3.2 RNases from specific contexts: RNase L, IRE1, and PMR1

This section discusses RNases requiring specific signals to become activated. RNase L and IRE1 are activated under signals from crisis situations and PMR1 is activated by a proto-oncogene signal (Garneau *et al.* 2007; Peng and Schoenberg 2007). RNase L functions in antiviral defense, but also in tumor suppression as its mutations are revealed to be implicated in different types of cancer (Li *et al.* 2007; Bisbal and Silverman 2007). Growing interests are drawn toward IRE1 that shows two opposite effects implicated in tumorigenesis and apoptosis, apart from its role in dealing with ER stress. Finally, evidence indicates an emerging link between PMR1 and cancer which remains dormant in normal conditions, but becomes activated to participate in mRNA decay.

i) RNase L

Human RNase L is an endoribonuclease expressed in a number of mammalian cell types. It has been shown in cell and cell-free systems to cleave both viral mRNA, rRNA, and several cellular mRNAs in the single stranded regions of UU and UA dinucleotides (Li *et al.* 2007; Daugherty *et al.* 2007). RNase L has been shown to control the stability of mitochondrial DNA-transcribed mRNAs in human and mice cells (Chandrasekaran *et al.* 2004; Le Roy *et al.* 2001) and destabilize mRNAs of genes induced by interferon response to viral infections (Bisbal *et al.* 2000). It was also reported to control the stability of MyoD mRNA and the differentiation of muscle cells (Li *et al.* 2000). Their main role, however, has been reported to be in innate immunity where its RNase activity can amplify an antiviral

response (Malathi *et al.* 2007; Bisbal and Silverman 2007; Liang *et al.* 2006). Recently, it has been shown to regulate interferon-induced apoptosis by controlling the stability of mitochondrial mRNAs (Le Roy *et al.* 2007). The activity and expression of RNase L are under tight regulation (Li *et al.* 2007; Bisbal and Silverman 2007). In normal conditions, it resides as a monomeric latent form and its activity is repressed by its inhibitor, RLI (Li *et al.* 2007). However, upon binding to 2',5'-linked oligoadenylates (2-5A) produced by 2-5A synthetase enzymes, it can dimerize and act as an activated RNase inside the cytoplasm. Analysis of its promoter sequence has found several sites for its tissue-specific and general expression accounting for its wide spread presence among mammalian cells (Zhou *et al.* 2005). Its expression is reported to be regulated at the mRNA level by ubiquitous RBPs, including HuR (Li *et al.* 2007).

Initially, RNase L was mapped to a region linked to susceptibility in hereditary prostate cancer (HPC) (Bisbal and Silverman 2007) and this is also consistent with the report that the human variants of RNase L are associated with aggressive metastasis (Noonan-Wheeler *et al.* 2006). There are significant differences in RNase activities of these variants and their effects have been observed in human cancers. A truncating variant, E265X, lacks 2–5A binding domain and this renders it completely inactive (Sun *et al.* 2007). Subsequently, higher frequency of heterozygosity in E265X mutation is found in hereditary prostate cancer (HPC) than in the controls (Rokman *et al.* 2002). R462Q shows a 3-fold reduction in its activity (Sun *et al.* 2007) and two studies have suggested this to be associated with higher risk of prostate cancer and its early onset (Rennert *et al.* 2005; Shook *et al.* 2007). There was also a correlation between risk of advanced prostate cancer and increased uptake of trans-fatty acid in carriers (R/Q) and in homozygous groups (Q/Q), showing that this susceptibility

gene can also have synergetic effect (Liu *et al.* 2007). D541E exhibits no loss in its RNase activity but a homozygous population (E/E) was found to have a significantly higher risk for developing prostate cancer than the D/D or D/E groups (Shook *et al.* 2007). The exact cause of this association still remains to be found and further reviews on population variants of RNase L to prostate cancer risk and progression are available (Bisbal and Silverman 2007; Liang *et al.* 2006; Sun *et al.* 2007). In addition, these variants have linkages to other types of cancers. Notably, the R462Q variant has been associated with colorectal (Krüger *et al.* 2005), and pancreatic cancers (Bartsch *et al.* 2005). Especially in the latter study, R462Q was found to be associated with increased aggressiveness and metastases of pancreatic cancer, and its homozygosity (Q/Q) was found to be more common in groups with cancers and possessed a higher risk.

The tumor suppressive function of RNase L has been well characterized especially under interferon signaling. RNase L is suggested to degrade mitochondrial mRNA which can lead to cytochrome-c release and caspase-3 activation during apoptosis induced by interferon-α or an anti-cancer agent (Le Roy *et al.* 2007; Naito *et al.* 2006). RNase L can also act by up-regulating tumor suppressor genes. Here, it's reported that RNase activity is required, but may not be sufficient to up-regulate the level of MIC-1/NAG-1. How RNase L activity raises the level of specific RNAs is still unknown, but there are speculations that it can destroy inhibitory miRNAs or rRNAs which results in the activation of transcriptional machineries (Malathi *et al.* 2005). RNase L was also found to act as a down stream effector of a tumor suppressor, BRCA1 activated upon interferon-γ signaling, to facilitate apoptosis in cancer cells (Mullan *et al.* 2005). Similarly, in prostate cells, one pathway that can antagonize interferon signaling is the dihydrotestosterone (DHT) pathway which promotes

cell survival and proliferation. It was shown in cancer cell lines that mutated RNase L can incur attenuation of interferon signaling and allow DHT pathway to take over (Bettoun *et al.* 2005). Reduction of RNase L activity may lead to diminished cleavage of DHT induced mRNAs and allow this pathway to promote cancer development. Accordingly, additive effect in RNase L activity results in inhibition of tumorigenesis (Krüger *et al.* 2005), confirming its role in suppressing cancer development. Moreover, RNase L shows tumor suppressor function in a mouse model of fibrosarcoma (Liu *et al.* 2007). Over-expression of human RNase L in mouse fibrosarcoma cells significantly delays tumor formation. As well, tumors over-expressing RNase L have more polygonal cells and shows increased tumor necrosis. Interestingly, these tumors start to grow once the ectopic expression of RNase L stops. Thus, it is concluded that RNase L can act as tumor suppressor of which its proper expression and activity are critical in regulating cell growth and survival.

ii) IRE1

Inositol-requiring enzyme 1 (IRE1) is a transmembrane endoribonuclease found in endoplasmic reticulum (ER). It has a functional endoribonuclease/kinase domain on the cytoplasmic side and stress sensor domain on the luminal side. Upon exposure to ER stress, its dimerization and autophosphorylation results in the activation of its RNase activity (Lee *et al.* 2008). To date, identified substrates for IRE1 are mRNAs encoding X-box binding protein 1 (XBP1), CD59, as well as its own mRNA (Tirasophon *et al.* 2000; Koong *et al.* 2006; Oikawa *et al.* 2007). IRE1 cleavage of XBP1 results in the splicing of this transcript which encodes a potent transcription factor, XBP1s, that activates genes necessary for unfolded protein response (UPR). UPR is a homeostatic signaling pathway which adjusts ER protein folding capacity according to the cellular need and, in a variety of contexts, it has

been shown to either promote cell survival or apoptosis (Bernales *et al.* 2006). How this decision is made is still unknown. Other than IRE1-XBP1s signaling, two other UPR activation signals have been found. It is speculated that the overall transcriptional output from combinations of these three signals ultimately determines the fate of the cell. Nonetheless, IRE1 acts in upstream to activate the UPR, and is an important RNase that directs cancer progression as well as cell death.

Its major implication in tumorigenesis comes from its production of XBP1s, a potent transcription factor that activates genes that are necessary for UPR initiation. For example, oncogene, LMP1, from Epstein Barr Virus, can induce IRE1-XBP1s pathway to activate UPR and its own synthesis (Lee and Sugden 2008). As well, its RNase activity has been suggested to influence the turn over of a significant number of mRNA in mammalian cells, including whose translation products regulate angiogenic processes (Drogat *et al.* 2007). For example, decreased expression of CD59 has been implicated in lung caner and an ectopic over-expression of IRE1 indeed down regulates its mRNA target (Oikawa *et al.* 2007). Indeed, this is consistent with the finding that the maintenance of IRE1 activity can promote cell survival (Lin *et al.* 2007). However, mounting evidence has linked XBP1s in tumor growth and progression under hypoxia, which is present in all solid tumors that incur ER stress. IRE1-XBP1s signaling has been found to promote cancer survival and progression. Over-expression of XBP1s in ER-positive breast cancer cells leads to estrogen-independent growth and reduced sensitivity to growth inhibition by the antiestrogens independent of functional p53 (Gomez *et al.* 2007). Moreover, signaling through IRE1-XBP1s is elevated in breast tumors with enhanced survival (Davies *et al.* 2008) and enhances the progression of liver cancer (Shuda *et al.* 2003).

But, UPR activation via IRE1 activation is also shown to mediate tumor suppression in multiple observations. For example, tumor suppressive mediators BAX and BAK modulate the UPR by directly interacting with IRE1alpha in cells and mice (Hetz *et al.* 2006). More importantly, IRE1-UPR pathway has been found to be used by various agents to induce cancer cell death and inhibition (Davenport *et al.* 2007; Guichard *et al.* 2006; Little *et al.* 2007). These evidence support IRE1 tumor suppressive activity which is also consistent with a report that showed its suppression resulting in synovial cell overgrowth (Gao *et al.* 2008). Therefore, definitive role of IRE1-UPR signaling in tumor development still need further clarifications. Particularly, future works should be focused on discovering a mechanism or a cellular environment that directs IRE1 activity to tumor progression or inhibition. It was reviewed that UPR signals are relayed and integrated to re-establish homeostasis in the cell's protein folding capacity or—if this cannot be achieved—commit cells to apoptosis (Bernales *et al.* 2006). Recent study suggests the balance between spliced and un-spliced form of XBP1 plays an important role in restoration of homeostasis, and this underscores the importance of understanding the regulation of IRE1 activity in deciding the fate of cancer cells (Davies *et al.* 2008). Additionally, investigating the regulation of IRE1 expression in cancers and ER stress can assist in understanding the role of IRE1 in deciding the cell's fate.

iii) <u>Polysomal ribonuclease 1 (PMR1)</u>

PMR1 is an endoribonuclease originally isolated from Xenopus liver polysomes but its orthologue was later found to be also present in mammalian cells (Yang *et al.* 2004). Uniformly found across the cytoplasm on polysomes, PMR1 has a unique sequence and structure that differentiate itself from other groups of RNases. Also, PMR1 is activated only upon being targeted to polysomes, and can initiate mRNA decay during its translation. This

critical step in regulation is mediated by c-Src phosphorylation of PMR1 at the tyrosine residue at C terminus (Peng and Schoenberg 2007). It was also found that this c-Src phosphorylation can be activated through EGFR signals which are well associated with tumorigenesis. Like the authors speculated, more external stimuli may be involved in PMR1 activation. Recent report revealed another layer of regulation of PMR1 activity. It was found that Hsp90 can bind to and stabilize PMR1 from proteasome degradation, sustaining its mRNA decay capabilities and accumulation inside the cell (Peng *et al.* 2007).

These findings indicate the potential role of PMR1 in cancer development and progression. c-Src is a well-known proto-oncogene in humans that is over-expressed or overtly activated in many cancers (Irby and Yeatman 2000). Its kinase activity can activate diverse number of transcription factors as well as signaling cascade that lead to cell growth and proliferation. The mechanistic model from Peng *et al.* suggests that c-Src may in part use PMR1 mRNA decay path as a route to destroy transcripts for tumor suppressors. In this, Hsp90 can prolong the longevity of PMR1 to sustain the process of mRNA decay. Since Hsp90 serves as an essential mediator for cellular proliferation (Calderwood *et al.* 2006), the mechanism mentioned above can be one of its ways to facilitate the destruction of mRNAs coding for growth regulators. Further studies to identify mRNA substrates of PMR1 should provide support to this model and the role of PMR1 in cancer. Further, assessing the relationship between PMR1 and EFGR over-expression and its elevated activity will clarify the role of PMR1 as a downstream effector in carrying out an oncogenic pathway. In addition, assessing its expression and activity in tumor samples or cell lines will give further support for its role in tumorigenesis.

1.3.3 RNases from miRNA pathway: Drosha, DICER, Argonaute 2

Growing evidence suggest dysregulation in microRNA (miRNA) expression pattern is associated with cancers (Hagan and Croce 2007). Subsequently, three major RNases involved in miRNA maturation and implementation can have critical effects in controlling miRNA expression and gene expression. This section discusses how alteration of these RNases can potentially lead to tumorigenesis.

i) Drosha/DGCR8

Maturation of miRNA begins with pri-miRNA processing. This step is carried out by the endoribonucleolytic function of Drosha complexed with DiGeorge syndrome Critical Region gene 8 (DGCR8). Drosha is part of the RNase III family responsible for giving the cleavage activity against double stranded RNAs and evidence suggests its implication as a proto-oncogene. In one study, elevated expression of Drosha and its mRNAs were found in esophageal cancers (Sugito *et al.* 2006). Moreover, its suppression in cancer cell lines resulted in inhibition of their proliferation. Another study showed a correlation between the elevation of Drosha mRNAs and gains in genomic copy-numbers in addition to reporting its increased copy numbers in clinical samples and cell lines of cervical squamous cell carcinoma (Muralidhar *et al.* 2007). Recently, in cervical cancer samples, Drosha was one of the genes that were over-expressed, further supporting its role as an oncoprotein (Scotto *et al.* 2008).

A few studies outline how Drosha might contribute to tumorigenesis. Its enhanced activity against pri-miRNAs can result from different signaling molecules, but has been found to influence the levels of miRNAs implicated in cancers. One study found increased accessibility of Drosha to pri-miRNA-191 resulted in miR-191 over-expression in leukemic

cell lines (Nakamura *et al.* 2007). Similarly, growth factors such as TGF-β and those from the family of bone morphogenetic proteins (BMPs) have been found to induce their downstream transducers which interact with Drosha and enhance its accessibility and/or activity towards pri-miRNA-21. This resulted in the rapid elevation of miR-21 in vascular smooth muscle cells (VSMC) and down-regulation of a tumor suppressor PDCD4. (Davis *et al.* 2008). The finding is in line with numerous clinical reports of miR-21 over-expression in different cancers (Iorio *et al.* 2005; Roldo *et al.* 2006; Slavy *et al.* 2007; Dillhoff *et al.* 2008; Markou *et al.* 2008; Connolly *et al.* 2008). Future studies can identify such signaling molecules, post-translational modifications, and structural changes in pri-miRNAs that can affect Drosha accessibility and activity. Further, studies can investigate on what alterations of these regulations can lead to altered pri-miRNA processing and tumorigenesis.

ii) DICER

DICER processes pre-miRNAs in the cytosol and is part of the RNase III family. A few studies reported of its role in destabilization of mRNAs and gene expression (Jing *et al.* 2005; Takahashi *et al.* 2006). Moreover, mounting evidence reveal its role as critical regulator of miRNA maturation and its deregulation in tumorigenesis. Whether DICER acts as a proto-oncogene or a tumor suppressor is unknown, considering its ability to process nearly all pre-miRNAs. In general, its over-expression has been predominantly associated with tumorigenesis which points toward its role as a proto-oncogene. In contrast, there is also evidence in support of DICER's role as a tumor suppressor. Nevertheless, these results converge on the notion that aberrant DICER function contributes to tumorigenesis. Several studies have reported its over-expression in a number of cancers including those of the salivary gland (Chiosea *et al.* 2008), lung (Chiosea *et al.* 2007), prostate (Chiosea *et al.*

2006), and ovary (Flavin *et al.* 2008) as well as in Burkitt's lymphoma (Kaul *et al.* 2004). Some of these studies pointed out that DICER over-expression can lead to a global up-regulation of oncogenic miRNAs such as miR-21 and others (Chiosea *et al.* 2006; Volinia *et al.* 2006). Future studies can focus on identifying those miRNAs of which their maturations are affected by DICER over-expression and the reason for their specificity. It has been shown that DICER can promote angiogenesis in endothelial cells and its expression can be controlled by miRNA let-7 which is known as a tumor suppressive miRNA (Kuehbacher *et al.* 2007; Tokumaru *et al.* 2008). Thus, these studies support the proto-oncogenic role of DICER.

In contrast, DICER reduction and subsequent reduction in global miRNA maturation can enhance tumor development (Blenkiron *et al.* 2007; Kumar *et al.* 2007). Reduction in miRNA species has potential to dysregulate oncogenes. A few clinical studies are consistent with this finding. Reduction of DICER was found to be a predictive marker for poor prognosis in lung cancer patients (Karube *et al.* 2005). Another study showed down-regulation of DICER being a strong predictor of relapse among non-small-cell lung cancer patients (Rosell *et al.* 2006). Further studies should unravel more on the role of DICER and its involvement in miRNA processing and in gene expression. For instance, it is warranted to identify more miRNAs targets affected by aberrant DICER function and elucidate how they can contribute to tumorigenesis.

iii) Argonaute 2

Pre-miRNAs are processed by DICER to become mature miRNAs that become part of a miRNA ribonucleoprotein (miRNP) complex. Part of this complex is Argonaute 2 (Ago2) which can destroy mRNAs having complementary sequences to the template miRNA

(Blenkiron *et al.* 2007). If a nearly perfect complementary association can not be reached in mRNA:miRNA binding, translational inhibition takes place. Ago2 has been reported to interact with DICER (Song *et al.* 2004) and suggested to assist its pre-miRNA processing (O'Carroll *et al.* 2007). It was shown to localize to the mRNA decay centres, known as cytoplasmic bodies, to exert miRNA-mediated gene regulation (Sen and Blau 2005). Ago2 is unique in that it is the only RNase from human Argonaute family comprised of eight members, four of which are Ago1 through Ago4 that are closely related and co-expressed in human cell lines (Meister *et al.* 2004; Rivas *et al.* 2005).

Recent reports highlight the altered levels of Ago2 in the deregulation of miRNA activities in cancer (Kovalchuk *et al.* 2008). One study showed elevated Ago2 levels in the more aggressive type of breast tumors (Blenkiron *et al.* 2007). Also, transfecting MCF7 cell line with Ago2 resulted in increased cell proliferation as well as transformation of cells into a phenotype undergoing endothelial-to-mesenchymal transition (Adams *et al.* 2008). How an increase in Ago2 levels lead to tumorigenesis is still unknown. Possible explanations include that the over-expression of Ago2 may relieve the competition implemented between different miRNA species to regulate gene expression (Vickers *et al.* 2007) and permit oncogenic miRNAs to better exert their effects. But, what seems to be more important is the maintenance of balance of Ago2 levels since its reduction also results in impairment of DICER's miRNA processing capabilities (O'Carroll *et al.* 2007). Future studies should identify unknown facilitating factors that may promote the association of oncogenic miRNAs to Ago2 and identify regulatory mechanisms exerted on Ago2. Recently, one of the transducers of the MAPK pathway has been found to phosphorylate Ago2 at a Ser residue and this enhanced its migration to the mRNA decay sites (Zeng *et al.* 2008). Identifying more

of such pathways will underscore the role of Ago2 as one of the down stream effector of external signals and may provide reasons behind the correlation between its elevated levels and tumorigenesis.

1.3.4 RNases of the nucleus/cytoplasm: Angiogenin, G3BP, and FEN1

Efforts are continuing to identify unknown RNases which play key role in the regulation of gene expression. But, a few proteins with unexpected RNase activity that have been identified were found to be linked to tumorigenesis and cancer progression. This section will discuss these evidences. Angiogenin is essential in angiogenic processes whose altered activity is implicated in cancer development. As well, G3BP is suggested to be the putative endoribonuclease affecting the turnover of c-myc mRNA in mouse fibroblasts (Tourriere *et al.* 2001) and its deregulated expression patterns were reported in cancer. Finally, the two enzymes, APE1 and FEN1, originally found to act on DNA, are receiving much attention due to their ability to cleave RNA and altered expressions reported in cancer.

i) Angiogenin

Angiogenin is part of a pancreatic RNase A superfamily. It was originally isolated as a human tumor-derived angiogenesis factor that has its activity towards UA or CA dinucleotides. It can specifically hydrolyze cellular tRNA to inhibit protein synthesis and though its activity is weaker by several orders of magnitude compared to RNase A, it is essential in angiogenesis (Curran *et al.* 1993). Unfortunately, its natural mRNA target has not been identified and its role in mRNA turnover has not been studied. However, it is speculated that its substrates may reside in the nucleolus of vascular endothelial cell where Angiogenin normally localizes (Kao *et al.* 2002). Clinical studies associating Angiogenin and a variety of cancers have been reviewed previously (Tello-Montoliu *et al.* 2006). Since it was initially

isolated as an angiogenesis factor from tumors, it is not a surprise to learn of its alterations implicated in different cancers. Several studies concordantly report its higher expression level correlated with higher proliferation of cancers. A study of a large cohort of prostatectomy specimens found an increasing expression of Angiogenin in the progression from benign prostate to high-grade prostatic intraepithelial neoplasia and ultimately to prostatic adenocarcinoma (Katona *et al.* 2005). Also, higher Angiogenin mRNA was reported in gastric carcinoma specimens than in the surrounding non-tumorous tissues (Chen *et al.* 2006) and recently, serum sample analysis of stage IV malignant melanoma reported marked elevation of Angiogenin among a sub-group of patients with progressive disease (Vihinen *et al.* 2007). Here, higher levels were significantly associated with poor treatment response with chemo-immunotherapy and the treatment-related survival was shorter in patients with above-median levels of Angiogenin than in those with below-median levels. Further, over-expression of Angiogenin was reported to enhance the tumorigenicity and angiogenesis in prostate cancer cell line while its knock-down exerted an opposite effect, in agreement with its oncogenic role (Kawada *et al.* 2007).

In turn, its reduction in activity inhibits cancer proliferation. In melanoma cell line, basic fibroblast growth factor cannot induce proliferation in the absence of Angiogenin (Song *et al.* 2006). Knock down studies in HeLa cells showed notable inhibition of proliferation, and in prostate adenocarcinoma cells, its knock down caused inhibition of rRNA transcription, cell proliferation, and xenograft growth in mice (Tsuji *et al.* 2005; Yoshioka *et al.* 2006). Six out of seven known variants are linked to amyotrophic lateral sclerosis and had marked reduction in RNase activity while three lowest ones showed significant decrease in angiogenic and proliferative activities (Crabtree *et al.* 2007). These reports are consistent and

demonstrate the importance of its activity in inducing cancer proliferation. It is also in line with the previous evidence from inhibition studies, which alluded that RNase activity controls the process of angiogenesis (Wang *et al.* 2005, Fu *et al.* 2005). Thus far, however, the molecular basis of Angiogenin in inducing cell proliferation is unknown and would require further studies to clearly elucidate its molecular mechanism (Gao *et al.* 2007).

ii) RasGAP Src homology 3 binding protein (G3BP)

RasGAP Src homology 3 binding protein 1 (G3BP) is an endoribonuclease ubiquitously expressed in the cytoplasm and in the nucleus. G3BP cleaves the 3' untranslated region of *c-myc* mRNA with a preference to cleave in between the CA dinucleotides. Its influence on mRNA turnover has been suggested when a defective form of G3BP was found in RasGAP deficient mouse embryonic fibroblasts that also showed delayed c-myc mRNA decay (Tourrière *et al.* 2001). However, there has not been a direct proof of G3BP acting as an endoribonuclease on c-myc mRNA *in vivo*. The endoribonuclease activity is dependent on phosphorylation of its serine residues and, in dividing cells, G3BP migrates toward plasma membrane and can interact with RasGAP, but not in quiescent cells (Tourrière *et al.* 2001; Gallouzi *et al.* 1998). Its essentiality in development is demonstrated by embryonic lethality and growth retardation in mice after its inactivation (Zekri *et al.* 2005).

Correlation of G3BP over-expression with a variety of cancers including that of breast, head and neck, colon and thyroid have been reviewed (Irvine *et al.* 2004). Recently, expression of G3BP has been studied in human esophageal squamous carcinoma (ESC) (Zhang *et al.* 2007) and in 71% of the cases, there was a positive expression rate for G3BP. Also, its expression in the lymph node metastasis group was significantly higher than that in the non-lymph node metastasis group and this expression was associated with shorter

survival time. However, like Angiogenin, the molecular mechanism behind this association is unknown and an opposing observation has also been made. One study reported the reduction of G3BP was associated with the metastatic lung carcinoma more so than the non-metastatic cells (Lie *et al.* 2001). It is possible that G3BP are predominantly found throughout the cytoplasm, but during arsenite or high temperature stress, it can localize specifically in a large cytoplasmic structures that resemble stress granules (SGs) (Tourrière *et al.* 2003). It is known that SGs are cytoplasmic aggregates of stalled translational complexes that accumulate during stress. One study proposed that the mRNA released from disassembled polysomes is sorted and remodeled at SGs, from which selected transcripts are delivered to processing bodies (PBs) for degradation (Kedersha *et al.* 2005). Whether G3BP associate with subset of these transcripts in SGs and can destroy them prematurely is still unknown. Future studies can clarify this by understanding the regulation of its localization to SGs and identifying its target mRNA associated with SGs.

iii) Flap endonuclease 1 (FEN1)

Human flap endonuclease 1 (FEN1) was discovered to have an endoribonuclease activity against synthetic and native RNAs *in vitro* (Stevens 1998). Whether FEN1 is capable of endonucleolytically cleaving RNA in cells is currently unknown. Human FEN1 is normally found in the nucleus and shows preference to cleave 5' endogenous stem structure of RNAs *in vitro*. Multiple functions of FEN1 include RNA primer removal during DNA replication, dsDNA 5' to 3' exonuclease, gap endonuclease, and RNase H activity (Robins *et al.* 1994; Shen *et al.* 2005). Interestingly, the exonuclease activity of FEN1 seemed to have a role in apoptotic DNA fragmentation while the gap endonuclease activity showed potential for repairing stalled DNA replication fork. Similarly to APE1, FEN1 may also be able to

regulate the levels of RNAs apart from its well known function in removing RNA primers during DNA replication. In cancers, it displays two opposing roles. Its over-expression has been reported to correlate with the aggressiveness of tumors (Sato *et al.* 2003; Lam *et al.* 2006). Mainly, its ability to assist in DNA replication via removal of RNA primers may promote cell proliferation. However, whether its endoribonuclease activity against other cellular RNAs plays a role in this development still needs to be assessed.

Its reduction in DNA endonuclease activity has also been associated with cancers. Its activity is reduced by a member of the signal transduction pathway promoting cell growth *in vitro* (Henneke *et al.* 2003). Previous studies have shown its haploinsufficiency contributes to rapid progression of tumours (Kucherlapati *et al.* 2002). A recent report from mice model found FEN-1 deficiency contributes to modest but a significant increase in tumor incidence and multiplicity (Kucherlapati *et al.* 2007). The loss in RNA primer removal as well as repairing stalled DNA replication fork may account for this observation. But, in another perspective, its ability to cleave RNAs may also play a role in such observations. In order to fully appreciate the extent of its deficiency, future studies should be carried out to look for its RNA targets. Also, in certain situations, it is retained in the cytoplasm with an unknown role. FEN1 has a nuclear localization signal (NLS) located at its C terminus, which directs its localization during S phase of the cell cycle and in response to DNA damage (Qiu *et al.* 2001). Truncation or alanine substitutions on the KRK residues of the NLS prevent its migration from the cytoplasm, but have no effect on its nuclease activity. Further studies can assess the effects of its retention in the cytoplasm that may involve regulating the levels of mRNAs.

1.4 Apurinic/apyrimidinic endonuclease1 (APE1) as an endoribonuclease

c-Myc, a proto-oncogene, has been implicated in the development of virtually all types of human cancers (Levens 2003). Like other cellular mRNAs, c-myc mRNAs, can be initiated to decay via exoRNases as described in section 1.1. However, c-myc mRNA can also be degraded endonucleolytically. Endonucleolytic cleavage of c-myc mRNA was first shown using a polysome-based *in vitro* mRNA decay assay (Bernstein *et al.* 1992). It was believed that a putative endoRNase targeted the specific exposed region of an endogenous polysome-associated c-myc mRNA referred to as the c-myc coding region determinant or CRD. Recent evidence suggested that translational pausing in CRD could result in ribosome-deficient region that is susceptible to endonucleolytic cleavage (20). Other studies have confirmed that the coding region of c-myc mRNA, including the CRD, is involved in the regulation of c-myc mRNA stability in cells (Levens 2003). Moreover, endoRNase decay intermediates for c-*myc* mRNA have been detected in cells (Hanson and Schoenberg 2001; Ioannidis *et al.* 1996; Herrick and Ross 1994) and this provided further support for the significance of c-*myc* mRNA decay initiated via an endoRNase. Later, it was discovered that apurinic/apyrimidinic endonuclease 1 (APE1) was the endoribonuclease that can bind to CRD region of c-myc mRNA, and specifically cleave in between the single stranded region of UA, CA, and UG dinucleotides (Barnes *et al.* 2009).

1.4.1 Possible role of APE1 in cancer

Apurinic/apyrimidinic endonuclease 1 (APE1) is an enzyme that has been found in the nucleus, cytoplasm, and mitochondria (Evans *et al.* 2000; Tell *et al.* 2005; Chattopadhyay *et al.* 2006). Its elevated expression has been observed in some cancers. In multiple myeloma, positive rate of APE1 expression was found in 65.6% of the patients (Yang *et al.*

2007). Similarly, elevated expression of APE1 was associated in osteosarcoma resistance and poor prognosis of patients (Wang *et al.* 2004). Altered subcellular localization of APE1 or its variants have also been reported in a variety of cancers (Tell *et al.* 2005). The cytoplasmic expression of APE1 is significantly higher in hepatocellular carcinoma than the surrounding tissues (Di Maso *et al.* 2007). In normal liver, they found no APE1 in the cytoplasm. A 3-fold increase of cytoplasmic expression in aggressive HCC patients compared to those with well-differentiated HCC and cytoplasmic localization was correlated with shorter survival time compared to those with negative cytoplasmic reactivity. APE1 was considered as a nuclear protein containing a nuclear localization signal near its N-terminus (Jackson *et al.* 2005; Chattopadhyay *et al.* 2006). However, re-distribution of APE1 between the nucleus and the cytoplasm in cancerous cells has raised many questions about its role in the cytoplasm. It is tempting to speculate that the RNase activity of APE1 in the cytoplasm is correlated with aggressive cancer phenotype. Also, cleavages of cellular RNAs, such as microRNAs or tumor suppressor mRNAs, can certainly trigger tumorigenesis as envisioned in the case of RNase L (Malathi *et al.* 2005). To test the above hypotheses, further studies are clearly required to identify RNA targets of APE1.

On the opposite side, APE1 may exert its RNase activity to destroy oncogenic mRNAs and miRNAs. This may be consistent with the fact that oncogenic Bcl2 suppresses the expression of APE1 while enhancing that of c-Myc (Jin *et al.* 2006). The authors were unclear of the molecular mechanism behind this process, but one model that can be deduced from this is that APE1 can destroy *c-myc* mRNA and regulate its turnover. This is supported by recent evidence that down regulation of APE1 leads to c-Myc over-expression (Barnes *et al.* 2009). In addition, there are seven substitution variants of DNA endonuclease domain of

APE1 in human population (Hadi *et al.* 2000). Several of these, notably, L104R, E126D, R237A, and D283G show 40-90% reductions in apurinic/apyrimidinic DNA endonuclease (AP-DNase) activity. D148E with an allele frequency of 0.38, surprisingly retains its AP-DNase activity as well as substrate binding. In cancer, homozygous individuals (E/E) for D148E variant were more associated with colon cancer (Pardini *et al.* 2007). Similarly, it was found in patients that D148E polymorphism was significantly associated with lung cancer risk (De Ruyck *et al.* 2007). Therefore, these reports indicate its AP-DNase activity cannot be responsible for this observation and suggest that alteration in the activity of APE1 may be associated with these cancers.

The post-translational (PT) modification of APE1 has also been linked to cancers. One study observed an abundance of post-translationally modified form of APE1 in leiomyoma extracts, suggesting its association with uterine smooth muscle tumorigenesis (Orii *et al.* 2002). It is unclear from this study what modification was done on APE1 but the authors suggested of multiple processing steps involving phosphorylation and proteolytic cleavage. Higher level of the modified APE1 (a larger sized APE1 compared to the regular molecular weight) was also observed in cell lines derived from leiomyosarcomas (Orii *et al.* 2002). Further, relative abundance of the phosphorylated APE1 was found to correlate with proliferating cell nuclear antigen levels, suggesting a correlation with increased proliferation. Here, the authors did not assess the effects of phosphorylation on AP-DNase activity nor on any of its known functions. At this stage, possibility of alteration in ribonuclease activity through PT modification can only be speculated. Recent study showed that APE1 nitrosation of C93 and C310, a consequence of oxidative stress caused by nitric oxide, eliminates its nuclear export to the cytoplasm (Qu *et al.* 2007). Preventing the channeling of APE1 to

different parts of the cell and interaction with different RNA substrates will most likely affect mRNA turnover and gene expression. On a similar note, APE1 was found to have 3-fold increase in its AP-DNase activity when its first 33 amino acid sequence is removed by proteolysis and exported out of the nucleus to the mitochondria (Chattopadhyay *et al.* 2006).

1.4.2 Abasic DNA incision activity of APE1

Discovery of APE1 as an endoribonuclease was unexpected and encouraged us to further characterize this activity *in vitro*. Its function as an endoRNase in any of the cellular compartments is completely unknown. Previous studies describe APE1 to possess multiple activities in cell-free and cellular systems. These activities included the cleavage of apurinic/apyrimidinic DNA (abasic DNA) (Kane and Linn 1991) and abasic-RNA (Berquist *et al.* 2008; Vascotto *et al.* 2009), redox activation of transcription factors implicated in apoptosis and cell growth (AP-1, Egr-1, NF-kappaB, p53, c-Jun, and HIF) (Tell *et al.* 2009), as well as 3' phosphodiesterase (Chen *et al.* 1991), 3'-5' exonucleases (Wilson *et al.* 1995), 3' phosphatase, and RNase H activities (Barzilay *et al.* 1995). APE1 is also referred to as redox effector factor 1 (Ref-1) because it was independently discovered to possess a redox activity.

In regards to its AP-DNA incision activity, it specifically recognizes the abasic site and facilitates the phosphodiester bond cleavage facilitated by divalent metal ions and water molecules. It cleaves the phosphodiester bond immediately 5' to the abasic site, generating products with 3' hydroxyls and 5'-deoxyribose phosphate termini (Demple and Harrison 1994). These products are then processed by enzymes such as DNA polymerases and ligases that fill the nucleotide gap and seal the nick in the DNA to complete the AP site repair (Evans *et al.* 2000). In mammalian cells, APE1 is the major protein involved in initiating the removal of abasic sites in DNA (Wilson and Barsky 2001).

Accordingly, efforts were put into identifying its active site and essential residues critical in abasic DNA incision. A few biochemical kinetic studies have found APE1 against abasic sites in ssDNA yielded an apparent K_m of 428 nM and a k_{cat} of 4.2 s^{-1}, while against abasic sites in dsDNA yielded an apparent K_m of 24 -33 nM and a k_{cat} of 3-4.1 s^{-1} (Sokhansanj *et al.* 2002; Marenstein *et al.* 2004). Several crystal structures in different conditions have been reported (Gorman *et al.* 1997; Mol *et al.* 2000; Beernink *et al.* 2001). Later, it was identified that ten amino acids constitute the active site of APE1 in carrying out abasic DNA incision, and was confirmed of their evolutionary conservation across different species (Tell *et al.* 2005).

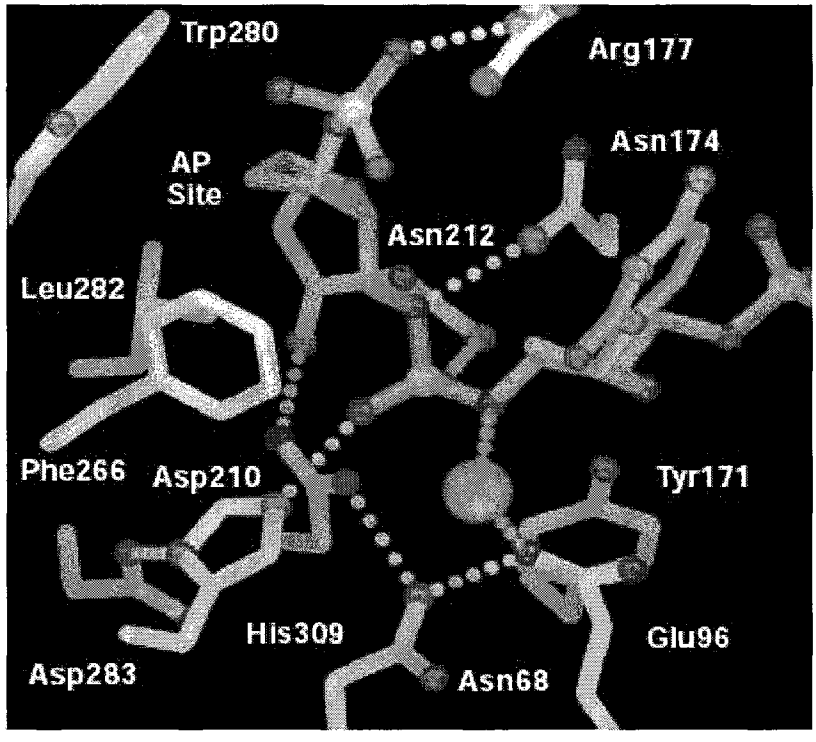

Figure 3: Abasic DNA cleaving active site model of APE1 based on X-ray crystallography (Mol *et al.* 2000). The XFIT generated model of APE1 active site. The orange lines represent phosphate backbone of abasic DNA strand while resides of the active site of APE1 is indicated by their numbers. The green sphere represents Mn^{2+} and dotted lines represent hydrogen bonds.

Amino acid residues Asp70, Asp90, Glu96, Tyr171, Asp210, Asn212, Asp219, Asp283, Asp308, and His309 have been noted as the critical amino acids in the active site (Figure 3). Substitution of any of these residues results in varying degrees of reduction in AP-DNA nuclease activity, and these findings are summarized in Table 1.

Table 1: Summary of abasic DNA incision activities of active site mutants (or structural mutants).

Mutants	Fold reduction in abasic DNA incision activity	Reference
N68A	600	Nguyen *et al.* 2000
D70A	Reduction	Nguyen *et al.* 2000
E96A	600 – 100000	Erzberger *et al.* 1999; Chou and Cheng 2003
Y171F	5000	Erzberger *et al.*1999
D210N	25000	Erzberger *et al.*1999
N212A	Not detectable	Rothwell and Hickson 1996
N212Q	300	Rothwell and Hickson 1996
F266A	6	Erzberger *et al.* 1998
D283N	10	Hadi *et al.* 2000
D308A	5-25	Erzberger *et al.* 1999; Barzilay *et al.* 1995
H309N	100000	Chou and Cheng 2003

It is noteworthy that substituting Asn212, for example, a polar residue to glutamine, another polar residue, resulted in a 300 fold reduction whereas mutating it to alanine, a hydrophobic residue, resulted in a complete abrogation of its nuclease activity (Rothwell and Hickson 1996). It is predicted that the amino group attached to the side chain of Asn212 can interact with oxygen on the phosphate backbone on the AP-DNA, helping to orient the scissile bond for incision to take place. Thus, it is thought that certain charge-charge interactions between the residues and the substrates are required to give abasic DNA incision activity.

Previous studies on abasic DNA catalysis and crystal structure of APE1:abasic DNA complex suggest that APE1 binds to nucleic acid structure that can adopt a uniquely kinked conformation. It seems that APE1 probes for substrates such as abasic DNA or single

nucleotide-gapped DNA that lack base-to-base stacking interaction and those that have increased backbone flexibility (Wilson and Barsky 2001). It is thought that during the binding of APE1 to abasic-DNA, the DNA undergoes a large extent of deformation in order to accommodate for a more stringent structural nature of APE1. APE1 was shown to have a preformed DNA binding surface that undergoes little conformational change while it uses its hydrophobic pocket to accommodate abasic site and exclude normal bases (Wilson and Barsky 2001).

In cleaving abasic DNA, APE1 is dependent on divalent metal ions and displays maximal activity in the range of 0.1mM to 2mM Mg^{2+} concentrations under *in vitro* assay conditions (6.6mM Tris-HCl, pH 7.5, 0.5mM $MgCl_2$, 0.1mM 2-mercaptoethanol) (Barzilay *et al.* 1995). It is thought that metal ions have no effect on substrate binding, but their role becomes critical during catalysis. They are predicted to be involved in substrate orientation, transition-state stabilization, and the dissociation of the incised product (Rothwell *et al.* 2000). This is supported by a metal-chelation experiment where EDTA inactivated nuclease activity of APE1 is rescued to a varying extent by addition of different metal ions. Among these, magnesium showed the highest rescue rate of nuclease activity followed by manganese, nickel, zinc, and potassium, in decreasing order. Also, APE1 can be induced to bind stably to abasic site-containing oligonucleotides (or oligonucleotides with modified abasic sites such as tetrahydrofuran) by chelation of the active site metal ion (Rothwell *et al.* 2000). In this way, the activity of APE1 can be 'trapped' in a stable complex with DNA at a stage subsequent to substrate recognition, but prior to phosphodiester backbone incision. Hence, the APE1 catalytic cycle can be viewed as being comprised of two steps that are separable both mechanistically and temporally.

1.4.3 Variants of APE1 identified in human populations

A few APE1 variants identified from the human population (Figure 4) were speculated to be associated with increased disease susceptibility (Hadi *et al.* 2000).

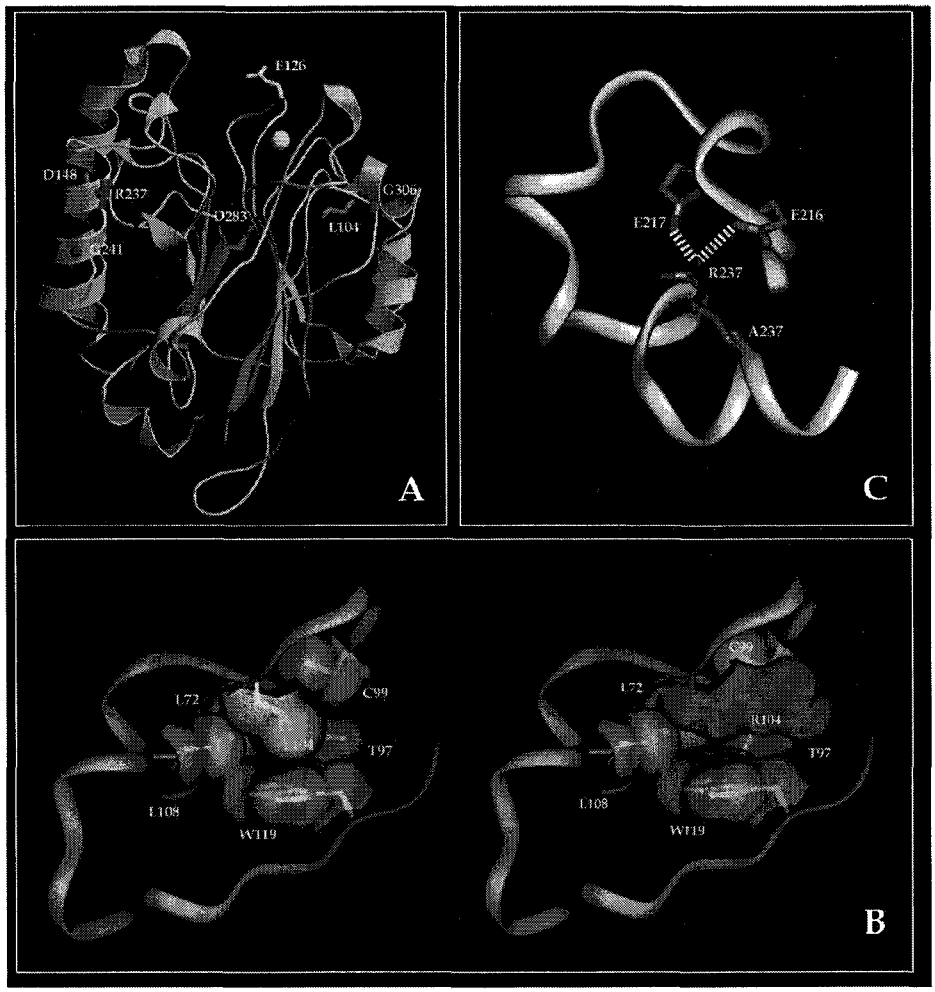

Figure 4: Molecular model of the positions of the residues found to be mutated in human population (Hadi *et al.* 2000). **(A)** Substitution mutations were found in these residues indicated by different colours: L104 (orange), E126 (green), D148 (peach), R237 (red), G241 (green), D283 (purple) and G306 (maroon). DNA binding groove is located at the top, with a metal cofactor represented as a ball. **(B)** Comparison of local structure in WT APE1 (left) versus L104R (right). The hydrophobic packaging of the local structure is predicted to be disrupted by the presence of R104. **(C)** Comparison of disruption in hydrogen bonding network of the WT versus R237A. Dashed lines indicate hydrogen bonds.

In a total of seven variants tested (L104R, E126D, D148E, R237A, G241R, D283G, and G306A), reductions in abasic DNA incision activity were observed in L104R, E126D, and R237A (Table 2). These variants were further discussed to have association with an increased risk of developing cancer (Hadi *et al.* 2000). Hadi *et al.* excluded a few of the variants that had mutations lying outside of the DNA endonuclease domain (L44C, Q51H, G57A and I64V). We included in our test Q51H and I64V, notably because these variants have never been assessed of their DNA endonuclease activities as well as RNA incision activity. With these, we tested the RNA incision activities of the six human variants except D283G.

Table 2: Summary of dissociation constants (K_d) and abasic DNA incision activities of APE1 population variants (Hadi *et al.* 2000).

	K_d (nM)	Incision
WT	25.8 ± 12.2	100
L104R	54.3 ± 19.7	56.71 ± 26.80
E126D	44.0 ± 7.2	60.43 ± 11.16
D148E	20.3 ± 3.4	94.36 ± 6.20
R237A	26.5 ± 14.1	35.71 ± 9.68
G241R	20.1 ± 0.1	108.73 ± 5.31
D283G	N/A	N/A
G306A	35.3 ± 13.9	107.22 ± 17.13

1.4.4 3'-5' Exonuclease activity of APE1

It was found that the strength of human APE1 3'-5' exonuclease activity is weaker than its abasic incision activity by 4-33 fold (Demple *et al.* 1991; Robson *et al.* 1991; Wilson *et al.* 1995). This is in contrast to the *E. coli* homolog of APE1, Exo III, which is a far better 3'-5' exonuclease, displaying its abasic endonuclease and exonuclease activities at a similar efficiency (Wilson *et al.* 1998). The active site residue difference seemed to account for this difference between the two enzymes.

In terms of substrate specificities, human APE1 showed varying efficiencies (K_{cat}/K_m) on different DNA substrates (5' overhang dsDNA = 1 nt gapped dsDNA > nicked dsDNA > 2 nt gapped dsDNA >> ssDNA = blunt ended dsDNA (Suh *et al.* 1997; Hadi *et al.* 2002), but appeared to exhibit a similar affinity (K_m value of ~250 nM) for these exonuclease substrates. It was concluded that human APE1 seemed to be mostly affected by the substrate context at the catalytic step (Wilson 2003). It was also found that APE1 is a non or poorly processive exonuclease (Wilson 2003), confirming that this activity of APE1 is weaker than its abasic DNA incision activity.

Nonetheless, its significance was re-examined after its exonuclease activity showed to remove various 3' termini blocking groups on DNA. Human APE1 has been found to remove 3'-phosphoglycolates. This excision is highly selective, with marked preference for gapped DNA substrates in comparison to single-stranded (ss) oligonucleotides or blunt end duplexes (Suh *et al.* 1997). It is also noteworthy that human APE1 can remove 3' mismatched nucleotides at least 50 times more efficiently than those matched correctly (Chou and Cheng 2002) which was recognized as another 3' proofreading function of APE1.

In linking its activity to biological relevance, human APE1 was also found to be a strong remover of stereochemically unnatural L-configuration anticancer nucleoside analogues (Chou *et al.* 2000), and beta-L-dioxolane-cytidine (Beta-L-OddC, BCH-4556; Troxacitabine) (Grove *et al.* 1995), and other beta-L-configuration nucleoside analogues from the 3' terminus of DNA in leukaemic cell nuclei. Also, in retroviral therapy against HIV, certain nucleoside analogues such as 3'-azido-3'-deoxythymidine (AZT) are often used to block viral DNA replication. APE1, in contrast to other cytosolic exonucleases, can remove this analogue from the 3' terminus of a nick efficiently (Chou and Cheng 2002). As

APE1 is expressed constitutively in human cells, it could therefore be used to limit the cytotoxicity of AZT and other anti-HIV compounds. Later, APE1 was found to remove 3'-tyrosyl residues, which could result from erroneous function of Topoisomerase I, via a phosphodiesterase or endonucleaselike activity, again depending on the DNA structural context (APE1 removes 3'-tyrosyl residues from 3'-recessed and nicked DNAs) (Wilson 2003).

1.5 Research objectives

There is increasing evidence that endoribonucleolytic mRNA decay plays a critical role in mammalian gene expression (Lebreton *et al.* 2008; Schaeffer *et al.* 2009; Eberle *et al.* 2009). Efforts are being added to identify and understand novel mammalian endoribonucleases (endoRNases). APE1 has been recently purified and determined to possess a novel endoRNase activity *in vitro* (Barnes *et al.* 2009). In order to further understand this activity and its biological significance, the following research objectives were established.

The first objective was to definitively assess whether the RNA-cleaving activity of APE1 shares the same active centre as abasic DNA endonuclease activity. To accomplish this, we assessed the RNA cleaving activities of previously generated active site mutants of APE1 used in elucidating abasic DNA endonuclease activity. The results obtained from testing the two RNA substrates (c-myc-1705-1792 CRD RNA, and Oligo IB) were expected to definitively identify the active site residues of APE1. Also, we intended to assess the RNA cleaving activities of variants of APE1 found in human population and compare them to the abasic DNA endonuclease activities. This was expected give us a better understanding in correlating some of these mutants and their aberrant RNA-cleaving activities in association

with tumorigenesis. Finally, to support our findings and to understand the RNA incision catalysis, the endoribonuclease activity of APE1 was subjected to further biochemical characterization.

The second objective was to confirm the preferred RNA structure and sequence specificity for endoRNase activity of APE1 as well as to assess the biological significance of the endoRNase activity of APE1. The first part of the objective was carried out using five RNA substrates with different secondary structures and sequence. The experiments were mainly done using RNA sequencing gels to identify the sites and local RNA structures that were preferentially cleaved by APE1. The second part of the objective was carried out in cultured HeLa cells and using siRNA technology to knock down the levels of APE1 to assess its influence in c-myc mRNA turnover. Also to support this assessment, we tested the effect of APE1 expression in the growth of *E. coli* Origami cells which has been previously used to assess the effects of ribonuclease activity of RNase A and Angiogenin (Smith and Raines 2006; Smith and Raines 2008).

CHAPTER 2

Identifying the critical amino acid residues for endoribonuclease activity of APE1 and characterizing its biochemical properties

Preliminary analysis showed APE1 is capable of cleaving at multiple sites of its substrate RNA (Barnes *et al.* 2009). However, its active site residues for carrying out its RNA cleavage were unknown and it is intriguing to assess if these residues were shared between APE1 endoribonuclease activity and AP-DNA endonuclease activity. By testing recombinant mutants of APE1 that have amino acid substitutions in critical residues for AP-DNA endonuclease activity (Table 1), we evaluated their importance during RNA cleavage. As part of a collaborative effort, we have obtained APE1 structural mutants from Dr. David Wilson's laboratory at National Institute on Aging, NIH. Also, APE1 variants identified in the human population were also obtained from Dr. Wilson and assessed for their alterations in RNA cleaving activity. A few of these variants have been found to possess functional AP-DNA endonuclease activities (Hadi *et al.* 2002), however they were reported to be associated with the development of cancer. Therefore, it was intriguing for us to find out if there were any disparities in AP-DNA and RNA cleaving activities of these variants.

Also, endoribonuclease activity of APE1 needed to be characterized under various biochemical settings. This information will provide clues to the catalysis mechanism in RNA cleavage and may become beneficial in the long run for developing APE1 in applications for therapeutic purposes. We characterized the effects of metal ions as well as identified the end of its RNA cleavage product. In addition, robustness of its RNA cleaving activity was assessed by testing its sensitivity to RNasin, and a known inhibitor of RNase.

2.1 Methodology

This section describes the methods implemented in identifying the critical amino acid residues in endoribonuclease activity of APE1 and understanding its biochemical properties.

2.1.1 Reagents and buffer preparation

These reagents shown in Table 3 were used through out the course of experiments including those in chapter 3.

Table 3: Composition of Reagents used in this chapter

Reagent	Composition
0.5x TBE	0.45 M Tris-HCl/Boric acid (Sigma) pH 8.3, 5 mM EDTA
10x T7 Transcription Buffer	400 mM Tris-HCl pH 7.6, 240 mM $MgCl_2$, 20 mM spermidine, 0.1 % Triton X-100
10x Glycogen	0.2 mg/mL Glycogen, 3M sodium acetate pH 5.2
RNA Elution Buffer	1x TE pH 7.5, 0.01 % SDS, 0.1 M NaCl
1x TE	10mM Tris-HCl pH 8, 1mM EDTA pH 8
10x Alkali Buffer	500 mM sodium bicarbonate pH 9.2 and 10 mM EDTA
Stopping Dye	9M Urea, 0.01% bromophenol blue, and 0.01% xylene cyanole FF
Agarose Loading Dye	0.25% bromophenol blue, 0.25% xylene cyanole FF, 15% ficoll

2.1.2 PCR generation of linear templates

The c-myc-1705-1792 CRD RNA was generated in the lab while Oligo IA, dOligo IA, and Oligo IB were commercially synthesized from IDT, San Diego, CA (Table 4). To prepare linear DNA templates for *in vitro* generation of RNA substrates, the pUC19 plasmids containing cDNAs of c-myc (nucleotides 1705 – 1792) CRD RNA was amplified via PCR in the region including the T7 promoter and cDNA sequence. The sequences of the primer used are shown in Table 5.

Table 4: List of RNA substrates used in assessing the RNA-cleaving activity of APE1 and its mutants. rU and dU indicate ribose and deoxyribose moieties linked to the Uridine bases, respectively.

RNA Substrate	cDNA/Oligonucleotide sequence
c-myc (nts 1705-1792) CRD RNA	5'-CCAGATCCCGGAGTTGGAAAACAATGAAAAGGCCC CCAAGGTAGTTATCCTTAAAAAAGCCACAGCATACA TCCTGTCCGTCCAAGC-3'
Oligo IA	5'-CAAGGTAGTrUATCCTTG-3'
dOligo IA	5'-CAAGGTAGTdUATCCTTG-3'
Oligo IB	5'-CAAGGrUAGTTATCCTTG-3'

To generate the linear template, a total reaction mixture of 50 µl containing 100 ng of pUC19 plasmids, 2U of Phusion DNA polymerase (Finnzymes), 0.3 mM dNTPs, 1x Phusion HF Reaction Buffer (Finnzymes), 45 pmoles of forward and reverse primers. The mixture was put into the PCR MiniCycler PCR machine (MJ Research Inc., Watertown, MA) which was programmed to incubate the mixture for 18 cycles of 45 secs at 95 °C, 45 secs at 55 °C, 10 mins at 68 °C, 20 min extension at 68 °C, hold at 4 °C to generate linear DNA template. Once the PCR was finished, the mixture was added with 2 µl of agarose loading dye and run in 1% agarose gel for 1hour at 120V. The PCR fragment was visualized under UV and excised. The PCR fragment was purified using QIAEX II Gel Extraction Kit (Qiagen Inc., Valencia CA) and following the manufacturer's protocol.

Table 5: PCR primers and their sequences used in the generation of linear DNA template for c-myc (1705-1792) CRD RNA by *in-vitro* RNA transcription.

Primers	Sequences
c-myc (1705-1792 or 1705-1886) CRD RNA Forward	5'-GGATCCTAATACGACTCACTATAGGACCA GATCCCGGAGTTGG-3'
c-myc (1705-1792) CRD RNA Reverse	5'-GCTTGGACGGACAGGATG-3'
c-myc (1705-1886) CRD RNA Reverse	5'-CGCACAAGAGTTCCGTAG-3'

2.1.3 Standard phenol/chloroform extraction and ethanol precipitation

To the reaction mixture of 200 µl, ½ volume of phenol (pH = 6.7, Sigma) and ½ volume of chloroform : isoamyl alcohol ($CHCl_3$: IAA = 49 : 1, Fluka) were added and vortexed. Note that for extracting RNA, phenol (pH = 4.3, Sigma) was used. The mixture was centrifuged at 12,000 rpm for 5 mins at 4 °C and the aqueous layer was aliquoted and transferred into a fresh tube. Next, 1 volume of $CHCl_3$: IAA = 49 : 1 was added and vortexed and centrifuged at 12,000 rpm for 5 mins. The aqueous layer was transferred into a fresh tube and $1/10^{th}$ volume of 3M sodium acetate (NaOAc) pH 5.3 was added followed by 2 volumes of 100% ethanol. The mixture was vortexed and stored at -20 °C for 20 mins. The mixture was centrifuged at 12,000 rpm for 10 mins to precipitate the plasmid and the supernatant was poured off. Next, the pellet was rinsed with 200 µl of 70% ethanol and centrifuged at 12,000 rpm for 5 mins. The supernatant was removed by pouring and the pellet was dried inside fume hood for 20 mins. The pellet was resuspended with 20 µl of autoclaved water to give a final concentration of 0.1 - 0.4 µg/µl measured by ND-1000 UV-Spectrophotometer (NanoDrop V.3.1.0, Wilmington, Delaware). The concentration was measured by using the relationship: DNA concentration (µg/ml) = (OD_{260}) x (dilution factor) x (50 µg DNA/ml) / (1 OD_{260} unit).

2.1.4 Generation of unlabeled RNA substrates

To generate RNA from linear plasmids, overnight *in vitro* transcription was performed. A typical 100 µl reaction contained ~4.5 µg of linear plasmid, 10 µl of 100 mM DTT (Promega, Madison, WI) 1 µl of 40 U/µl RNasin (Promega, Madison, WI), 10 µl of 10x T7 transcription buffer (Table 3), 5 µl each of 100 mM ATP, CTP, GTP, UTP, 5 µl of 19 U/µl T7 RNA Polymerase (Promega, Madison, WI) and adjusted to the volume with

diethylpyrocarbonate (DEPC) (Sigma) treated Milli-Q-ddH_2O. The reaction was done at 37 °C for typically 16 hrs. After incubation, the sample was centrifuged at 12,000 rpm for 1 min and 1 µl of the supernatant was aliquoted into a fresh tube. The rest of the supernatant was transferred into a fresh tube and 10 µl of 1 U/µl RNase-free RQ1 DNase (Promega, Madison, WI) was added and incubated at 37 °C for 30 mins. 1 µl of the reaction mixture was aliquoted into a fresh tube and loaded along with the pre-treated sample (1 µl) on a 2.5% agarose gel to confirm the digestion of plasmid. The gel was prepared and visualized similarly to the method described in 2.1.2 except 1.25 g of agarose was used and the gel ran for about 50 mins. Next, 5 µl of phenol (pH = 4.3, Sigma) was added to the DNase treated sample and vortexed. Then ProbeQuant™ G-50 micro columns (GE Healthcare, Buckinghamshire, UK) were vortexed and the bottom closure was snapped off followed by centrifuge at 3,000 rpm for 1 min and flow through discarded. The vortexed DNase treated sample was split into two 50 µl samples and each was applied to the column resin and centrifuged at 3,000 rpm for 2 mins. The flow throughs were collected and combined (~120 µl). Standard ethanol precipitation was performed. 1/10th volume of (12 µl) of 3 M NaOAc pH 5.2 and 2 volumes (240 µl) of 100% ethanol were added and the sample was stored in -20 °C for 20 mins. After, the sample was centrifuged at 12,000 rpm for 10 mins and its supernatant removed by pouring. Then, 200 µl of 70% ethanol was added to rinse the pellets and centrifuged at 12,000 rpm for 5 mins. The supernatant was poured off and the pellet was dried in fume hood for 20 mins. The pellet was resuspended with 80 µl of DEPC treated water and its RNA concentration was determined by ND-1000 UV-Spectrophotometer (NanoDrop V.3.1.0, Wilmington, Delaware). The concentration was measured by using the relationship: RNA concentration (µg/ml) = (OD_{260}) x (dilution factor) x (40 µg RNA/ml) / (1 OD_{260} unit).

2.1.5 Generation of 5'-radiolabeled RNA substrates

First, *in vitro* transcribed RNA (0.2 – 1.0 μg/μl) was dephosphorylated at the 5' end. Typically two reactions were performed in parallel to produce a higher yield of dephosphorylated RNA after extraction. A typical 200 μl dephosphorylation reaction contained 10 μg of RNA (e.g. 333 pmol of c-myc 1705-1792 CRD RNA), 20 μl of 10x NEB Buffer 3 (New England Biolabs, Beverly, MA), 0.5 μl of 5 U/μl Calf Intestine Phophatase (New England Biolabs, Beverly, MA) diluted from 10 U/μl in 1x NEB Buffer 3, and volume adjusted with DEPC treated water. The reaction was carried out at 37 °C for 60 mins. Next, 1 μl of 0.5M EDTA pH 8, 4 μl of 5M NaCl, and 10 μl of 20% SDS were added to the mix. Then, RNA was subjected to a standard phenol/chloroform extraction and ethanol precipitation as described in 2.1.3. Only exceptions from this protocol were the usage of pH 4.3 phenol (Sigma) and resuspending the RNA from two reactions in 20 μl of DEPC treated water to give a concentration around 0.25 – 0.8 μg/μl.

The 5'-radiolabeling of the dephosphorylated transcript was performed in a 12.5 μl final volume consisting of 0.38 μg of the dephosphorylated transcript (e.g. 12.5 pmol of c-myc 1705-1792 CRD RNA) and 38 μCi or 12.5 pmol of γ-^{32}P-ATP (PerkinElmer, Boston, MA), 0.5μl of 1 U/μl of T4 Polynucleotide Kinase (PNK) (New England Biolabs, Beverly, MA), 1.25 μl of 10x PNK buffer, and DEPC treated water. The reaction mix was incubated for 1 hour at 37 °C. The reaction mix was stopped by adding 25 μl of Stopping Dye which contains 9M Urea, 0.01% bromophenol blue, and 0.01% xylene cyanole FF. Subsequently, the stopped mixture was loaded onto an 8% polyacrylamide (29:1, acrylamide: N,N'=metheylenebisacrylamide) gel containing 7M urea (Invitrogen) and ran at 20 mA with 0.5x TBE buffer (0.45 M Tris-HCl/Boric acid (Sigma), 0.01 M EDTA pH 8.3 for 1 hour or

until the bromophenol blue dye was near the bottom of the gel. The gel was exposed onto a Cyclone Storage Phosphor Screen System (Packard, Meriden, CT) and gel image was developed using Cyclone PhosphoImager and visualized by the OptiQuant software (Hewlett Packard, Palo Alto, CA). The polyacrylamide gel containing the radiolabeled transcript was sliced out and put into a tube containing 400 µl of RNA Elution Buffer (1x TE pH 7.5, 0.01 % SDS, 0.1 M NaCl) and 200 µl of phenol (pH = 4.3, Sigma). The elution reaction lasted 5 hrs at 45 °C, followed by standard phenol/chloroform extraction and ethanol precipitation. The RNA was resuspended in 50 µl of DEPC treated water and diluted appropriately in order to give a final count of approximately 100,000 c.p.m./µl.

2.1.6 Generation of 5'-radiolabeled abasic DNA substrate

Commercially available 18-mer oligonucleotide, 5'-GTCACCGTG**F**TACGACTC-3' (IDT, San Diego, CA) that contained the model analog of an abasic site, tetrahydrofuran (F) (Figure 5) (Hadi *et al.* 2000) was used. The sequence of its complementary strand was 5'-GAGTCGTAACACGGTGAC-3' (IDT, San Diego, CA). The oligonucleotides were adjusted to a concentration of 1 µg/µl or 187 pmol/µl for sense strand and 1 µg/µl or 177 pmol/µl for anti-sense strand by addition of autoclaved water.

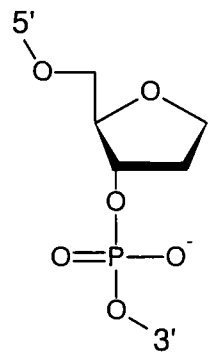

Figure 5: Chemical structure of abasic site analog represented as F in the cDNA sequence.

Dephosphorylation

The oligonucleotide containing the abasic site was dephosphorylated in a typical reaction of 80 µl that contained 4 µg of oligonucleotide, 1x NEB buffer 3 (New England Biolabs, Beverly, MA), 2 U of Calf Intestine Phophatase (New England Biolabs, Beverly, MA) diluted from 10 U/µl in 1x NEB Buffer 3, and autoclaved water. The reaction was done at 37 °C for 60 mins

Standard phenol/chloroform extraction

Next, 120 µl of autoclaved water was added to the reaction mix followed by the addition of 1 µl of 0.5M EDTA pH 8, 4 µl of 5M NaCl, and 10 µl of 20% SDS. Then, the dephosphorylated oligonucleotide was subjected to a standard phenol/chloroform extraction and ethanol precipitation as described in 2.1.3. Only exceptions from this protocol were the replacement of 3M sodium acetate (NaOAc) pH 5.3 with 10x glycogen (0.2 mg/ml), which was added at a final concentration of 20 µg/mL to the aqueous layer before the addition of 100% ethanol. This was to improve the precipitation of shorter length oligonucleotides. The precipitated oligonucleotide was resuspended in 20 µl of autoclaved water to give a concentration of approximately 0.2 µg/µl.

5'-radiolabeling and hybridization

The 5'-radiolabeling of the dephosphorylated oligonucleotide was performed in a 25 µl final volume consisting of 0.13 µg (25 pmol) of the dephosphorylated oligonucleotide and 75 µCi (25 pmol) of γ-^{32}P-ATP (Amersham GE Healthcare, Montreal, QC), 10 U of T4 Polynucleotide Kinase (PNK) (New England Biolabs, Beverly, MA), 1x PNK buffer (New England Biolabs, Beverly, MA), and autoclaved water. The reaction mix was incubated for 1 hour at 37 °C. The reaction was stopped by heating at 95 °C for 2 mins and icing the reaction

for 1 min. Molar excess (177 pmol) of anti-sense oligonucleotide was added to the stopped kinase reaction mixture and the mixture was heated to 56 °C for 10 mins. Next, the reaction was placed at room temperature for 60 mins and at 4 °C overnight for hybridization.

Removal of free γ-^{32}P-ATP and quantification of radioactivity

ProbeQuant G-50 Micro Column (GE Healthcare) was prepared by vortexing the resin in the column and spinning the column at 3000 rpm for 1 min. The flow-through was discarded and 26 µl of hybridization mixture was applied to the resin. The column was placed into a new eppendorf tube and spun at 3000 rpm for 2 mins. The abasic DNA was collected in the eppendorf tube which was transferred to another eppendorf tube. 1 µl of purified abasic DNA was measured of its activity in counts per min (c.p.m.) using Packard 1600 TR liquid scintillation analyzer. The abasic DNA was diluted to give a final count of 100,000 c.p.m./µl.

2.1.7 SDS-PAGE analysis on recombinant human APE1

12 % SDS-PAGE resolving gel mix (12 % acrylamide/0.32 % bisacrylamide, 0.3 M Tris-HCl pH 8.8, 0.1 % SDS) was made by mixing 2.5 mL of 30% acrylamide/0.8 % bisacrylamide, 1.5 mL of 4 x Lower Gel Buffer (Table 6), and 2 mL of autoclaved water. 5mL of this mixture was mixed with 10 µl of 20 % ammonium persulfate (APS), and 3 µl of TEMED (Sigma) and cast into the assembled gel apparatus (Biorad, Hercules, CA). The surface of the resolving gel was evened out by pipetting in 1 mL isopropanol. The resolving gel was left to solidify for 30 minutes. After, the isoproanol was removed and the surface of the resolving gel dried. Similarly, 5 % SDS-PAGE stacking gel mix (5 % acrylamide/0.13 % bisacrylamide, 0.1 M Tris-HCl pH 6.9, 0.1 % SDS) was made by mixing 0.32 mL of 30%

acrylamide/0.8 % bisacrylamide, 0.5 mL of 4 x Upper Gel Buffer, and 1.18 mL of autoclaved water.

Table 6: Composition of reagents for SDS-PAGE.

Reagents	**Composition**
10 x Running Buffer	0.19 M Tris-HCl, 1 % SDS, 1.9 M Glycine
4 x Lower Gel Buffer	1.15 M Tris-HCl pH 8.8, 0.4 % SDS
4 x Upper Gel Buffer	0.38 M Tris-HCl pH 6.9, 0.4 % SDS
2 x SDS Loading Dye	0.1 M Tris-HCl pH 8.8, 0.4 % SDS, 20 % Glycerol, 0.00004 % Bromophenol Blue, 10 % β-mercaptoethanol
30 % acrylamide/0.8 % bisacrylamide	14.6 g acrylamide, 0.4 g bisacrylamide in 50 mL autoclaved water, Filter sterilized
20 % ammonium persulfate	2 g ammonium persulfate in 10 mL of autoclaved water

2mL of this mixture was mixed with 5 µl of 20 % ammonium persulfate, and 2 µl of TEMED (Sigma) and cast on top of the resolving gel already solidified and dried from the previous step. Immediately, the comb was inserted on to the stacking gel and the gel was left to solidify for 20 mins.

All protein samples were prepared as follows. 10 µl of protein sample (40 µg) was mixed with 10 µl of 2 x SDS Loading Dye and boiled in water bath for 4 mins. The 20 µl mix was spun briefly and subsequently loaded onto the 12 % SDS-PAGE gel. As a control, 10 µl of Full Range Rainbow Molecular Weight Markers (Amersham Biosciences, Buckinghamshire, UK) was also loaded. The gel was run at 120 V with 1 x Running Buffer (20 mM Tris-HCl, 0.1 % SDS, 0.2 M Glycine) prepared from its 10 x stock in MilliQ water. The gel was run for 60 mins or until the Bromophenol Blue dye front had reached the bottom of the gel.

Table 7: SDS-PAGE gel staining & destaining reagents.

Reagents	Composition
Coomassie staining solution	50 % methanol, 10 % acetic acid, 0.1 % (= 0.1g) Coomassie Brilliant Blue R-250
Destaining solution	50 % methanol, 10 % acetic acid

The gel was removed from the apparatus and stained in 50 mL of Coomassie staining solution (Table 7) overnight with gentle shaking at room temperature. The gel was then destained using Destaining solution for 1 hr. The gel was visualized and imaged under white light transillumination using ChemiImager™ System (Alpha Innotech Corporation, San Leandro, CA).

2.1.8 Endoribonuclease assays using 5'-radiolabeled RNA

The buffer system used in the standard endoribonuclease assay contained Tris-Cl. A typical 20 µl reaction condition contained the following ingredients: 10 mM Tris-Cl pH 8 and 2 mM DTT, 25 nM of 5'-^{32}P-lableled substrate (100,000 c.p.m.), and varying concentration of APE1. The reaction is carried out at 37 °C for varying amount of time. Once the reaction is complete, the reaction mixture is stopped by adding 40 µl of Stopping Dye. Ten microliters of stopped mixture was loaded onto 8% polyacrylamide (29:1, acrylamide: N,N'=metheylenebisacrylamide) gel containing 7M urea (Invitrogen) and ran at 20 mA with 0.5x TBE buffer (0.45 M Tris-HCl/Boric acid (Sigma), 0.01 M EDTA pH 8.3) for 60 mins. The gel was transferred onto a filter paper and dried on a gel dryer (LABCONO, Kansas City, MO) for 45 mins at 80 °C and exposed overnight to a Cyclone Storage Phosphor Screen System (Packard, Meriden, CT). On the following day, the gel image was developed using Cyclone PhosphoImager and visualized by the OptiQuant software (Hewlett Packard, Palo Alto, CA).

2.1.9 Abasic DNA endonuclease assays using 5'-radiolabeled abasic DNA

The established protocol for APE1 abasic DNA endonuclease assay was used with modifications (Mantha *et al.* 2008). A typical reaction mixture of 15 µl contained 80,000 c.p.m. (0.1 pmoles) of abasic DNA, 25 pg (0.7 fmoles) of APE1, 50 mM Tris–HCl (pH 8), 50 mM KCl, 1 mM DTT, 0.1 m M EDTA, 2 mM $MgCl_2$ and 100 µg/mL bovine serum albumin. The reaction was carried out at 37 °C for 3 mins. Next, 30 µl of the Stopping Dye was added to the reaction mixture and 9 µl of the sample was loaded onto an 8% polyacrylamide (29:1, acrylamide: N,N'=metheylenebisacrylamide) gel containing 7M urea (Invitrogen) and ran at 20 mA with 0.5x TBE buffer (0.45 M Tris-HCl/Boric acid (Sigma), 0.01 M EDTA pH 8.3) for 40 mins or until the bromophenol blue dye was separated from the xylene cyanole FF by 3 cm. The remainder of the procedure was identical to that described above (section 2.1.8).

2.1.10 Dialysis of APE1

For experiments designed to assess the effects of divalent metal ions, recombinant APE1 produced from Dr. Mitra's laboratory was dialyzed additionally in a metal-free buffer. 50 µl aliquot of APE1 was treated with 2 µl of 6 M Guanidine-HCl with 20% β-mercaptoethanol to allow for denaturation of the protein. A total of 10 µl of the 6M Guanidine-HCl with 20% β-mercaptoethanol was added in sequential steps by adding 2 µl at a time. Once the protein was denatured, the aliquots were transferred to the Slide-A-Lyzer Mini Dialysis Units (Pierce, Rockford, IL) and put into the beaker holding 500 mL of dialysis buffer (20 mM Tris-HCl pH 8, 300 mM NaCl, 1 mM DTT, 0.1 mM EDTA, and 50% glycerol) with gentle stirring. The dialysis was carried out in the cold room for a total of 5 hrs with one change of dialysis buffer after the first 2.5 hrs. The protein was quantified later with ND-1000 NanoDrop V.3.1.0 Protein A280 method (Wilmington, Delaware).

2.1.11 Determination of the nature of 3'-end of the RNA cleavage product

To determine whether APE1 generates RNA products with a 3′phosphate or a 3′hydroxyl group, we adopted the method described by Schoenberg and co-workers (Chernokalskaya et al. 1997) which uses snake venom exonuclease's (Sigma) ability to digest only products bearing 3′hydroxyl. The c-*myc* CRD RNA nts 1705-1792 was used as a substrate. RNase T1 generates products with 3′phosphates, and these can not be processed by the exonuclease. In contrast, S1 nuclease generates decay products with 3'hydroxyls and these can be degraded upon treatment with the exonuclease. Hence, APE1 treated RNA decay products can also be treated the exonuclease to determine the characteristic of their 3' ends.

i) <u>RNase T1</u>

A typical 20 µl reaction contained ~250,000 c.p.m. of 5'-radiolabeled RNA, 1 U of RNase T1 in RNase T1 Buffer (25 mM Tris-HCl pH 7.2, 2.5 mM $MgCl_2$, 25 mM KCl). The reaction was carried out 37 °C for 5 mins.

ii) <u>S1 Nuclease</u>

A typical 20 µl reaction contained ~250,000 c.p.m. of 5'-radiolabeled RNA, 10 U of S1 Nuclease in 1x S1 Nuclease Buffer (Invitrogen Life Technologies, Carlsbad, CA). The reaction was carried out at 37 °C for 5 mins.

iii) <u>APE1</u>

A typical 20 µl reaction contained ~250,000 c.p.m. of 5'-radiolabeled RNA, 0.3 µg of APE1 in APE1 reaction mixture including 10 mM Tris-HCl pH 7.4, 2 mM DTT, and 2 mM magnesium acetate. The reaction was carried out 37 °C for 5 mins.

iv) **RNA Product Extraction and Resuspension**

After reactions, 130 µl of DEPC treated water was added to raise the volume to 200 µl, followed by a standard phenol/chloroform extraction and ethanol precipitation as described in section 2.1.2. Exceptions from this section were the usage of pH 4.3 phenol (Sigma) and the resuspension of the extracted RNA in 12 µl of snake venom phosphatase reaction buffer (100 mM Tris-HCl pH 8.7, 100 mM NaCl, and 14 mM $MgCl_2$).

v) **Snake Venom Phosphatase Reaction**

To 4 µl of resuspended RNA, 1 µl of $3.2x10^{-5}$ U/µl of snake venom phosphatase (Sigma, St. Louis, MO) was added and the reaction was carried out at 25 °C for 10 mins. The reaction was stopped by adding 5 µl of the Stopping Dye and 3 µl of the stopped mixture was loaded on to an 8% polyacrylamide (29:1, acrylamide: N,N'=metheylenebisacrylamide) gel containing 7M urea (Invitrogen) and ran at 20 mA with 0.5x TBE buffer (0.45 M Tris-HCl/Boric acid (Sigma), 0.01 M EDTA pH 8.3) for 1 hour or until the bromophenol blue dye was near the bottom of the gel. The gel was transferred to a filter paper and dried on a gel dryer (LABCONO, Kansas City, MO) for 45 mins at 80 °C and exposed overnight to a Cyclone Storage Phosphor Screen System (Packard, Meriden, CT). On the following day, the gel image was developed using Cyclone PhosphoImager and visualized by the OptiQuant software (Hewlett Packard, Palo Alto, CA).

2.1.12 Electrophoretic mobility shift assay (EMSA)

To assess the RNA binding abilities of APE1 and its mutants, electrophoretic mobility shift assay (EMSA) was used.

i) Generation of internally radiolabeled RNA

For our EMSA, internal radiolabeling of the c-myc 1705-1886 CRD RNA was done through *in vitro* transcription reaction. A typical reaction mixture of 20 µl was made up by mixing 4 µl of 5x Transcription Buffer (Promega, Wyoming, MI), 1 µl of 40 U/µl RNasin (Promega, Madison, WI), 2 µl of 100 mM DTT (Promega, Madison, WI), 1 µls of 10 mM ATP, CTP, and GTP, and 2.5 µl of 100 µM of UTP, 2 µl of 19 U/µl T7 RNA Polymerase (Promega, Madison, WI), 0.5 to 1 µg of linear DNA template, and 3 µl of Uridine 5'-triphosphate (α-^{32}P) (PerkinElmer, Boston, MA) and adjusted to the volume with diethylpyrocarbonate (DEPC) (Sigma) treated Milli-Q-ddH_2O. The reaction was incubated at 37°C for 1 hr. Next, 10 µl of 1 U/µl RNase-free RQ1 DNase (Promega, Madison, WI) was added and incubated at 37 °C for 10 mins and the reaction was stopped with 10 µl of Stopping Dye (Table 3). Subsequently, the sample was loaded onto an 8% polyacrylamide (29:1, acrylamide: N,N'=metheylenebisacrylamide) gel containing 7M urea (Invitrogen) and ran at 25 mA with 0.5x TBE buffer (Table 3) for 1.5 hour. The gel was exposed onto a Cyclone Storage Phosphor Screen System (Packard, Meriden, CT) and the image was developed using Cyclone PhosphoImager and visualized by the OptiQuant software (Hewlett Packard, Palo Alto, CA). The polyacrylamide gel containing the radiolabeled transcript was sliced out and put into a tube containing 400 µl of RNA Elution Buffer (Table 3) and 200 µl of phenol (pH = 4.3, Sigma). The elution lasted 5 hrs at 45 °C, followed by standard phenol/chloroform extraction and ethanol precipitation (refer to section 2.1.3). The RNA was resuspended in 40 µl of DEPC treated water to give a final count of ~600,000 c.p.m./µl. The RNA was quantified by diluting 5 µl of RNA samples in 800 µl of DEPC water in a spectrophotometer cuvette (VWR International). The sample was loaded onto Ultraspec 1000 (Biochrom)

UV/visible spectrophotometer and measured of its absorbance at wavelength 260 nm. The concentration of the RNA was calculated by the equation, Abs_{260nm} x 6.4 = sample in μg/μl. A typical concentration was ~0.75 μg/μl.

ii) Electrophoretic Mobility Shift Assay (EMSA)

For one EMSA reaction, 6.625 μl of Binding Buffer Cocktail (BBC) was prepared by mixing 4 μl of Binding Buffer (Table 8), 1 μl of 10 mg/ml of yeast tRNA, 1 μl of 10 mg/ml of BSA (Sigma), 0.125 μl of 40 U/μl RNasin (Promega, Madison, WI), and volume adjusted with DEPC water. A typical 20 μl EMSA reaction contained 6.625 μl of BBC, 30 nM of internally radiolabeled RNA and different amounts of APE1. The mixture was incubated at 35°C for 15 mins. 2 μl of EMSA Loading Dye was added and the mixture was loaded on to pre-running 8% native polyacrylamide (29:1, acrylamide: N,N'=metheylenebisacrylamide) gel. The gel was run for 2 hrs at 25 mA or until the xylene phenol FF dye reached the bottom of the gel. The subsequent process was identical to that of the endoribonuclease assay in section 2.1.8.

Table 8: The composition of reagents used in EMSA experiments.

Reagents	**Composition**
Binding Buffer	50 mM Tris-Cl pH 7.4, 12.5 mM EDTA, 10 mM DTT, 25 % glycerol, 0.01 % Triton-X
EMSA Loading Dye	250 mM Tris-Cl pH 7.4, 0.07 % Bromophenol blue, 0.07% Xylene cyanol FF

2.2 Results and Discussion

2.2.1 Generation of unlabeled and 5'-radiolabeled RNA

For certain plasmids, it was more convenient to perform PCR amplification to generate DNA templates for use in *in vitro* transcription rather than linearizing plasmids. So, it was decided that the PCR fragment should be used as a DNA template for *in vitro* transcription of c-myc 1705-1792 CRD RNA. Primer sets were designed (Table 5) and used to amplify the DNA templates coding for c-myc-1705-1792 CRD RNA identical in sequence to the one inserted in pUC19-c-myc-1705-1792. Figure 6A shows the *in vitro* transcribed unlabeled RNA substrate generated using the PCR templates. Both lanes 2 and 3 confirmed the presence of intact RNA substrate before and after DNase I treatment for eliminating DNA template. Both lanes 2 and 3 confirmed the presence of intact RNA substrate before and after DNase I treatment for eliminating DNA template. The RNA substrate showed multiple bands when migrated on a non-denaturing agarose gel. These bands may have been produced due to the inherent formation of RNA secondary structures under the non-denaturing condition. It should be noted that the non-denaturing agarose gel analysis is a rapid method to quickly visualize whether the transcription has occurred, but it does not provide an accurate estimation on the size of the RNA substrate. To estimate the size of the RNA, the RNA should be run on a 1% formaldehyde gel. However, later it was confirmed that when c-myc-1705-1792 CRD RNA, were phosphorylated with γ-^{32}P-ATP, only a single band of high activity was observed in an 8% denaturing polyacrylamide gel (Figure 6B; left gel), confirming that the *in vitro* transcribed RNA is indeed the right product. The size of the radiolabeled RNA was estimated using the internal standards, xylene cyanol and bromophenol blue.

Commercially obtained RNA oligonucleotides (Table 4) were also radiolabeled in a similar way and were subjected to purification by excision and elution. Oligo IB is shown in the right panel of Figure 6B. Other substrates (Oligo IA and dOligo IA) are not shown.

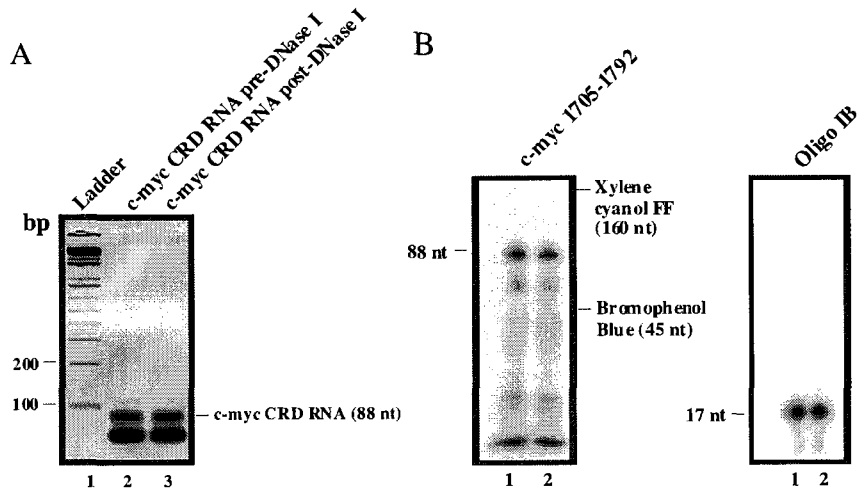

Figure 6: Agarose and polyacrylamide gel analyses showing the *in vitro* transcribed RNA substrate and the generation of 5'-radiolabeled RNA substrates. **(A)** 2% non-denaturing agarose gel showing *in vitro* transcribed c-myc 1705-1792 CRD RNA (lane 3) after DNase I treatment for 30 mins. **(B)** 8% polyacrylamide denaturing gel showing the products of 5'-end radiolabeling phosphorylation reactions using γ-^{32}P-ATP and T4 polynucleotide kinase and unlabeled c-myc-1702-1792 CRD RNA (left). On the right, 8% polyacrylamide denaturing gel shows the products of Oligo IB RNA substrate 5'-radiolabeled in an identical way as c-myc-1702-1792 CRD RNA.

2.2.2 Identification of essential residues for RNA incision activity of APE1

Recombinant APE1, APE1 structural mutants that have mutation on one of the active site residues, and APE1 population variants obtained from Dr. David Wilson's laboratory were all run on an SDS-PAGE gel to confirm their purity (Figure 7). All samples showed one band at an estimated molecular weight of 35.5 kDa with the exception of D308A mutant, which showed two bands of approximate size of 35.5 kDa and 33.5 kDa. It was known previously that an N-terminal truncated form of APE1 was observed (Chattopadhyay *et al.* 2006) and that APE1 can undergo hydrolysis during boiling of the protein samples, losing its

N-terminal region of 32-33 amino acids. In fact, previous WT APE1 produced in Dr. Mitra Sankar's laboratory also showed two bands when ran on an SDS-PAGE gel (Barnes *et al.* 2009).

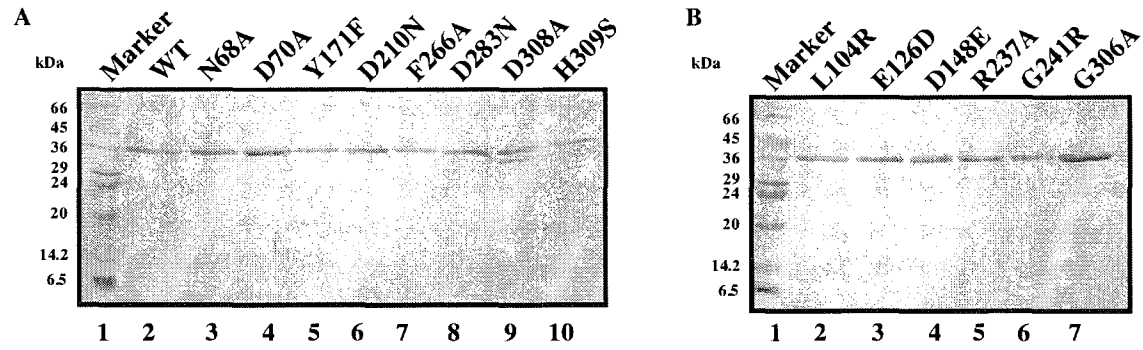

Figure 7: SDS-PAGE analysis of 1 µg of APE1 WT and mutants. The proteins were loaded on to each well and the gel was stained with Coomassie Blue. In lane 1 of each gel, Low Molecular Weight Marker was loaded. **(A)** APE1 WT (lane 2) and structural (active site) mutants (lanes 3 to 10). **(B)** APE1 human population variants (lanes 2 to 7).

The activities of these structural mutants were tested against their typical, 18 nt abasic DNA, substrate (Figure 8A). When the reduction of their activities were calculated by measuring the ratio of density of the product over those of the substrate plus product, D70A and H309S showed 7-fold and 158-fold reduction in their activities, respectively (Table 9). Compared to the previous reports, our results showed that N68A and D308A exhibited less reduction in their activities (~58-fold and ~1.4-fold, respectively compared to the WT) whereas F266A and D283N showed greater reduction (~30-fold and ~573-fold, respectively compared to the WT).

This may be due to the different assay conditions that we used in our laboratory as compared to those used by the other groups. There are disparities in the reported literature in regards to fold reductions observed in DNA endonuclease activity. For example, E96A mutant (not tested here) showed variations in reduction of its DNA endonuclease activity up

to 100 fold when tested in different enzyme amounts that fell in the range between 100 and 1000 pg (Erzberger *et al.* 1998; Chou and Cheng 2003). The amount of F266A and D283N used in our assay were both 25 pg in a reaction volume of 15 µl, which were suggested to give a linear reaction rate in abasic DNA incision (Mantha *et al.* 2008). In other studies, however, the same mutants were used in higher amounts (Erzberger *et al.* 1998; Masuda *et al.* 1998) that the reduction in their activities was reported to be less. Nevertheless, reductions observed in APE1 structural mutants relative to one another correlated to the suggested importance of these residues and the roles they play in the DNA endonuclease activity. These details are discussed further in conjunction with the results on RNA incision activity.

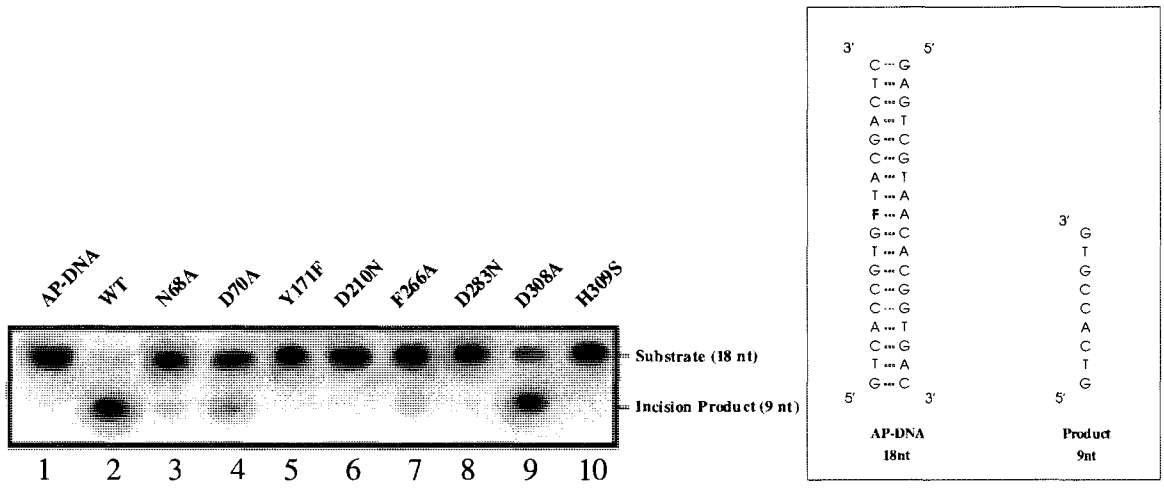

Figure 8: Abasic DNA endonuclease activity of WT APE1 and APE1 structural mutants. **(A)** 0.14 nM of APE1 (lanes 2 to 10) was tested against 25 nM of 5'- γ-^{32}P-radiolabeled abasic DNA in a total reaction volume of 15 µl for 3 mins at 37°C. **(B)** Structure and sequence of the abasic DNA (AP-DNA) and its incised product.

Table 9: Summary of fold reduction in WT APE1 and structural mutants.

Mutants	Reference	Fold reduction in abasic DNA incision in literatures	Fold reduction in abasic DNA incision (Figure 8A)	Fold reduction in RNA incision (Figure 10A)
N68A	Nguyen *et al.* 2000	600	58.7	Abolished
D70A	Nguyen *et al.* 2000	Reduction	6.7	55.6
E96A	Erzberger *et al.* 1999; Chou and Cheng 2003	600 – 100000	Not tested	Not tested
Y171F	Erzberger *et al.*1999	5000	Abolished	17.7
D210N	Erzberger *et al.*1999	25000	Abolished	8312.6
N212A	Rothwell and Hickson 1996	Not detectable	Not tested	Not tested
F266A	Erzberger *et al.* 1998	6	30.4	Abolished
D283N	Hadi *et al.* 2000	10	572.6	4.0
D308A	Erzberger *et al.* 1999; Barzilay *et al.* 1995	5-25	1.4	9.0
H309N	Chou and Cheng 2003	100000	Not tested	Reduction (Barnes *et al.* 2009)
H309S	Nguyen *et al.* 2000	Not tested	158.3	6.0

When the structural mutants were challenged with c-myc CRD RNA, most of the mutants, except D283N, showed reduced or abrogation of RNA incision activity at both concentrations tested (Figure 9A and B). Compared to the WT, the D283N mutant showed similar or greater activity, and though reduced, D308A, seemed to retain some RNA-cleaving activity.

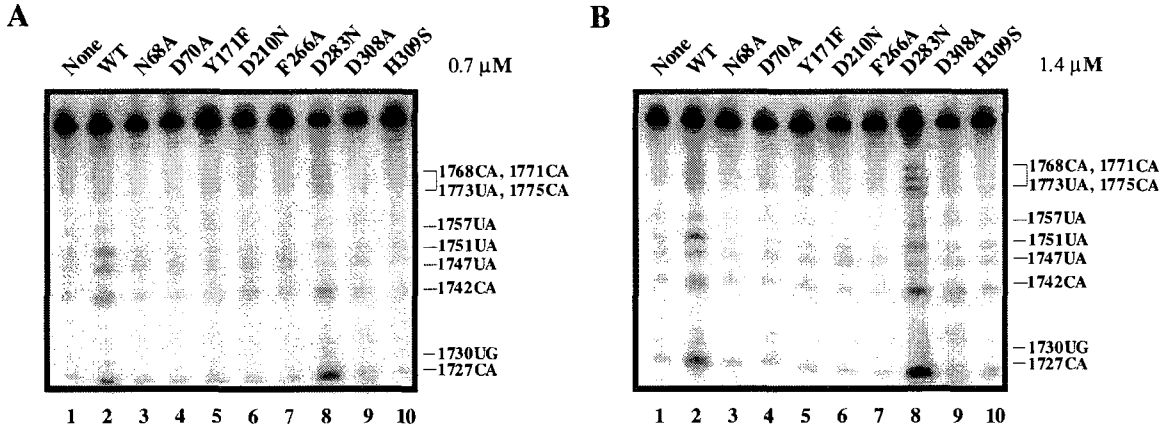

Figure 9: Endoribonuclease activity of APE1 and its structural mutants on c-myc-1705-1792 CRD RNA. (A) 0.7μM of APE1 (lanes 2 to 10) was tested against 25 nM of 5'- γ-^{32}P-radiolabeled c-myc-1705-1792 CRD RNA in a total reaction volume of 20 μl for 25 mins at 37°C. **(B)** Same condition as A with 1.4 μM of APE1 mutants.

The test of these mutants showed that the active site for cleaving abasic DNA is also important in cleaving RNA, despite a subtle difference for D283 which does not seem to be required for giving RNA incision activity. The same set of enzymes were also challenged with the 17nt RNA substrate, Oligo IB, which can form a single stem and a hairpin structure (Figure 10B) and has an identical sequence to the c-myc CRD region of 1741-1757 (Figure 15B). Oligo IB is composed entirely of deoxyribose-phosphate backbone except at base position 6, where a Uridine base is bonded to a ribose sugar. This was to confirm the reduction in activity seen with testing c-myc 1705-1792 CRD RNA (88nt). By measuring the ratio of density of the products (5 nt & 6 nt) over those of the substrate plus product, we could quantify the degree of reduction observed in these mutants. It was found that the reduced activities of structural mutants were also observed with Oligo IB (Table 9 and Figure 10A), confirming that these residues are indeed critical for giving RNA incision activity of APE1.

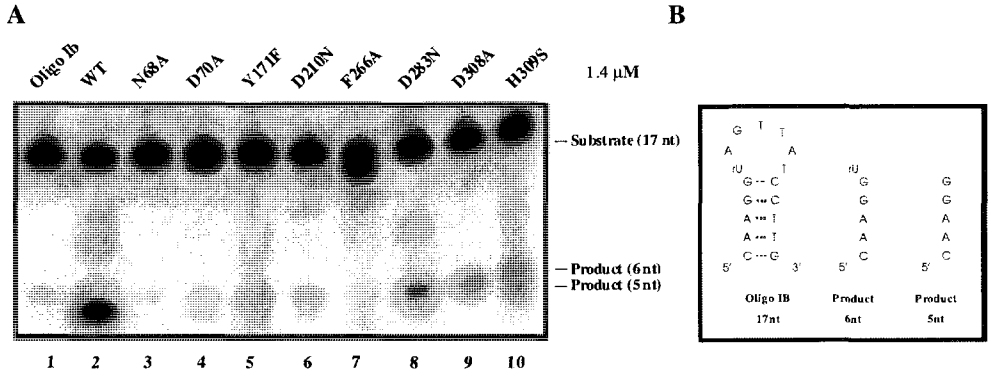

Figure 10: Endoribonuclease activity of APE1 and its structural mutants on Oligo IB RNA. **(A)** 1.4 μM of APE1 mutants (lanes 2 to 10) were tested against 25 nM of 5'- γ-^{32}P-radiolabeled Oligo IB RNA in a total reaction volume of 20 μl for 25 mins at 37°C. **(B)** Secondary structure of Oligo IB predicted through Mfold showing its APE1 RNA incision product (6nt) and 3' phosphodiesterase product (5nt).

One noteworthy observation was that there were two cleavage products of similar intensities were generated by D70A, Y171F, D210N, and D309S mutants (lanes 4, 5, 6, and 10, Figure 10A). The identity of the 6nt product seemed to have resulted from the RNA incision activity of APE1 cutting in between rUpA dinucleotides where as the 5nt product may have resulted from DNA 3' exonuclease activity of APE1 (Chen *et al.* 1991). The strong 5nt band produced by the WT (lane 2) compared to the weaker bands produced by the structural mutants showed that the WT can remove rU that hangs on to the recessed strand of the DNA structure. This suggests that WT APE1 possesses 3' exoribonuclease activity that is reduced in structural mutants. However, further investigation would be required to confirm this proposal. The finding is also in line with the suggestion that APE1 shares a common active site for its DNA endonuclease and 3'-5' exonuclease activities (Chou and Cheng 2003).

In general, human APE1 has been found to be a non- or poorly-processive 3'-5' exonuclease (Wilson 2003). 3'-5' exonuclease activity of APE1 is about 0.03% of the abasic DNA incision activity (Wilson *et al.* 1995) and shows similar affinities (K_m) towards 3' termini, but varying degrees of turnover (k_{cat}) in decreasing order for 3' recessed DNA, 1 nt gapped DNA, nicked DNA, and 2nt gapped DNA (Wilson 2003). The WT 3'-exonuclease activity is not detectable on blunt end of duplex DNA (Suh *et al.* 1997; Hadi *et al.* 2002) or on ssDNA (Wilson 2003). Also, human APE1 has been shown to remove 3' mismatched nucleotides at least 50 times more efficiently than those that are matched correctly. The mismatched nucleotide was removed more efficiently from nicked DNA than from recessed DNA (Chou and Cheng 2002). Thus, we speculate that after rUpA is cleaved by the WT APE1 RNA incision activity, the remaining rU must have been further removed by its 3'-5'

exoribonuclease activity of APE1, but this linear deletion could not have proceeded beyond the removal of rU.

The degree of reduction for each structural mutant in abasic DNA and RNA incision activity (Table 9) corresponds to the residue's importance in both of the reactions. For example, reductions seen in D70 and D308 do not seem to be severe as these two residues are predicted to coordinate metal ions (Erzberger and Wilson 1999) during the abasic DNA incision that are thought to orient the substrate, stabilize transition state, and facilitate the dissociation of product. In abasic DNA incision, their mutations are thought to have relatively minor effects compared to other mutations in other residues with only ~6.7-fold and ~1.4-fold reduction in their DNA endonuclease activities and ~56-fold and ~9-fold reduction in RNA incision activities (as in Figure 10) for D70A and D308A, respectively. It can be speculated that the absence of one of these residues may be relieved by the other and the mutant APE1 would be able to retain its DNA endonuclease activity.

In molecular mapping through crystal structure, N68, E96, Y171, and D283 are hydrogen bonded to their neighboring residues and create an environment for abasic DNA incision to occur (Figure 11).

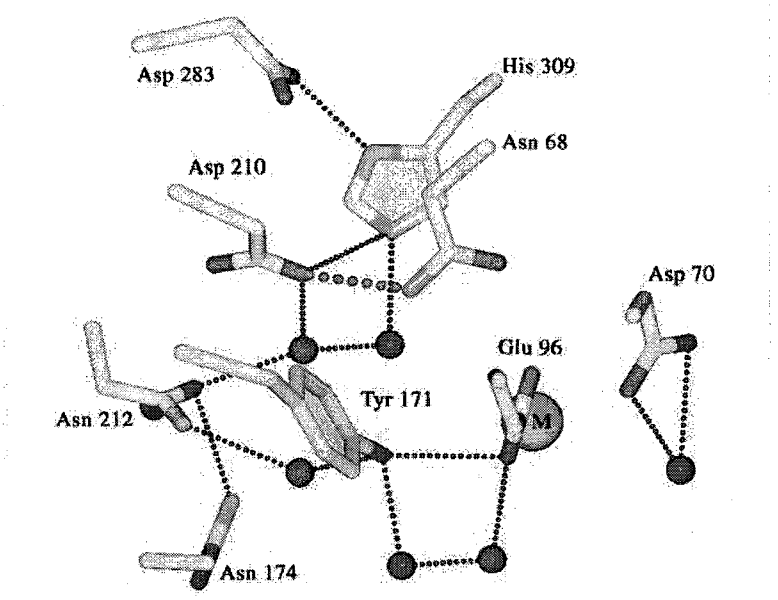

Figure 11: Molecular model of APE1 active site (Rothwell *et al.* 2000). Blue spheres represent water molecules and orange sphere represents the bound metal ion. The thick dotted line represents a hydrogen bond between Asp 210 and Asn 68. The thin dotted lines represent various hydrogen bonds between side chains of active site residues.

N68 is thought to hydrogen bond to D210 and H309, which supposedly creates a favorable environment for catalysis (Nguyen *et al.* 2000) and its mutation to alanine would logically be detrimental for RNA incision activity (Table 9). E96, originally considered to serve in the coordination of a metal ion (Beernink *et al.* 2001; Chou and Cheng 2003), is also thought to be critical in establishing the appropriate active site environment via a hydrogen-bonding network involving Y171 (Erzberger and Wilson 1999). The RNA cleaving activity of E96A has been found to be non detectable (Barnes *et al.* 2009) and a mutation of Y171F also gives reduction in RNA incision activity, confirming that the hydroxyl group on the phenyl ring is an important component in formation of hydrogen bonds to E96. One noteworthy observation is that D283N mutant exhibited RNA incision activity and this was a

significant contrast to what has been known about D283. Also, D283N showed to some degree of 3' exonuclease activity and indicated that this residue is not as critical as in RNA incision as in 3' exonuclease activity of APE1. Its role is to orient H309 through hydrogen bonding and act to stabilize its positive charge (Hadi *et al.* 2000), and the presence Oligo IB incision activity indicated that the significance of D283-H309 dyad in RNA cleavage is not so critical compared to cleaving abasic DNA. However, H309S mutant showed less RNA cleaving activity than D283, and this was more evident against c-myc 1705-1792 CRD RNA, which indicated that the role of H309 is more important than D283 in RNA catalysis. Similarly, a previous report from Dr. Lee's laboratory also showed a significant reduction in endoribonuclease activity with H309N, suggesting a critical role for H309 in RNA incision (Barnes *et al.* 2009). Its role in abasic DNA cleavage is also thought to be critical in aligning and polarizing the scissile bond linking the normal base and the abasic sugar (Rothwell *et al.* 2000), and our observation thus far also pointed to similar role in RNA incision activity.

Initially, the role of D210 was described as the proton donor of the incised leaving group (Erzberger and Wilson 1999). However, later it was proposed that the reaction mechanism for abasic DNA incision relied on an elevated pKa for D210 in that the carboxylate on side chain can be protonated to generate the nucleophilic hydroxyl group from a water molecule (Mol *et al.* 2000). Indeed, substitution of this residue strongly diminishes abasic DNA incision activity, while stabilizing the binding of APE1 to its substrates (Rothwell *et al.* 2000). In RNA incision, this trend was also observed (Figures 8 and 9), suggesting that an additional role of D210 may also be in the generation of the nucleophile. Residue F266 has been found to be a part of a hydrophobic pocket comprised of F266, W280 and L282 that accommodates abasic sugar moiety during the abasic DNA

incision (Mol *et al.* 2000, Hadi *et al.* 2002). In RNA incision, we observed significant reductions both on Oligo IB (Figure 10) and c-myc 1705-1792 CRD RNA (Figure 9), which suggested that F266 may serve a similar role in recognizing RNA bases. F266A showed greater reduction in RNA incision with its activity being not detectable compared to cleaving abasic DNA (30-fold reduction). This suggested that the alteration in this residue or the hydrophobic pocket were less tolerant for RNA catalysis than for abasic DNA. In addition, F266A mutant was shown to possess an enhanced DNA 3'-exonuclease activity compared to the WT on an array of DNA substrates (including single-stranded DNA, and duplex DNAs containing either a nick, single nucleotide gap, blunt end or 3′ flap) (Hadi *et al.* 2002) and this fact may account for the appearance of DNA 3'-exonucleolytic product in lane 7 (Figure 10). The difficulty for detecting 3' exonucleolytic products of F266A on abasic duplex DNA (lane 7; Figure 8A) may be due to its preference for 3' termini in the nicked structure or within a partial duplex DNA over fully complementary or blunt-ended DNA substrates with matched 3' ends (Hadi *et al.* 2002). Hence, F266A showed 3' exonuclease activity on a single stranded DNA-RNA hybrid (Oligo IB) that can form a dynamic hairpin structure, but this activity was not observable in an abasic DNA duplex.

2.2.3 Assessing the RNA-binding abilities of APE1 structural mutants

We tested the RNA-binding abilities of a few selected structural mutants using electrophoretic mobility shift assay (EMSA). Preliminary analysis showed that the WT (lanes 2 to 4) and E96A (lanes 6 to 8) both exhibited similar binding abilities to c-myc 1705-1886 CRD RNA, while H309N (lanes 10 to 12) showed lesser binding (Figure 12A). It also was found that N68A (lanes 6 to 8), Y171F (lanes 10 to 12), and D210N (lanes 14 to 16) displayed comparable binding abilities to that of the WT (lanes 2 to 4) to the same substrate

(Figure 12B). Interestingly, D283N at lower amounts (250 ng and 500 ng), showed lesser binding, but at higher amount (1000 ng), showed stronger binding compared to the WT (lanes 2 to 4) (Figure 12B).

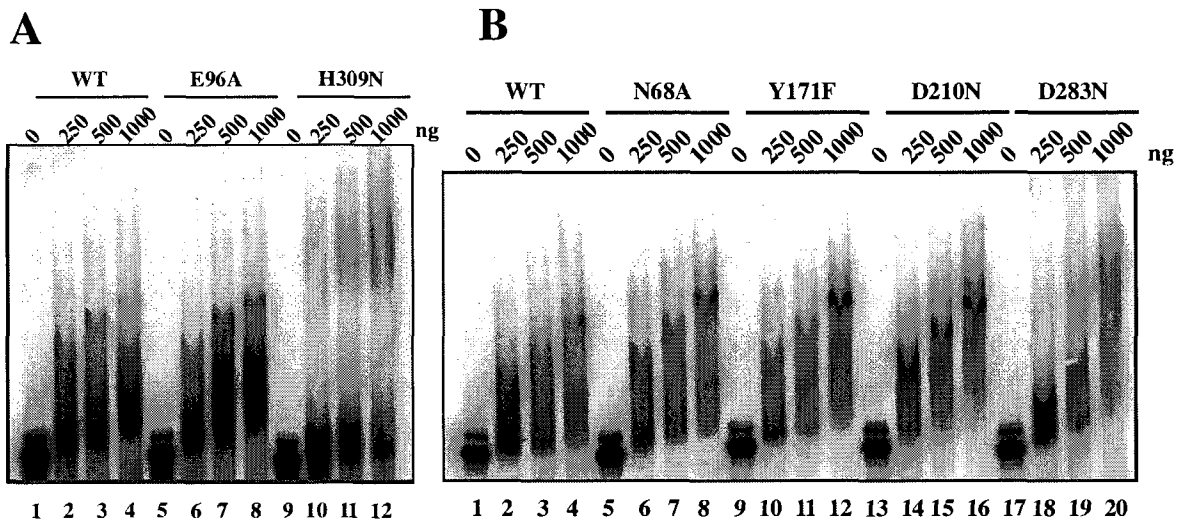

Figure 12: RNA-binding abilities of APE1 and its structural mutants on c-myc 1705-1886 CRD RNA. Increasing amount of APE1 or structural mutants were tested against 50 nM of ^{32}P-internally radiolabeled c-myc 1705-1886 CRD RNA in a total binding volume of 20 µl for 15 mins at 35°C in a standard electrophoretic mobility shift assay (EMSA). (**A**) EMSA gel showing APE1 WT (lanes 2 to 4), E96A (lanes 6 to 8), and H309N (lanes 10 to 12). (**B**) EMSA gel showing APE1 WT (lanes 2 to 4), N68A (lanes 6 to 8), Y171F (lanes 10 to 12), D210N (lanes 14 to 16), and D283N (lanes 18 to 20).

The role of some of these residues in RNA-binding may not be as critical as our results have shown. The discussion on specific residues and how they may or may not be involved in the RNA-binding as well as abasic DNA-binding are further discussed in section 5.4.

2.2.4 RNA incision activity of the population variants of APE1

When these selected population variants were tested on an abasic DNA, they displayed a similar reduction for all variants previously tested (Hadi *et al.* 2000), except for E126D (lane 7) which showed an activity close to that of the WT (Figure 13). The quantification of the appearance of product over a total density of substrate and product

showed that these variants possessed comparable DNA endonuclease activities relative to the WT (100%) as the following: Q51H (~101%), I64V (~103%), L104R (~74%), E126D (~102%), D148E (~101%), R237A (~0.1%), G241R (~101%), and G306A (~97%).

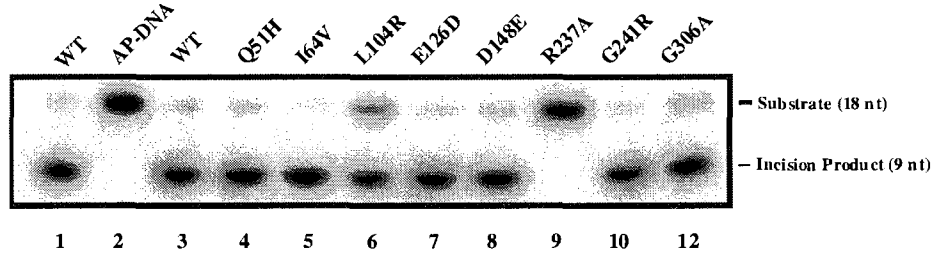

Figure 13: Abasic DNA endonuclease activity of population variants of APE1. **(A)** 0.14 nM of APE1 (lanes 2 to 10) was tested against 25 nM of 5'- γ-^{32}P-radiolabeled abasic DNA in a total reaction volume of 15 µl for 3 mins at 37°C.

It is possible that the increased cleavage activity observed in E126D may have been due to our increased amount of enzymes in the reaction condition (75 pg vs 2.5 pg) compared to the previous report (Hadi *et al.* 2000). Apart from this, we have discovered that Q51H and I64V showed similar activities as the WT, agreeing with the fact that these residues lie outside of the DNA endonuclease domain as viewed by X-ray crystallography (Mol *et al.* 2000). Overall, this assay verified that these population variants possessed abasic DNA endonuclease activities and could be tested against RNA substrates.

Table 10: Summary of abasic DNA and RNA incision activities of human population variants of APE1. ND indicates non-detectable level of activity. *The ratios of density of the products (5 nt & 6 nt) over those of the substrate plus product were measured using OptiQuant software (Hewlett Packard, Palo Alto, CA) to quantify activities

APE1 Proteins	Activity on Abasic DNA (%) (Hadi et al. 2000)	Activity on Abasic DNA (%) (Figure	Activity on CRD RNA (%) (Figure	Activity on Oligo IB (%) (Figure
WT	100	100	100	100
Q51H	Not Tested	101	23.1	12.5
I64V	Not Tested	103	15.6	Abolished
L104R	56.71 ± 26.80	74	60.0	0.9
E126D	60.43 ± 11.16	102	41.4	8.0
D148E	94.36 ± 6.20	101	23.3	6.8
R237A	35.71 ± 9.68	0.1	6.0	Abolished
G241R	108.73 ± 5.31	101	24.3	12.2
G306A	107.22 ± 17.13	97	20.4	5.5

In endoribonuclease assay against c-myc-1705-1792 CRD RNA as the substrate, we found that L104R (lane 5 in Figure 14) and E126D (lane 6 in Figure 14) retained RNA incision activity (~60% and ~40%, respectively), but their cleavage sites were altered. In contrast to the report on abasic DNA incision (Hadi *et al.* 2000), we found D148E (lane 7), R237A (lane 8), G241R (lane 9), and G306A (lane 10) to have reduced RNA cleaving activity (Table 10). This was also confirmed with Oligo IB RNA in lanes 6 to 9 after quantification of the activities that were reduced down to ~5.5%-12% compared to the WT (Figure 15 and Table 10). These results showed that these variants have reduced RNA incision activity and warrants further investigation on their role in human diseases like cancer and ALS (Hadi *et al.* 2002).

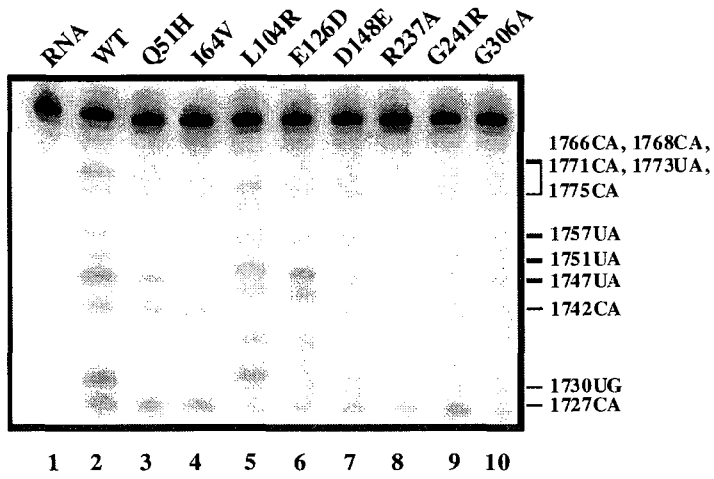

Figure 14: Endoribonuclease activity of human population variants APE1 on c-myc-1705-1792 CRD RNA. (A) 1.4μM of APE1 (lanes 2 to 10) were tested against 25 nM of 5'-γ-^{32}P-radiolabeled c-myc-1705-1792 CRD RNA in a total reaction volume of 20 μl for 25 mins at 37°C.

For the first time, we discovered that the activities of Q51H and I64V were also notably reduced (~23% and ~15.6%, respectively) against c-myc RNA (lane 3 and 4, Figure 14) especially those sites of 1730 UG, 1747UA, 1751UA, 1757UA, and 1773 UA, but not 1727 CA, 1742 CA, 1766 CA, 1768 CA, 1771 CA, and 1775 CA sites. The reduction of RNA incision activity at specific region was confirmed through testing the variants on Oligo IB RNA designed to mimic the c-myc CRD region of 1741-1757 which also provides an analogous site of cleavage for APE1 at 1747 UA site. Indeed, the RNA incision activities of Q51H and I64V were reduced down to ~0-13% (Table 10). The reason behind such reduction for specific dinucleotides sequence is unknown and warrants further investigation on identifying regions of APE1 that give cleavage specificity. Nonetheless, this showed that Q51H and I64V have reduced RNA incision activity and warranted further characterization of their properties.

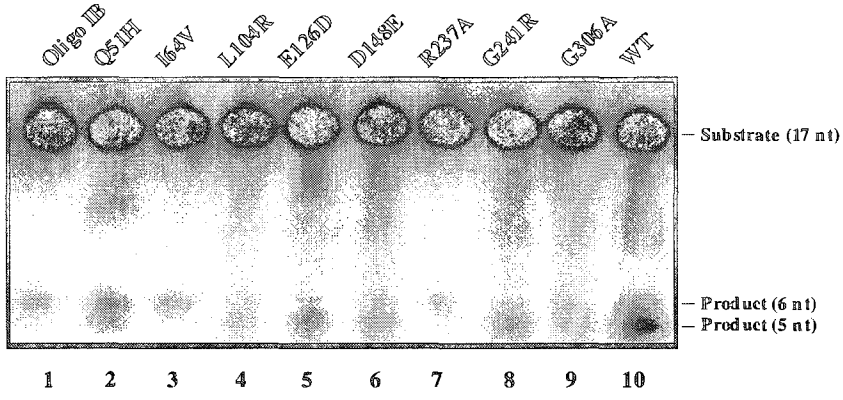

Figure 15: Endoribonuclease activity of human population variants of APE1 on Oligo IB RNA. 1.4 μM of APE1 (lanes 2 to 10) were tested against 25 nM of 5'- γ-^{32}P-radiolabeled Oligo IB RNA in a total reaction volume of 20 μl for 25 mins at 37°C.

In addition, we have mapped the altered cleavage sites of L104R and E126D on a sequencing gel (Figure 16). For reference, an alkaline hydrolysis ladder was generated as shown (lane 1). Numbering on the left indicates guanosine residue sites cleaved by RNase T1 under denaturing conditions (lane 3), whereas numbering on the right indicates the sites cleaved by APE1 WT (lane 4) and its variants (lanes 5 and 6). It was determined that L104R produced cleavages at 1727 CA, 1731 GA, 1742 CA, 1747 UA, 1749 GU, 1751 UA, 1768 CA, 1770 GC, 1771 CA, 1773 UA, 1775 CA. It is noteworthy that L104R was capable of cleaving after guanine bases (1731 GA, 1749 GU, and 1770 GC). For E126D, the cleavage pattern was suggestive of exoribonucleolytic decays occurring at regions of 1715-1734, 1741-1751, and 1758-1775. Notably, E126D variant was capable of prominently cleaving 1731 GA, 1748 AG, and 1749 GU. Such observation suggested that these residues are not only important in giving endonuclease activity (abasic DNA and RNA incision), but also in giving the specificity of cleavage of APE1.

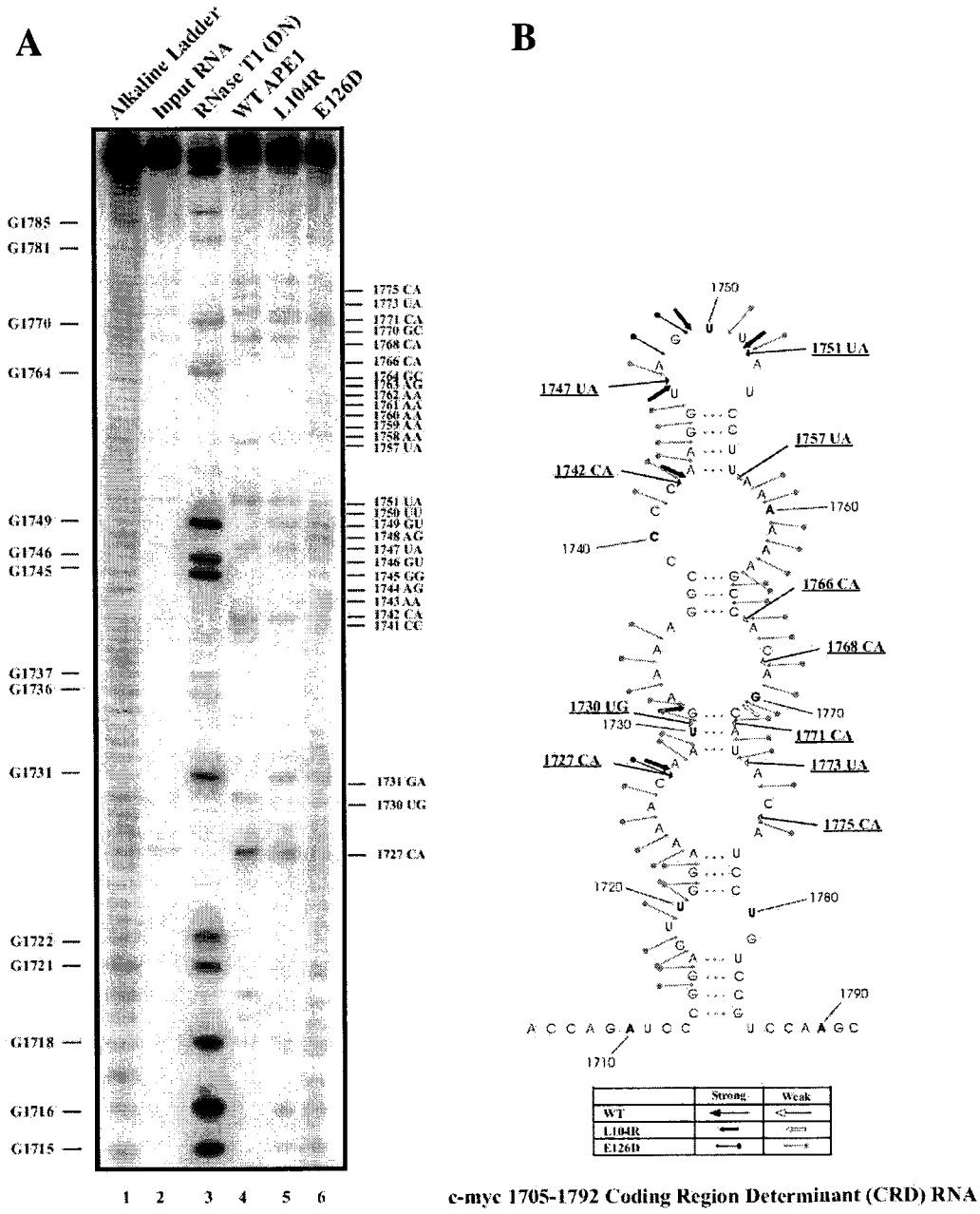

Figure 16: Mapping of the cleavage sites generated by L104R and E126D variants of APE1. **(A)** 1.4 μM of APE1 WT, L104R, and E126D variants (lanes 4 to 6) were tested against 25 nM of 5'- γ-^{32}P-radiolabeled c-myc-1705-1792 CRD RNA in a total reaction volume of 20 μl for 25 mins at 37°C. The products were resolved on a 12% polyacrylamide gel as described in section 3.1.2. **(B)** Secondary structure of c-myc 1705-1792 CRD RNA and the positions of cleavage sites for WT, L104R, and E126D.

2.2.5 Assessing the RNA binding abilities of APE1 population variants

We tested APE1 population variants in an electrophoretic mobility shift assay (EMSA) on c-myc 1705-1886 CRD RNA. It was found that the WT and the six population variants all exhibited similar binding abilities (Figure 17). L104R (lanes 6 to 8, Figure 17A) and E126D (lanes 10 to 12, Figure 17A) were expected to bind to RNA since they showed RNA-cleaving activities in previous experiments (Figures 14 to 16). Comparable binding abilities of D148E (lanes 14 to 16, Figure 17A), R237A (lanes 14 to 16, Figure 17B), G241R (lanes 10 to 12, Figure 17B), and G306A (lanes 6 to 8, Figure 17B) to that of the WT (lanes 2 to 4, Figure 17A-B) indicated that these residues likely affect the catalytic step of RNA incision and not the RNA-binding process.

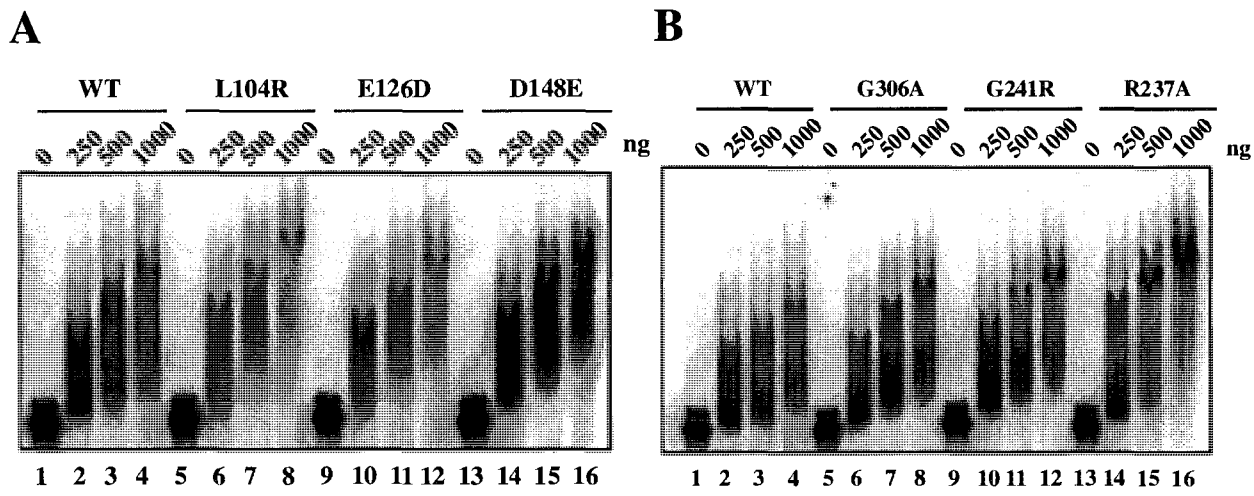

Figure 17: RNA-binding abilities of APE1 and its population variants on c-myc 1705-1886 CRD RNA. Increasing amount of APE1 and its population variants were tested against 50 nM of ^{32}P-internally radiolabeled c-myc 1705-1886 CRD RNA in a total binding volume of 20 µl for 15 mins at 35°C in a standard electrophoretic mobility shift assay (EMSA). (**A**) EMSA gel showing APE1 WT (lanes 2 to 4) and L104R (lanes 6 to 8), E126D (lanes 10 to 12), and D148E (lanes 14 to 16). (**B**) EMSA gel showing APE1 WT (lanes 2 to 4), G306A (lanes 6 to 8), G241R (lanes 10 to 12), R237A (lanes 14 to 16).

Intriguingly, L104R and E126D appeared to retain RNA-cleaving activities despite in the presence of RNasin in the EMSA binding reaction. This was visualized by lighter intensities of APE1-RNA complex (lanes 6-8, 10-12) compared to the WT (lanes 2 to 4) and D148E (lanes 14 to 16) (Figure 17A). Also, the appearance of RNA incision products from L104R (lanes 6 to 8) and E126D (lanes 10 to 12) were clearly visible below the APE1-RNA complex in the same EMSA gel (Figure 18). Hence, in the binding reaction, the digestion of RNA took place for L104R and E126D, and we could observe the APE1-RNA complex shifting, but at the same time, we could also visualize the presence of decay products. Therefore, our results have revealed not only an alteration in the cleavage pattern of these variants (Figure 16), but also a potentially novel RNasin-resistant activity (Figure 18). Future studies should confirm the existence of this activity and characterize the difference in the strengths of L104R and E126D compared to the WT and other mutants in the presence of RNasin. If this novel activity is found to be truly originating from L104R and E126D, the biological impact of their RNasin-resistant activities should also be assessed.

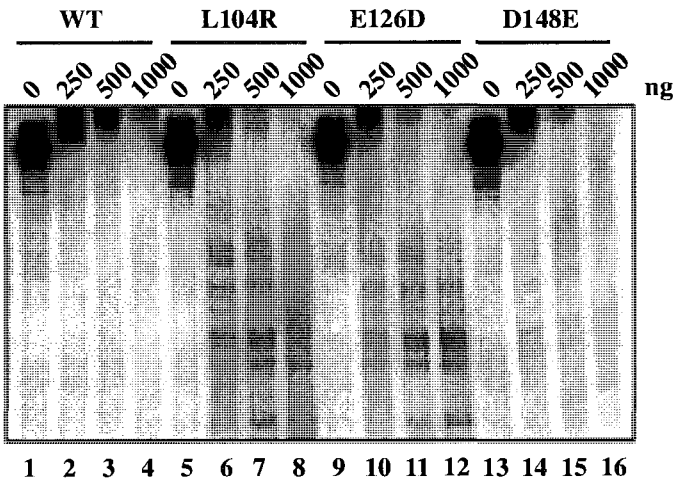

Figure 18: RNasin-resistant activity of L104R and E126D on c-myc 1705-1886 CRD RNA. From the same EMSA gel in Figure 17A, RNA cleavage products were more visible in samples treated with L104R (lanes 6 to 8) and E126D (lanes 10 to 12) than those treated with the WT (lanes 2 to 4) and D148E (lanes 14 to 16).

2.2.6 Possible mechanism of RNA incision by APE1

To further understand the RNA cleavage mechanism of APE1, we first tested to see whether APE1 generated RNA products with a 3'phosphate or a 3'hydroxyl group (Figure 19). This was done using the ability of snake venom exonuclease that digests only the products bearing 3'hydroxyl group (Chernokalskaya *et al.* 1997). The distinct product generated by RNase T1 (asterisk in lane 2) remained visible after digestion with exonuclease (lane 3). This is consistent with fact that RNase T1 generates products with 3'phosphates. In contrast, S1 nuclease generated decay products (marked with asterisks in lane 5) were completely degraded upon treatment with the exonuclease (lane 6). This is consistent with the notion that S1 nuclease generates products with 3'hydroxyls. Fig. 16 shows that the distinct decay products generated by APE1 (marked with asterisks in lane 9) were still visible upon treatment with the exonuclease (lane 8). However, we also observed the disappearance of products in the range of 1766 to 1775 after treatment with the exonuclease (Lane 8), raising the possibility that perhaps these bands were produced by the 3'-5' exonuclease activity of APE1. What mechanism by which these products were generated is up for speculation and will require further experimentation. At the least, however, we found that APE1 can generate endoribonucleolytic products with 3'phosphates.

Determining the 3'end of RNA products generated by APE1 provides insights into the role of APE1 in mRNA metabolism. APE1 produces those RNA products with 3' phosphates and 5' hydroxyls (Figure 19), and such products are expected to be less efficient for clearance by 3'-5' exosome (Chernokalskaya *et al.* 1997). Nevertheless, APE1 activity may still be a part of mRNA decay machinery. APE1 generated products can be further degraded by any one or combinations of the following paths. Activity of exosome itself

which possesses both endoribonucleolytic and exonucleolytic activities can clear these transcripts despite at a reduced rate for 3' phosphate bearing single stranded RNAs (Schaeffer *et al.* 2009). XRN1, a 5'-3' exoribonuclease, can degrade these RNAs from their 5' ends after decapping takes place (Garneau *et al.* 2007).

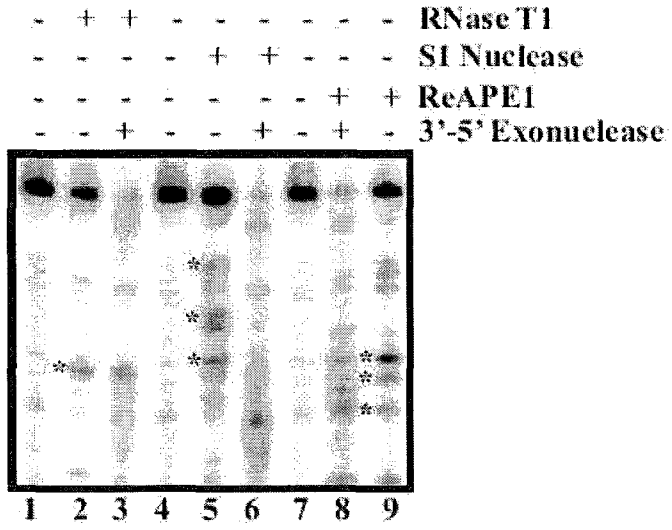

Figure 19: APE1 generates RNA products with 3'phosphates. 25 nM 5'-labeled c-*myc* CRD RNA was digested with 1 U RNase T1 (lanes 2 and 3) for 1 min at 37°C, or with 10 U S1 nuclease (lanes 5 and 6) or 8.5 μM purified APE1 (lanes 8 and 9) for 5 min at 37°C under the standard endonuclease assay. The products were then incubated with 3 x 10^{-5} U snake venom exonuclease for 10 min at 25°C (lanes 3, 6, and 8), and electrophoresed on a 8% polyacrylamide/urea gel. Asterisks indicate the decay of products generated by RNase T1 (lane 2), S1 nuclease (lane 5), or ReAPE1 (lane 9).

Since APE1 is ubiquitously expressed and its localization reported to differ perhaps due to its ability to serve multiple functions in different cell types (Duguid *et al.* 1995), its RNA cleaving activity has the potential to play an important role in mRNA decay. On the other hand, RNA-cleaving activity of APE1 may also have biological significance during mRNA processing. This speculation is in line with the finding that APE1 serves as a nuclear enzyme. Also, APE1 has been found to interact with a global regulator of mRNA splicing,

hetergenous nuclear ribonucleoprotein L (hnRNP L) which associates with transcribed RNAs in the nucleus (Kuninger *et al.* 2002).

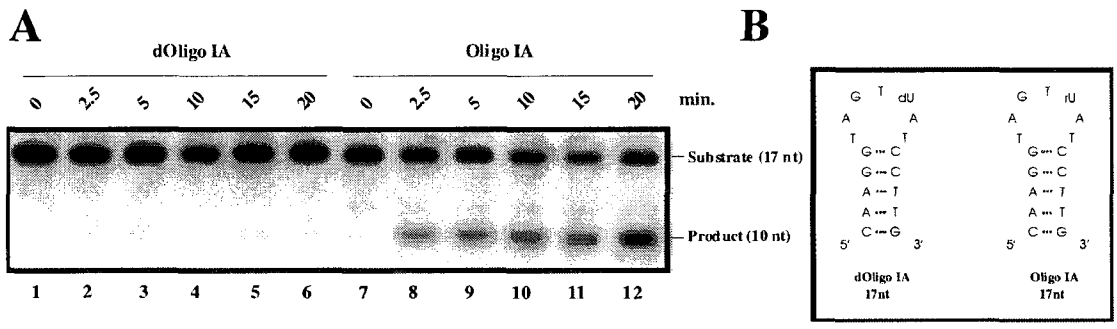

Figure 20: RNA incision activity of APE1 requires 2'-OH on the sugar moiety. (**A**) 1.4 μM of APE1 were tested against 25 nM of 5'- γ-^{32}P-radiolabeled dOligo IA (lanes 1-6) or Oligo IA (lanes 7-12) RNA in a total reaction volume of 20 μl for varying time points at 37°C. (**B**) Secondary structure of dOligo IA and Oligo IA predicted through Mfold.

In understanding APE1 mechanism of catalysis, producing an RNA product with 3' phosphate end is different from a typical abasic DNA cleavage product with a 3' hydroxyl group (Doetsch and Cunningham 1990; Demple and Harrison 1994; Friedberg *et al.* 1995). The active site residues in APE1 abasic DNA cleavage could be involved differently in RNA cleaving, perhaps providing an environment that promotes a general acid-base RNA catalysis that utilizes 2'-OH group on the sugar moiety as exemplified by RNase A (Raines 1998). If this were not the case, residues involved in abasic DNA cleavage may still be able to generate a hydroxyl nucleophile from a water molecule. Next, this nucleophile can attack the phosphodiester bond from the side opposite to where it is proposed to attack during the abasic DNA cleavage, generating an O5' leaving group and a final product with 3' phosphate.

To test whether 2'-OH group is important in RNA catalysis of APE1, APE1 was tested on a modified form of Oligo IA, which has a deoxyribose sugar at base position 10

(Table 4, Figure 20). APE1 can not cleave the dUA bond in dOligo IA (lanes 2-6) whereas the rUA bond in Oligo IA was cleaved over time (lanes 8-12). This result suggested that indeed during APE1 RNA cleavage, 2'-OH is essentially involved in the catalysis, and that APE1 utilizes residues from the active site, and not H_2O molecules to carry out the catalysis.

2.2.7 The effect of divalent metal ions in APE1 RNA catalysis

The abasic DNA incision activity of APE1 has been shown to be divalent metal ion dependent (Masuda *et al.* 1998; Erzberger and Wilson 1999; Beernink *et al.* 2001; Oezguen *et al.* 2007). We therefore determined the effect of divalent metal ions on RNA cleavage by APE1. For the purpose of the following experiments, protein samples were denatured and refolded in metal ion-free buffer, as described in section 2.1.10, to ensure complete removal of metal ions. Figure 21 shows that APE1 has the ability to cleave c-*myc* RNA in the absence of added divalent metal ions (lanes 1-3). In the assumption that the denaturation/refolding step had successfully removed all of the divalent metal ions from the APE1 buffer, this result helped us to conclude that APE1 is able to cleave RNA without the presence of divalent metal ions. APE1 exhibited activity in the presence of Mg^{2+} (lanes 4-5), Ca^{2+} (lanes 6-7), and Mn^{2+} (lanes 12-13). In contrast, at 2 mM, Zn^{2+} (lanes 8-9), Ni^{2+} (lanes 10-11), Cu^{2+} (lanes 14-15), and Co^{2+} (lanes 16-17), all had inhibitory effect on RNA-cleaving activity of APE1. As in DNA cleavage reactions, RNA cleaving activity of APE1 is present and/or enhanced by the addition of metal ions, particularly Mg^{2+}. Whether the presence of metal ion enhances the affinity of APE1 to abasic DNA or RNA is currently unkown and this question needs to be further explored. However, our observation is in line with reports on APE1 requiring Mg^{2+} concentration of around 0.1mM-0.5mM for its 3'-5' DNA exonuclease activity and 2 mM-10 mM for its abasic DNA incision activity (Chou and Cheng 2003; Wilson 2005). APE1 has

also been shown to exert EDTA-resistant activity towards (Erzberger and Wilson 1999) acyclic DNA substrates that are considered to have better flexibility than abasic DNA and even shown a weak incision activity for a regular abasic DNA in the presence of EDTA (Masuda *et al.* 1998).

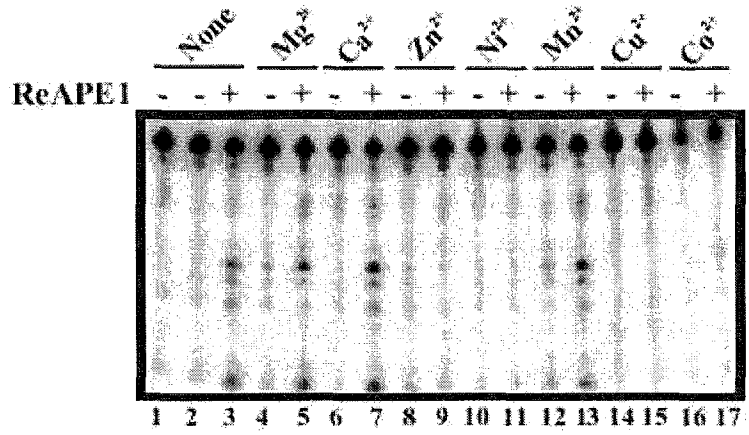

Figure 21: Effect of divalent metal ions on RNA-cleaving activity of APE1. 12.5 nM of 5'-labeled c-myc-1705-1792 CRD RNA were treated with purified APE1 for 5 min at 37°C in the presence (lanes 4-17) or absence (lanes 1-3) of 2 mM various divalent metal ions as indicated under the standard endoribonuclease assay. Samples were run on 8% polyarylamide/7 M urea gel. The background reaction buffere contained (10 mM Tris-Cl pH 8 and 2 mM DTT).

Single stranded RNA structures that form secondary structures (e.g. hairpin loops) are particularly more flexible than duplex RNAs or abasic duplex DNAs, which may explain the RNA cleaving activity observed even at 0 mM Mg^{2+} (lane 1 and 2). The effect of Mg^{2+} was further assessed by testing a range of concentrations (0 mM - 200 mM) (Figure 22). Lane 2 shows that APE1 has the ability to cleave RNA at 0 mM Mg^{2+} and at 5 mM (lane 4), APE1 showed the most activity in cleaving RNA. The increasing amount of Mg^{2+} gradually decreased the activity of APE1 where at 100 mM and 200 mM the activity was clearly inhibited (lanes 8 and 9). Interestingly, we also observed a change in cleavage pattern at 20

mM and 50 mM concentrations (lanes 6 and 7), suggesting metal ions may either alter the RNA secondary structure or the RNA binding affinity of APE1. This was clarified later by EMSA experiment using WT APE1 against c-myc-1705-1886 CRD RNA under increasing concentrations of Mg^{2+} (Figure 22B). This showed that the binding affinity of APE1 was not dramatically altered by the increasing divalent metal ion. Hence, our results indicated that the likely reason behind altered cleavage pattern is due to the alterations in RNA secondary structure.

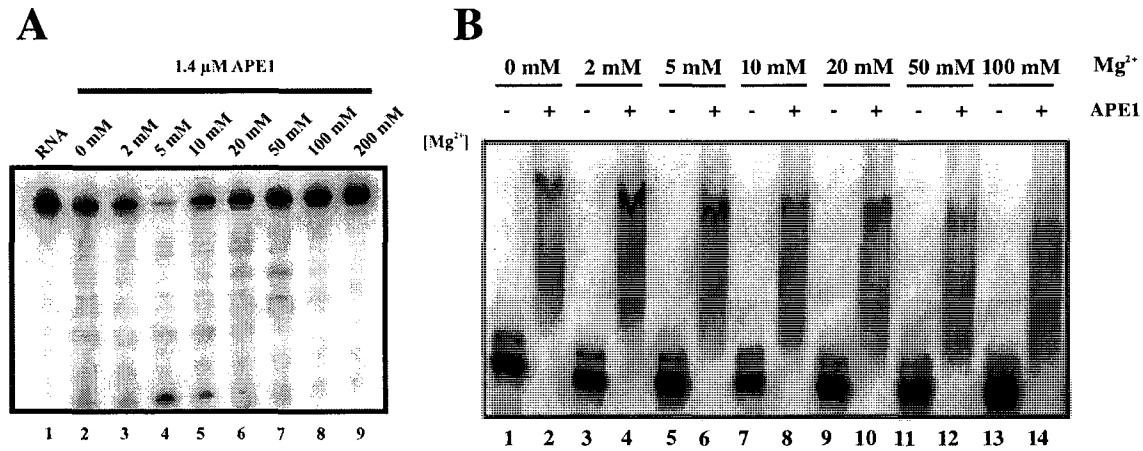

Figure 22: Differing concentrations of magnesium in the reaction mixture affects the specificity and the incision activity of APE1. **(A)** 1.4 μM of APE1 (lanes 2 - 9) were tested against 25 nM of 5'- γ-^{32}P-radiolabeled c-myc-1705-1792 CRD RNA in a total reaction volume of 20 μl for 25 mins at 37°C. Each lane contains differing magnesium concentration as indicated. **(B)** APE1 WT was tested against 50 nM of ^{32}P-internally radiolabeled c-myc 1705-1886 CRD RNA in a total binding volume of 20 μl for 15 mins at 35°C in a standard electrophoretic mobility shift assay (EMSA) under increasing concentrations of Mg^{2+}.

2.2.8 The effect of RNase inhibitors on APE1 activity

A set of experiments showed that APE1 RNA cleaving activity can be inhibited by the treatments of typical RNase inhibitors: Diethyl pyrocarbonate (DEPC) and Ribonuclease Inhibitor (RNasin). It is thought that DEPC is an effective inhibitor that reacts with enzymes containing -NH, -SH, or -OH groups in their active sites. Hence, APE1 that has active site residues consisting of Asp, Glu, His, and Asn will likely be inhibited when DEPC reacts with

any of these groups. Indeed, titration of DEPC showed that at 1.43 mM of DEPC was enough to clearly inhibit the activity of APE1 (Figure 23A). Electrostatic forces between ribonuclease and RNasin are known to allow their binding and sterically hinder substrate-ribonuclease interaction (Kobe and Deisenhofer 1996). This may also be the case with APE1. It was found that 1 unit of RNasin was able to inhibit 84 nM of APE1 activity (Figure 23B), which suggested that RNasin may also interact with APE1 and sterically prevent RNA substrate from interacting with residues of the active site.

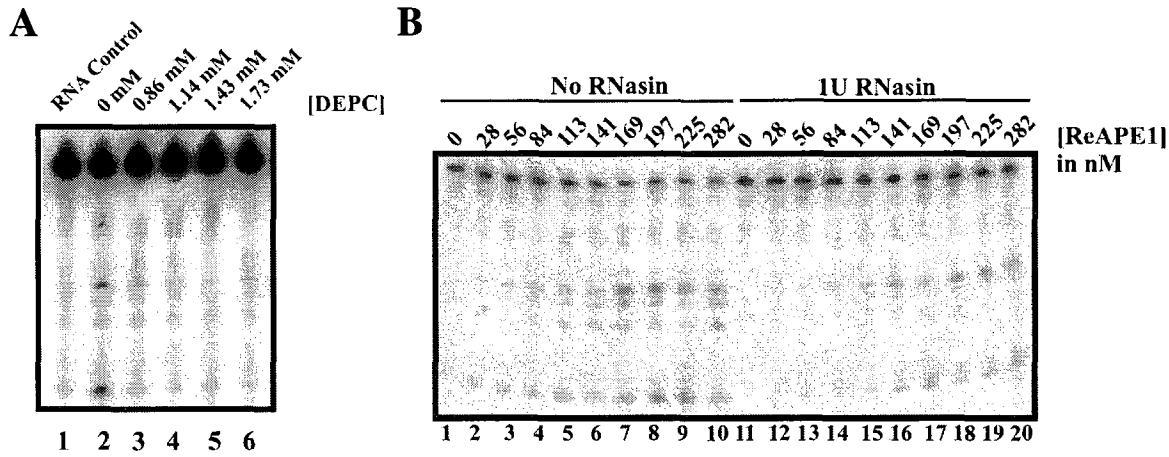

Figure 23: RNA incision activity of APE1 is inhibited by DEPC and RNase Inhibitor (RNasin). **(A)** 0.2 μM of APE1 (lanes 2 - 6) were tested against 12.5 nM of 5'- γ-^{32}P-radiolabeled c-myc-1705-1792 CRD RNA in the presence of increasing concentration of DEPC dissolved in 0.1% ethanol. **(B)** Specified concentration of APE1 was tested in the absence or presence of 1 unit of RNasin against 12.5 nM of substrate RNA.

Future studies can focus on revealing whether this inhibition of RNA cleaving activity is due to the alterations in RNA binding or in incison step. Testing of APE1 binding to the RNA substrate in the presence of DEPC or RNasin may give clearer distinction between the inhibitions via alteration of binding or incision activity of APE1.

CHAPTER 3

Establishing the RNA structure and sequence cleaved by APE1

This chapter presents the methods and discusses the results of the experiments used to determine the RNA structure and sequences that are preferentially cleaved by APE1. The purified recombinant human APE1 has thus far been tested only against c-*myc* CRD RNA (Barnes *et al.* 2009). To determine if APE1 can also cleave other RNAs, to further confirm the sequence and structural cleavage specificity of APE1, and to initiate studies into future possible use of the enzyme as an anti-viral and anti-cancer agent, we challenged APE1 with three RNA components, Spike, Orf1b and Orf3 RNAs, which are derived from proteins important for the life cycle of the SARS-corona virus (Tan *et al.* 2005) and two miRNA substrates, miR-10b and miR-21 which are known to be associated with cancer (Ma and Weinberg 2008; Gramantieri *et al.* 2008). Spike or S protein mediates binding of the virus to host receptors and in membrane fusion (Tan *et al.* 2005). Orf1b is one of the replicases essential for replication of the virus, and Orf3 is a protein with endocytotic properties and which does not have homology to other coronaviruses and is expressed during SARS-CoV infection (Tan *et al.* 2005).

Sequences of human-pri-miR-10b (pri-miR-10b) and human-pri-miR-21 (pri-miR-21) were also tested. Notably, miR-10b has been reported to be associated with metastasis of breast tumors (Ma *et al.* 2007), of which its expression has been thought to be induced after the activation of an oncogenic transcription factor, twist. Similarly, miR-21 has been reported to reduce the expression of a tumor suppressor and increases the abilities for cellular invasion (Asangani *et al.* 2007). In addition, over expression of miR-21 has been reported in

various cancer samples including, cholangiocarcinoma (Selaru *et al.* 2009), esophageal squamous cell carcinoma (Hiyoshi *et al.* 2009), breast carcinoma (Qian *et al.* 2008; Yan *et al.* 2008), hepatocarcinoma, (Connolly *et al.* 2008), and cervical cancer (Lui *et al.* 2007).

3.1 Methodology

3.1.1 Plasmid linearization and PCR generation of linear templates

To prepare linear DNA templates for *in vitro* generation of RNA substrates, the pUC19 plasmids containing cDNAs of Spike, Orf1b, and Orf3 were all linearized. The sequences of these cDNAs are shown in Table 11. These plasmids also contained T7 promoter on the 5' side of cDNA sequences. These plasmids were linearized with the restriction enzyme *EcoRI* (Invitrogen). A 35 µl digestion reaction contained 2 to 8 µg of plasmid, 10 µl of *EcoRI* (10 U/µl), 1x reaction buffer (ReACT 3 from Invitrogen), and made up to volume with autoclaved water. The digestion was done at 37 °C for 3 hrs in a water bath. After digestion, 1 µl of linearized samples and 1 µl of original plasmids as well as 1 µl of 1 kb DNA ladder (Invitrogen) were loaded onto 1% agarose (Invitrogen) gel to check for completion of the reaction. To prepare the gel, 0.5 g of agarose was added to a 50 ml of 0.5x TBE buffer (Table 3) and heated by microwave to completely dissolve the residues. The gel mix was cooled and 15 µl of 10 mg/ml ethidium bromide was added to the mix before casting on the gel apparatus.

Table 11: List of RNA substrates generated and their cDNA sequences from plasmid

RNA Substrate	cDNA Sequence
Spike	5'-CTAAACGAACATGTTTATTTTCTTATTATTTCTTACT CTCACTAGTGGTAGTGACCTTGACCGGTGCA-3'
Orf1b	5'-AGGATGTAAACTGACATAGCTCGCGTCTCAGTTTCA AGGAACTTTTAGTGTATGCTGCTGATCCAGCTAT-3'
Orf3	5'-CGAACTTATGGATTTGTTTATGAGATTTTTTACTCT TAGATCAATTACTGCACAGCCAGTAAAAATTGACAATG CTTCTC-3'
hsa-miR-10b	5'-CCAGAGGTTGTAACGTTGTCTATATATACCCTGT AGAACCGAATTTGTGTGGTATCCGTATAGTCACAGATT CGATTCTAGGGGAATATATGGTCGATGCAAAAACTT CA-3'
hsa-miR-21	5'-TGTCGGGTAGCTTATCAGACTGATGTTGACTGTT GAATCTCATGGCAACACCAGTCGATGGGCTGTCTGA CA-3'
5'-GG-pre-miR-10b	5'-TACCCTGTAGAACCGAATTTGTGTGGTATCCGTA TAGTCACAGATTCGATTCTAGGGGAAT-3'
5'-GG-pre-miR-21	5'-TAGCTTATCAGACTGATGTTGACTGTTGAATCTC ATGGCAACACCAGTCGATGGGCTGT-3'

The gel ran for 1.5 hour at 85 V in 0.5x TBE buffer and visualized under UV-transillumination using ChemiImager™ System (Alpha Innotech Corporation, San Leandro, CA). Next, 2 µl of Proteinase K (20mg/ml, Roche Diagnostics Inc, Mannheim, Germany) were added into each linearized samples and incubated at 37 °C for 30 mins. The reaction mixtures were made up to 200 µl with autoclaved water for standard phenol/chloroform extraction and ethanol precipitation. For miR substrates, hsa-miR-10b, hsa-miR-21, 5'-GG-pre-miR-10b and 5'-GG-pre-miR-21, pMIF-cGFP-Zeo-hsa-miR-10b (System Biosciences, Mountain View, CA) and pSIF-Neo-Ires-GFP-hsa-miR-21 (gift from Dr. Yong Li, University of Louisville) were used to generate linear cDNA templates by PCR that included the T7 promoter and the miR cDNA sequence. The sequences of the primer used are shown in Table 12.

Table 12: List of primers and their sequences used in the generation of cDNA templates by PCR for *in-vitro* RNA transcription.

cDNA Template	Sequence
hsa-miR-10b Forward	5'-GGATCCTAATACGACTCACTATAG GCCAGAGGTTGTAACGTTG-3'
hsa-miR-10b Reverse	5'-TGAAGTTTTTGCATCGAC-3'
hsa-miR-21 Forward	5'-GGATCCTAATACGACTCACTATAG GTGTCGGGTAGCTTATCA-3'
hsa-miR-21 Reverse	5'-TGTCAGACAGCCCATCGA-3'
5'-GG-pre-miR10b Forward	5'-GGATCCTAATACGACTCACTATAG GTACCCTGTAGAACCGAAT-3'
5'-GG-pre-miR10b Reverse	5'-ATTCCCCTAGAATCGAAT-3'
5'-GG-pre-miR21 Forward	5'-GGATCCTAATACGACTCACTATAG GTAGCTTATCAGACTGATG-3'
5'-GG-pre-miR21 Reverse	5'-ACAGCCCATCGACTGGTG-3'

3.1.2 Utilization of enzyme probes for secondary structure determination

The 5'-radiolabeled RNA transcript (50,000 c.p.m.) was partially digested with RNase T1 (Roche Diagnostics Inc, Mannheim, Germany) which cleaves 3' to single-stranded guanosines, RNase T2 (Invitrogen Life Technologies, Carlsbad, CA) which preferentially cleaves 3' to single-stranded adenosines, but also 3' to the other three nucleotides, RNase A (Ambion, Inc., Austin, Texas) which cleaves 3' to single-stranded uridines and cytidines, and RNase V1 (Ambion, Inc., Austin, Texas) which cleaves 3' to paired nucleotides or stacked bases (Ehresmann *et al.* 1987).

i) <u>Alkali digestion</u>

A partial alkaline digestion of the 5'-radiolabeled transcript was carried out to generate an RNA ladder used to identify the cleavage sites. A typical reaction mixture of 10 µl included 5'-radiolabeled transcript (100,000 c.p.m.), 1 µl of 10x Alkali buffer, and DEPC treated water. The reaction was carried out at 95 °C for 3 mins, iced for 1 min, followed by the addition of 5 µl Stopping Dye. Subsequently, 3 µl of the stopped mixture was loaded onto

a 12% polyacrylamide (29:1, acrylamide : N,N'= metheylenebisacrylamide) gel containing 7M urea (Invitrogen).

For the following enzymatic reactions, the 5'-radiolabeled transcripts were initially denatured at 55 °C for 5 mins and re-natured at 4 °C for 5 mins in their respective enzymatic buffers in the absence of their RNases. This procedure had ensured that all RNAs were correctly folded into their native secondary structures.

ii) <u>RNase T1</u>

RNase T1 digestion was carried out under RNA native and denaturing conditions in order to confirm the strandedness of the guanosine residues. Denaturing condition was applied by setting up a reaction mixture of 10 µl including 50,000 c.p.m. radiolabeled transcript, 3 U of RNase T1, 1x sequencing buffer (Ambion, Inc., Austin, Texas) consisting of 20 mM sodium citrate pH 5, 7 M Urea, and 1mM EDTA, and DEPC treated water. The reaction was carried out under room temperature for 5 mins and stopped by adding 20 µl of the Stopping Dye. Subsequently, 6 µl of the stopped mixture was loaded onto the 12% polyacrylamide gel described above. Under native conditions, a total reaction volume of 10 µl included 50,000 c.p.m. radiolabeled transcript, 3 U of RNase T1, 2.5 mM Tris-HCl pH 7.2, 2.5 mM $MgCl_2$, 25 mM KCl, and DEPC treated water. The reaction was carried out under room temperature for 5 mins and stopped by adding 20 µl of the Stopping Dye (Table 3). Subsequently, 6 µl of the stopped mixture was loaded onto the 12% polyacrylamide gel described above.

ii) <u>RNases T2, V1, A</u>

For RNase T2, RNase V1, and RNase A digestions, reaction mixtures of 10 µl was set up that included 50,000 c.p.m. radiolabeled transcript, one of the RNases (1U of RNase

T2, 1 mU of RNase V1, 0.2 ng of RNase A), 1x structure buffer consisting of 10 mM Tris pH 7, 100 mM KCl, 10 mM $MgCl_2$ (Ambion, Inc., Austin, Texas), and DEPC treated water. The mixtures were incubated under room temperature for 5 mins and stopped by adding 20 µl of the Stopping Dye (Table 3). Subsequently, 6 µl of the stopped mixture was loaded onto the 12% polyacrylamide gel described above. For checking the RNA integrity, undigested transcripts were also loaded and ran on the polyacrylamide gel.

iii) Separation by PAGE

The polyacrylamide gel was ran at 20 mA with 0.5x TBE buffer (0.45 M Tris-HCl/Boric acid (Sigma), 0.01 M EDTA pH 8.3 for 45 mins initially, followed by the loading of another batch of the same stopped reaction mixtures to empty wells and ran under the same condition for another 1 hour to resolve the cleavage sites near the 5' end. The gel was transferred to a filter paper and dried on a gel dryer (LABCONO, Kansas City, MO) for 45 mins at 80 °C and exposed overnight to a Cyclone Storage Phosphor Screen System (Packard, Meriden, CT). On the following day, the gel image was developed using Cyclone PhosphorImager and visualized by the OptiQuant software (Hewlett Packard, Palo Alto, CA).

3.1.3 *In vitro* effects of APE1 RNase activity on DICER product formation

APE1/DICER reaction

The reaction was carried out in two steps. First, a 10µl reaction mix containing 1 µM of recombinant APE1 and 25 nM of 5'-^{32}P-labeled *in vitro* transcribed pre-miRNA analog (50,000 c.p.m/µl) in 8.8 mM Tris-HCl pH 7.4 and 2 mM magnesium acetate was incubated at 37°C for 30 mins. Recombinant APE1 purified and prepared in 20 mM Tris-HCl pH 8, 300 mM NaCl, 1 mM DTT, 0.1 mM EDTA, 50% glycerol was used in this reaction. Second, 10 µl mixture containing 0.4 x DICER Reaction Buffer (Ambion), 0.25 U DICER (Ambion),

and DEPC treated water was added to the first reaction and incubated at 37°C for 30 mins. Addition of 0.4x DICER Reaction Buffer (120 mM NaCl, 8 mM HEPES, 2 mM $MgCl_2$, and 20 mM Tris-HCl pH 9.0) gives the final reaction mix a salt and pH condition similar to that of the 1x DICER Reaction Buffer which allows for optimal DICER activity. DICER (Ambion) was prepared to 0.25U/µl from 1 U/µl stock in storage buffer (100 mM NaCl, 20 mM Tris (pH7.5), 1mM EDTA, and 50% Glycerol) before combining with the DICER Reaction Buffer. 0.4x DICER Reaction Buffer was prepared from 5X DICER Reaction Buffer (Ambion, 1.5 M NaCl, 100 mM HEPES, 25 mM $MgCl_2$, and 250 mM Tris-HCl pH 9.0). The reaction was stopped by adding 40 µl of the Stopping Dye (Table 3) and 6 µl was loaded onto the 8% polyacrylamide gel.

Alkaline Ladder reaction

A 10 µl reaction mix containing 75 nM (100,000 c.p.m) of 5'-^{32}P-labeled *in vitro* transcribed pre-miRNA analog, 500 mM sodium bicarbonate pH 9.2 and 10 mM EDTA was incubated at 95 °C for 3 mins and on ice for 1 min before adding 5 µl of Stopping Dye (Table 3). 3 µl of the reaction mixture was loaded onto the 8% polyacrylamide gel

RNase T1 reaction

A 10µl reaction mix containing 25 nM (50,000 c.p.m) of 5'-^{32}P-labeled *in vitro* transcribed pre-miRNA analog, 0.6x Sequence Buffer (9751G, Ambion), and 0.3 U/µl RNase T1 was incubated at room temperature for 5 mins and stopped by adding 5 µl of Stopping Dye (Table 3). 3 µl of the reaction mixture was loaded onto the 8% polyacrylamide gel

3.2 Results and discussion

3.2.1 Generation of unlabeled and 5'-radiolabeled RNA

The linearization of pUC19 vectors containing cDNA sequences for Spike and Orf3 with a restriction enzyme, *EcoRI*, generated discrete single bands sized between 2000bp and 3000bp in lane 3 and 5, respectively (Figure 24A). Undigested plasmids in lane 2 and 4 migrated differently compared to their linearized counterparts. *EcoRI* digestion result for Orf1b is not shown, however, it can be confirmed that a proper digestion had took place which resulted in generation of proper sized RNA of ~79 nt (Figure 24C). Once the digestion had taken place, the linearized plasmids were subjected to *in vitro* transcription to generate unlabeled RNA substrates (Figure 24B-C). Lanes 3 and 5 in Figure 24B and Lane 3 in Figure 24C confirmed the elimination of DNA templates after transcription. Similarly to c-myc 1705-1792 CRD RNA (Figure 6A), the non-denaturing agarose gel showed multiple bands of substrate RNAs due to their inherent abilities to form secondary structures. For the two substrates (5'GG-pre-miR10b and 5'GG-pre-miR21) used for assessing APE1 interference in DICER activity, their DNA template was PCR amplified that included their T7 promoter and their cDNA sequences (Table 12). Once we obtained linear PCR fragments, RNAs were *in vitro* transcribed following the procedure described in 2.1.4 (Figure 24D).

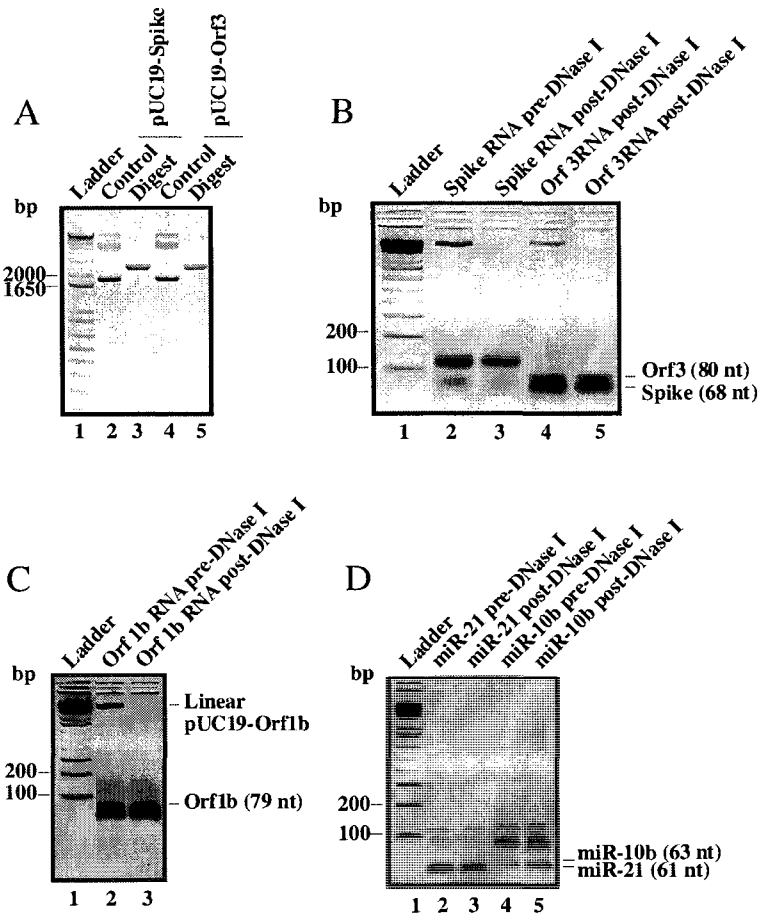

Figure 24: Agarose gel analysis showing the digestion of plasmids used for *in vitro* transcription and the generation of unlabeled RNA substrates. (A) 1% agarose gel showing the undigested plasmids pUC19-Spike and pUC19-Orf3 (lanes 2 and 4) and digested plasmids (lanes 3 and 5) after treatment with 10 U of *EcoRI*. **(B)** Non-denaturing 2% agarose gel showing the *in vitro* transcribed RNAs of Spike (lane 3) and Orf3 (lane 5) after DNase I treatment for 30 mins. **(C)** Orf 1b (lane 3). **(D)** hsa-miR-21 and hsa-miR-10b (lane 3 and 5).

3.2.2 APE1 cleaves RNA components of SARS-corona virus at specific sites

The secondary structure of Spike nts 21481-21548 was also predicted using M-fold program (Zuker 2003), and the RNase structure probing data were then used as a constraint with the structure generated by Mfold to obtain a structure that best fit the probing data (Figure 25). In using the 68 nt Spike RNA as substrate, following are the key observations.

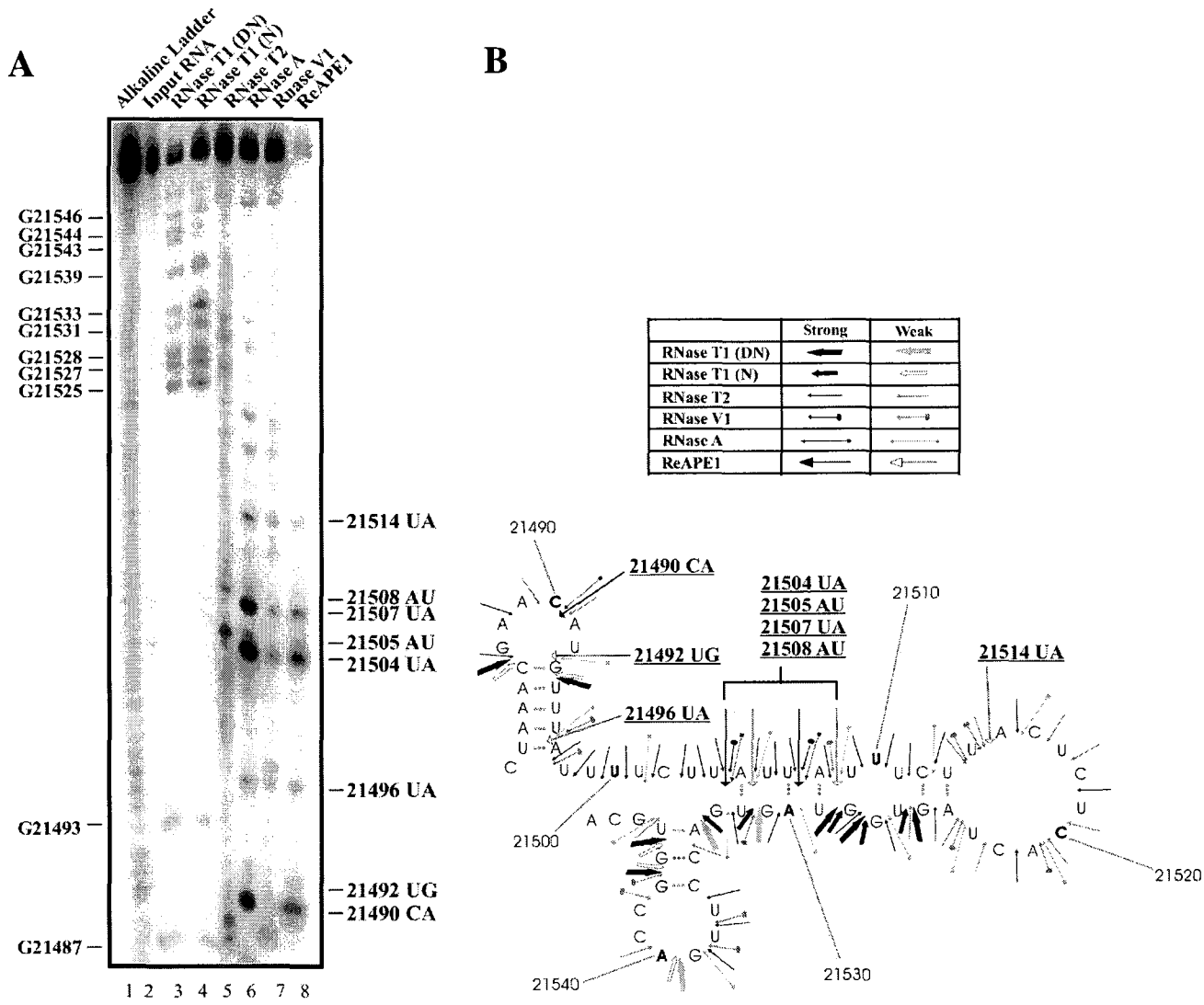

Figure 25: Ribonuclease secondary structure probing of Spike RNA. (A) *In vitro* transcribed RNA corresponding to the indicated nucleotides was 5'-end-labelled with ^{32}P and refolded prior to probing with the indicated RNases. For reference, an alkaline hydrolysis ladder was generated as shown. Numbering on the left indicates guanosine residue sites cleaved by RNase T1 under denaturing conditions, whereas numbering on the right indicates some of the sites cleaved by APE1. **(B)** The RNA secondary structure model shows locations of bases accessible for enzyme probes. The structure was obtained by using the probing data in the top panel as constraint with the Mfold program (Zuker 2003). Fully-filled symbols represent strong cleavage while moderately-filled symbols represent moderate to weak cleavage. D denotes cleavage by RNase T1 under denaturing conditions, and N denotes cleavage by RNase T1 under native conditions.

(i) APE1 cleaves strongly at 21490CA, 21504UA, and 21507UA, (ii) APE1 can cut weakly in between UA at stem region as exemplified by weak cleavage at 21496UA, (iii) APE1 can cut weakly in 21492UG and 21514UA, (iv) APE1 can cut weakly at AU at weak stem region as exemplified by cleavages at 21505AU and 21508AU.

The secondary structure of Orf1b RNA nts 14439-14508 was predicted using M-fold program (Zuker 2003), and the RNase structure probing data using RNases T1, T2, A, and VI, as shown Figure 26 were then used as a constraint with the structure generated by Mfold to obtain a structure that best fit the probing data (Figure 26B). APE1 cleavage sites on Orf1b RNA were then mapped as shown in Figure 26A (lane 8). Moderate to major cleavage sites generated by APE1 are 14445UA, 14453CA, 14455UA, 14473CA, 14484UA, and 14489UA, while weak cleavages are at 14443UG, 14448AC, 14449CU, 14462CG, 144464UC, 14467CA, and 15587UG. Several key observations can be drawn from this result: (i) there is preference for UA over UG as exemplified by more intense cleavage at 14445UA over 14443UG, (ii) cleavages can occur at CA, UA, and UC at weak stems as exemplified by 14464UC, 14467CA, 14473CA, and 14484UA, (iii) for the first time, APE1 is shown to cut very weakly at CU, AC and CG at single-stranded region as exemplified by 14448AC, 14449CU, and 14462CG sites. Similarly, the secondary structure of Orf3 RNA nts 25260-25339 was predicted using M-fold program (Zuker 2003), and the RNase structure probing data as shown in the left panel of Figure 27A were then used to generate a structure that best fit the probing data (Figure 27B). Moderate to strong cleavage by APE1 are at the following sites: 25266UA, 25278UA, 25290UA, 25312CA, 25319UA, and 25329CA.

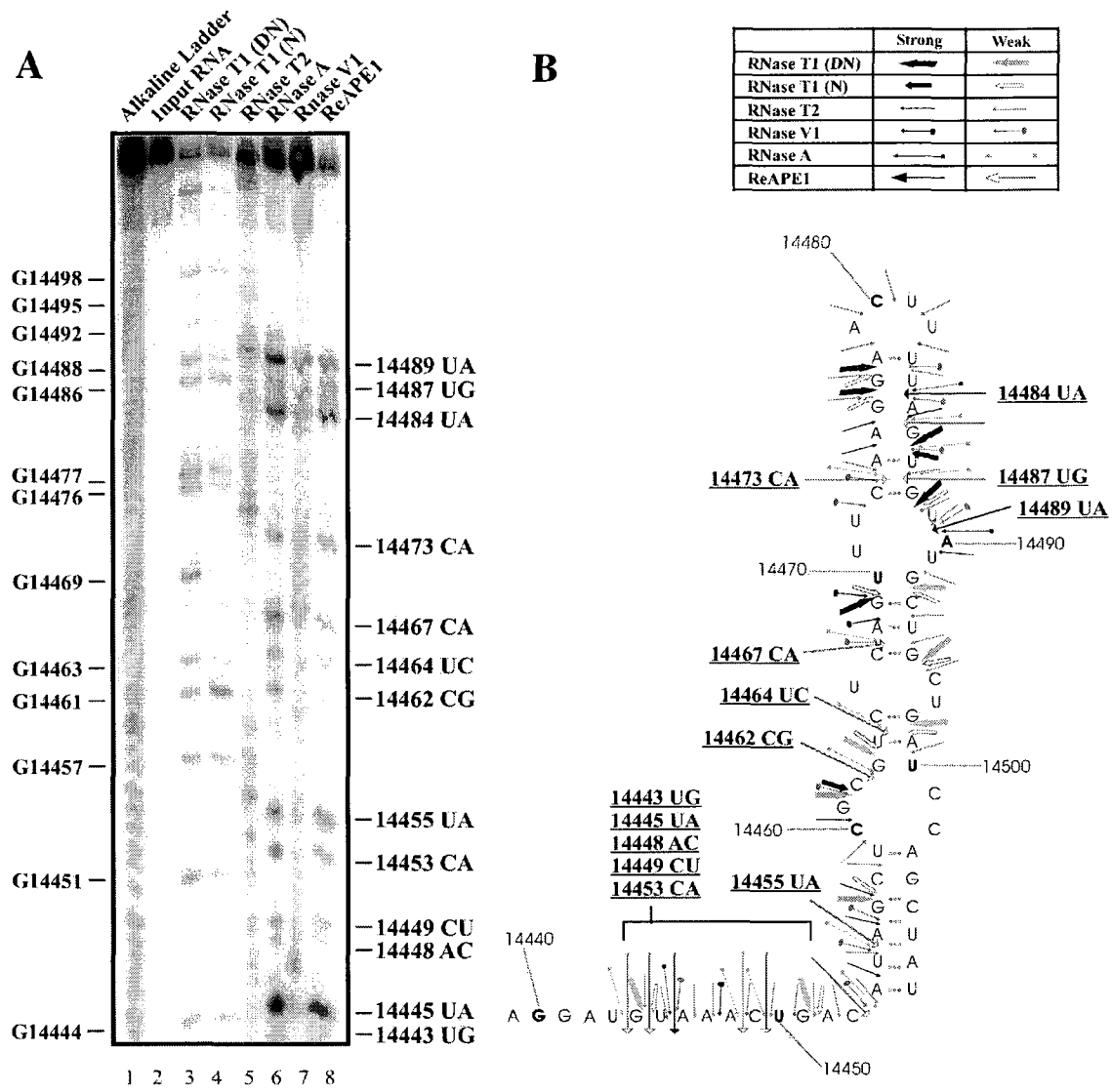

Figure 26: Ribonuclease secondary structure probing Orf1b RNA. (A) *In vitro* transcribed RNA corresponding to the indicated nucleotides was 5'-end-labelled with ^{32}P and refolded prior to probing with the indicated RNases. For reference, an alkaline hydrolysis ladder was generated as shown. Numbering on the left indicates guanosine residue sites cleaved by RNase T1 under denaturing conditions, whereas numbering on the right indicates some of the sites cleaved by APE1. **(B)** The RNA secondary structure model shows locations of bases accessible for enzyme probes. The structure was obtained by using the probing data in the top panel as constraint with the Mfold program (Zuker 2003). Fully-filled symbols represent strong cleavage while moderately-filled symbols represent moderate to weak cleavage. D denotes cleavage by RNase T1 under denaturing conditions, and N denotes cleavage by RNase T1 under native conditions.

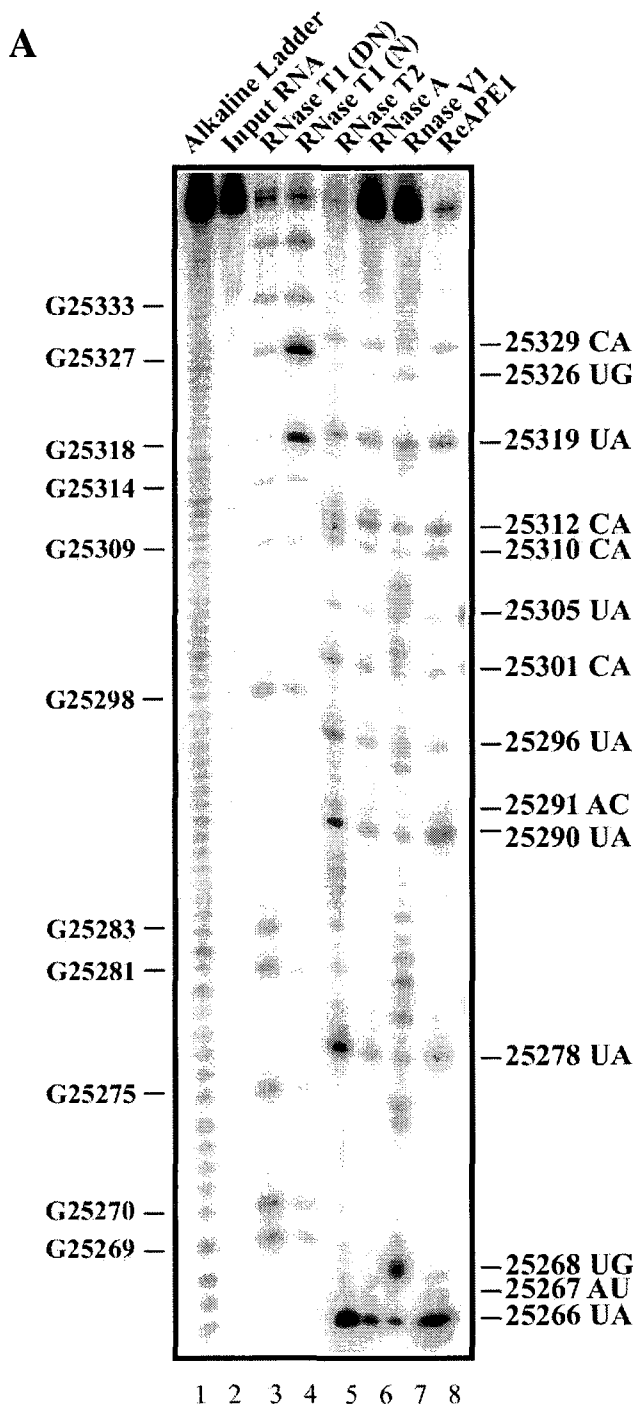

Figure 27: Ribonuclease secondary structure probing of Orf3 RNA. (A) *In vitro* transcribed RNA corresponding to the indicated nucleotides was 5'-end-labelled with ^{32}P and refolded prior to probing with the indicated RNases. For reference, an alkaline hydrolysis ladder was generated as shown. Numbering on the left indicates guanosine residue sites cleaved by RNase T1 under denaturing conditions, whereas numbering on the right indicates some of the sites cleaved by APE1.

B

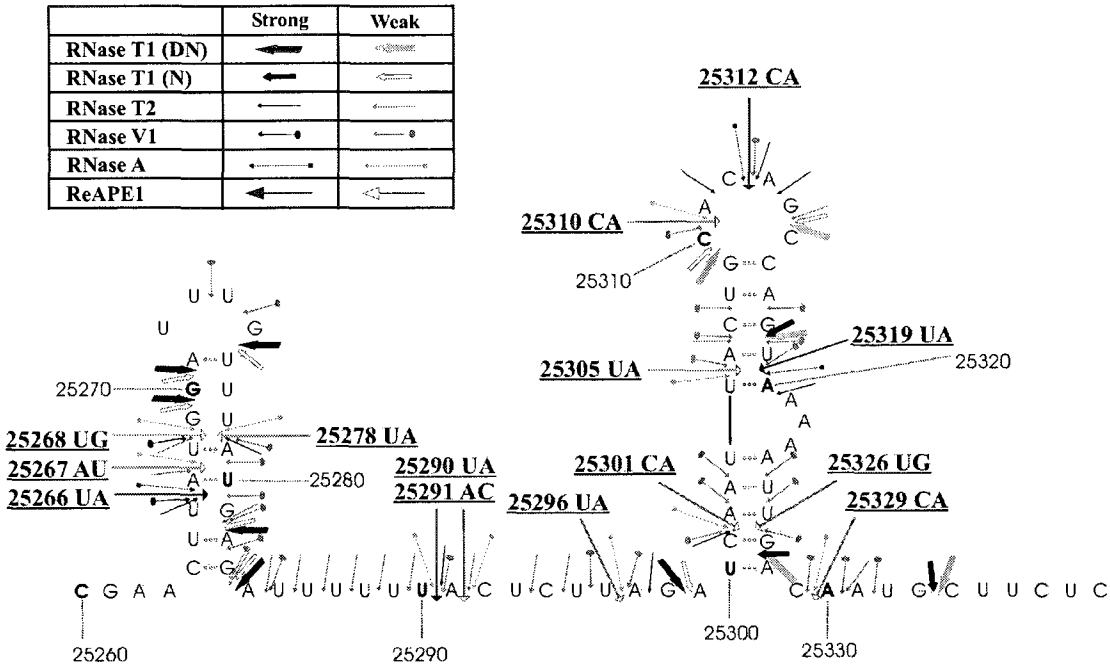

Figure 27: Ribonuclease secondary structure probing of Orf3 RNA. (B) The RNA secondary structure model shows locations of bases accessible for enzyme probes. The structure was obtained by using the probing data in the top panel as constraint with the Mfold program (Zuker 2003). Fully-filled symbols represent strong cleavage while moderately-filled symbols represent moderate to weak cleavage. D denotes cleavage by RNase T1 under denaturing conditions, and N denotes cleavage by RNase T1 under native conditions.

Weaker but significant cleavage sites are observed at 25291AC, 25296UA, 25301CA, 25305UA, 25310CA, and 25326UG (Figure 27A). The following observations are noted: (i) cleavage at UA at weak stem as exemplified by 25266UA, 25278UA, and 25319UA, (ii) APE1 cuts weakly at AC as exemplified by cleavage at 25291AC, (iii) APE1 can cut weakly at CA at stem region as exemplified with 25301CA.

3.2.3 APE1 cleaves pri-miR-21 and pri-miR-10b at specific sites

In our effort to further confirm the sequence and structural cleavage specificity of APE1 and to initiate studies into the possible future use of APE1 in degrading oncogenic miRNAs, we challenged *in vitro* transcribed pri-miR-21 and pri-miR-10b with the purified

recombinant human APE1. The secondary structure of pri-miR-10b was predicted using Mfold program (Zuker 2003) and as before, RNase probing experiments were conducted (Figure 28A). The data was used as a constraint with the structure generated by Mfold to obtain a structure that best fit the probing data (Figure 28B). The major cleavage sites generated by APE1 are 11UA, 53UA, and 59UA, while weaker sites are observed at 34UA, 50UG, and 61UA. Key observations for this result are: (i) APE1 cleaves UA at weak stems as shown by cleavages at 34UA and 53UA, (ii) APE1 does not cut in between UA, CA, UG, and UC at strong stem regions as exemplified by the absence of cleavage at 21UA, 23UA, 25UA, 48UG, 65CA, and 71UC.

Similarly, RNase probing experiments were performed on pri-miR-21 and the secondary structure generated upon constraining the experimental data (Figure 29A) with structure predicted by Mfold, is shown on the right panel of Figure 29B. As shown, the major cleavage sites generated by APE1 are 34UG, 38UC, and 41CA, while weaker cleavage sites are seen at 13UA, 16CA, 31UG, 33UU, and 40UC. The following are key observations from this result: (i) APE1 cleaves CA, UG, and UC at weak stems as shown by 34UG, 38UC, and 41CA, (ii) APE1 does not cut in between UG, CA, and UU at strong stems as indicated by the absence of cleavage at 12UU, 24UG, 26UU, 27UG, 43UG, 46CA, 49CA, 52CA, and 55UC.

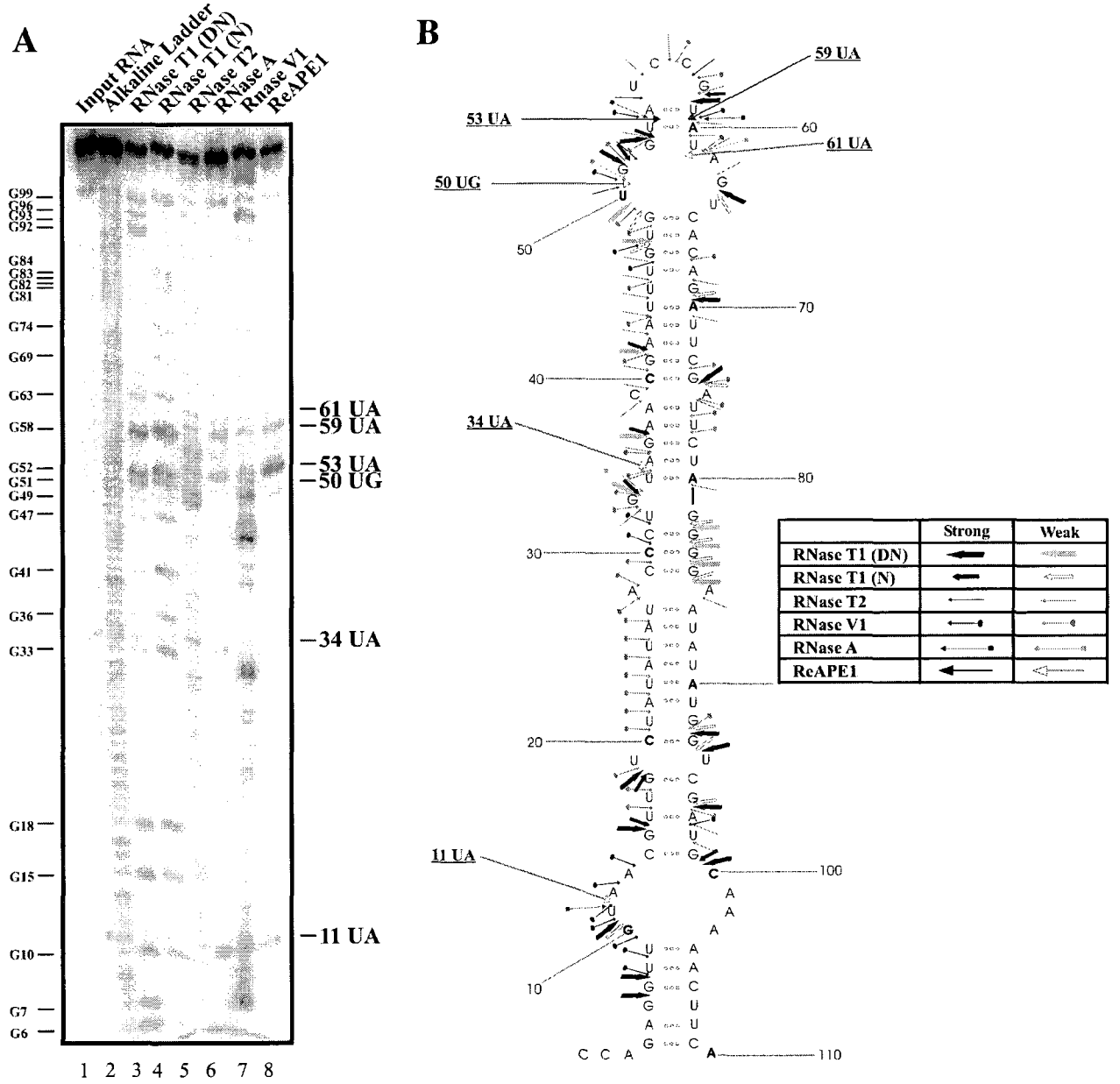

Figure 28: Ribonuclease secondary structure probing pre-miR-10b RNA. (A) *In vitro* transcribed RNA corresponding to the indicated nucleotides was 5'-end-labelled with ^{32}P and refolded prior to probing with the indicated RNases. For reference, an alkaline hydrolysis ladder was generated as shown. Numbering on the left indicates guanosine residue sites cleaved by RNase T1 under denaturing conditions, whereas numbering on the right indicates some of the sites cleaved by APE1. **(B)** The RNA secondary structure model shows locations of bases accessible for enzyme probes. The structure was obtained by using the probing data in the top panel as constraint with the Mfold program (Zuker 2003). Fully-filled symbols represent strong cleavage while moderately-filled symbols represent moderate to weak cleavage. D denotes cleavage by RNase T1 under denaturing conditions, and N denotes cleavage by RNase T1 under native conditions.

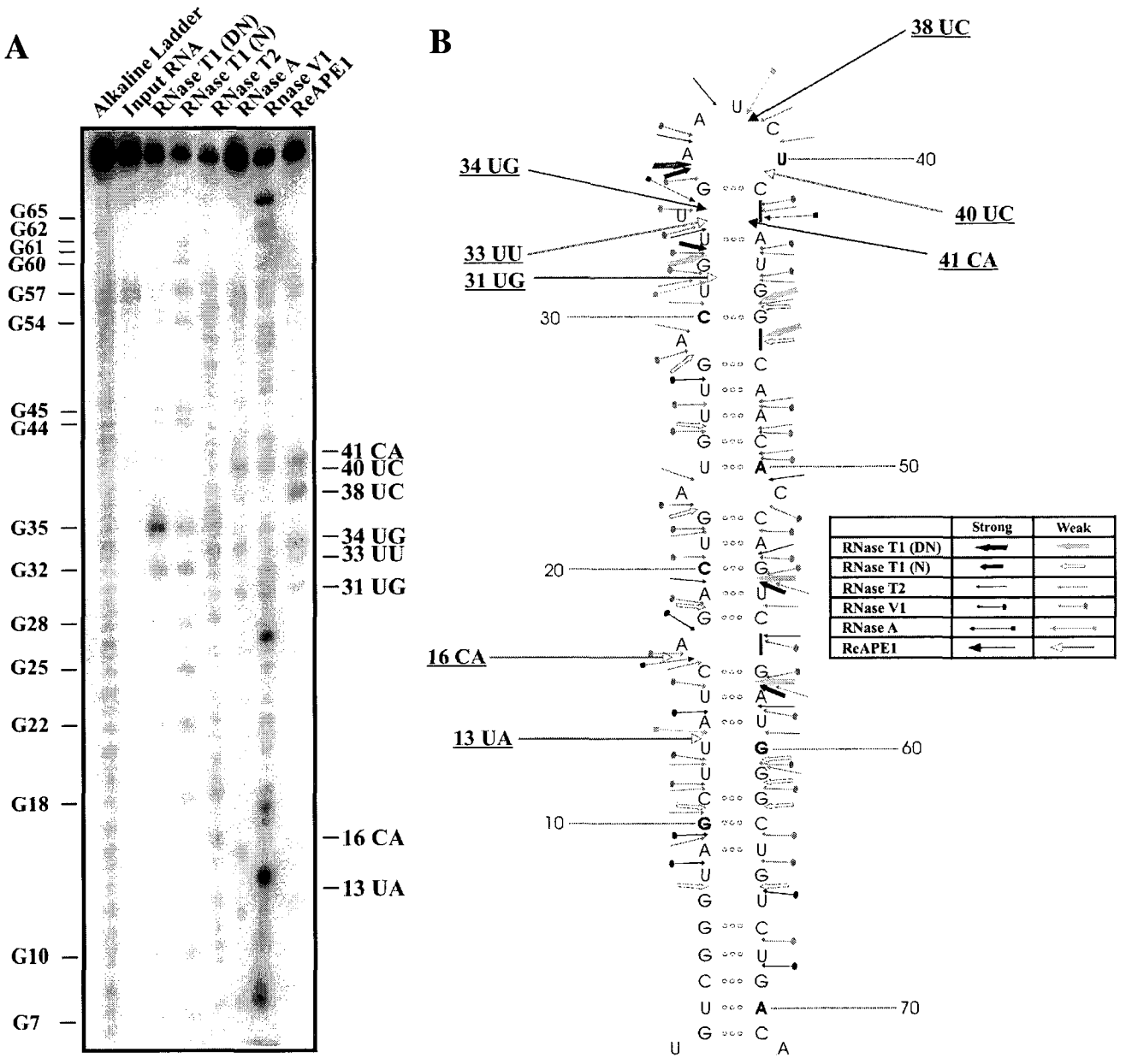

Figure 29: Ribonuclease secondary structure probing pre-miR-21 RNA. (A) *In vitro* transcribed RNA corresponding to the indicated nucleotides was 5'-end-labelled with ^{32}P and refolded prior to probing with the indicated RNases. For reference, an alkaline hydrolysis ladder was generated as shown. Numbering on the left indicates guanosine residue sites cleaved by RNase T1 under denaturing conditions, whereas numbering on the right indicates some of the sites cleaved by APE1. **(B)** The RNA secondary structure model shows locations of bases accessible for enzyme probes. The structure was obtained by using the probing data in the top panel as constraint with the Mfold program (Zuker 2003). Fully-filled symbols represent strong cleavage while moderately-filled symbols represent moderate to weak cleavage. D denotes cleavage by RNase T1 under denaturing conditions, and N denotes cleavage by RNase T1 under native conditions.

3.2.4 Pre-treatment with APE1 interferes with processing of pre-miR-10b and pre-miR-21 by DICER

To assess if APE1 can potentially interfere with the processing of pre-miRNAs by DICER, we treated pre-miR-10b and pre-miR-21 with 1 μM of APE1 prior to incubation with DICER. Figure 30A shows the cleavage of APE1 on pre-miR10b at 26UG, 29UA, 35UA, and 37UA. On the other hand, 0.25 Units of DICER alone cleaves pre-miR-10b to generate two major products, 25 nt Product 1 and 26 nt Product 2. Pre-treatment of pre-miR-10b with 1 μM of APE1 appeared to substantially suppress the ability of DICER to process pre-miR-10b as evident from the significant reduction in Products 1 (~6.2 fold) and 2 (~6.7 fold). Figure 31A shows 1 μM of APE1 cleaves pre-miR-21 at 26UG, 28UU, 29UG, 33UC, and 36CA. 0.25 Units of DICER cleaves pre-miR-21 to generate a single major product of 26 nt size as shown in Figure 31A. Pre-treatment with APE1 significantly reduce the ability of DICER to process pre-miR-21 as evident by the significant reduction of the 26 nt major DICER product by ~6.2 fold. Comparison of the two lanes in Figure 31A and B, notably, APE1 alone and APE1/DICER treated lanes, showed that APE1-generated products (29 UG, 33 UC, and 36 CA in lane 4 of Figure 31A and in lane 4 of Figure 31B) and pre-miR-21 substrate did not differ much, but at the same time, significant reduction in major DICER product (26nt DICER product in lanes 3 and 4 of Figure 31B) was observed. This indicated that prior destruction of the miR-21 substrate by APE1 can substantially abrogate the production of mature miRNA by DICER. The alkaline ladder reaction (lane 1) was also loaded onto lane 2, RNase T1 reaction, by accident (Figure 31A).

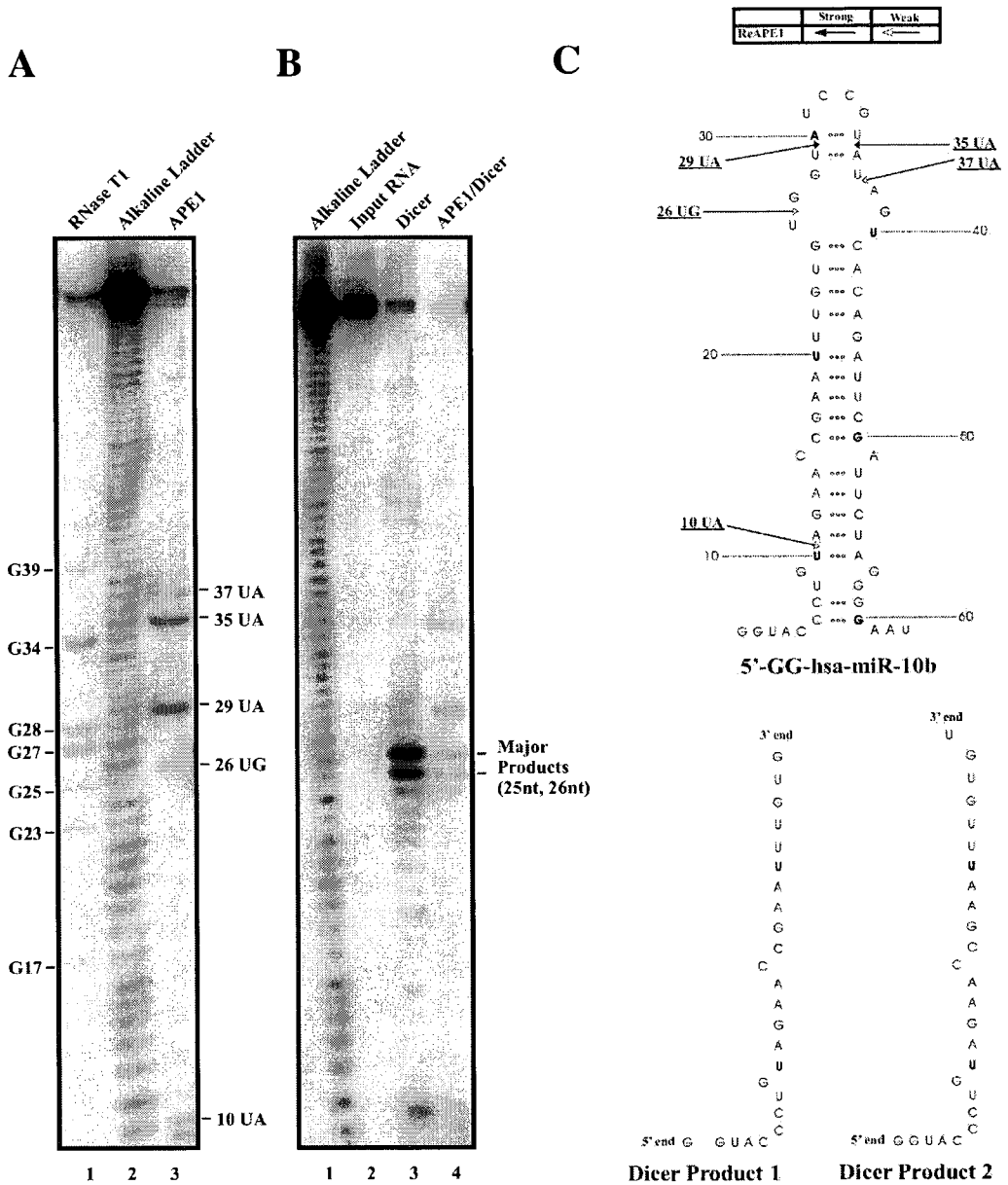

Figure 30: Effect of pre-treatment with APE1 on DICER's ability to process 5'GG-pre-hsa-miR-10b. **(A)** 25 nM ^{32}P-5'-labeled 5'-GG-pre-hsa-miR-10b were treated with purified APE1 (lane 3) for 60 mins at 37°C under the standard endonuclease assay. For reference, an alkaline hydrolysis ladder was generated (lane 2). Numbering on the left indicates guanosine residue sites cleaved by RNase T1 under denaturing conditions (lane 1), whereas numbering on the right indicates sites cleaved by APE1. **(B)** The major cleavage products 1 and 2 generated by DICER are shown with numbering on the right. ^{32}P-5'-labeled 5'-GG-pre-hsa-miR-10b pre-treated with (lane 4) or without (lane 3) APE1 for 30 mins at 37°C prior to incubation with 0.25 units of DICER for additional 30 mins. **(C)** The RNA secondary

structure of 5'-GG-pre-hsa-miR-10b shows locations of cleavage sites by APE1. DICER products 1 and 2 are shown.

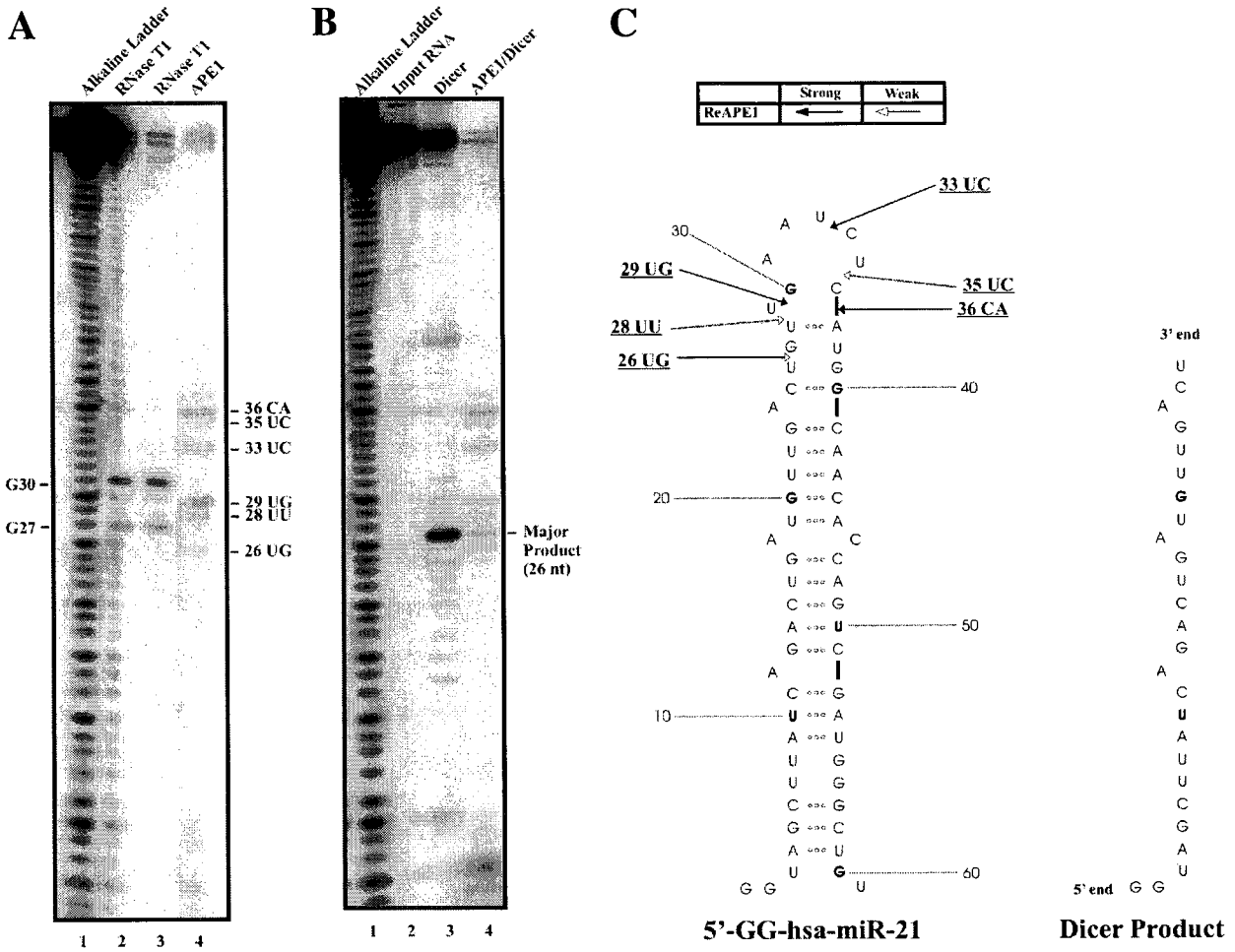

Figure 31: Effect of pre-treatment with APE1 on DICER's ability to process 5'GG-pre-hsa-miR-21. **(A)** 25 nM ^{32}P-5'-labeled 5'GG-pre-hsa-miR-21 were treated with purified APE1 (lane 4) for 60 mins at 37°C under the standard endonuclease assay. For reference, an alkaline hydrolysis ladder was generated (lane 1). Numbering on the left indicates guanosine residue sites cleaved by RNase T1 under denaturing conditions (lane 2), whereas numbering on the right indicates sites cleaved by APE1. **(B)** Numbering on the right indicates the major cleavage product generated by DICER. ^{32}P-5'-labeled 5'GG-pre-hsa-miR-21 pre-treated with (lane 4) or without (lane 3) APE1 for 30 mins at 37°C prior to incubation with 0.25 units of DICER for additional 30 mins. **(C)** The RNA secondary structure of 5'GG-pre-hsa-miR-21 shows locations of cleavage sites by APE1. The major DICER product is shown.

CHAPTER 4

Assessing the endoribonuclease activity of APE1 in biological systems

In chapter 2, we demonstrated that APE1 has the ability to cleave c-myc CRD RNA *in vitro*. c-Myc is a major oncogene that is known to promote cell survival and proliferation (Dang *et al.* 2005). Similarly, over-expression of c-myc mRNA has been found in virtually all types of cancers and the fact that APE1 can cleave c-myc mRNA *in vitro* warranted further study to confirm this observation in cultured cell line. This would be the first study to assess the RNA cleaving activity of APE1 in a biological system. The first part of this chapter investigates the involvement of APE1 in the turnover of c-myc mRNA in cultured HeLa cervical cancer cells. By treating cells with DICER substrate for RNA interference specific for APE1 mRNA (APE1-dsRNAi), we could reduce the levels of APE1 expression in these cells. Total RNA from these cells were harvested and subjected to quantitative Real-Time PCR (qRT-PCR) to measure the levels of specific mRNAs of interest. By observing the relevant ratios of c-myc mRNA to that of a housekeeping gene (β-actin), we could compare the changes in the levels of c-myc mRNA in APE1-dsRNAi and control-dsRNAi treated samples. In addition, we assessed the stability of c-myc mRNA in APE1-dsRNAi and control-dsRNAi treated samples to assess the role of APE1 in c-myc mRNA stability.

The second part of this chapter tested the validity of applying a bacterial-based genetic selection system to identify amino acid residues important for the RNA cleaving activity of APE1 in cells. This was carried out by expressing APE1 and its amino acid substitution mutants in *E. coli* Origami cells, a genetic selection system which have been previously used in determining the essential residues for endoribonucleases such as RNase A

and Angiogenin (Figure 32). This system takes advantage of the ability of a ribonuclease to cleave cellular RNA and hence cause cell death (Smith and Raines 2006). In general, RNase A and its homologs are not toxic when expressed in typical *E. coli* strains. This is so because these ribonucleases contain three or four disulfide bonds, and the reducing environment of a typical *E. coli* cytosol will not allow appropriate formation of these bonds. Consequently, the enzymes are not folded properly to their active state and cellular RNAs are not cleaved. However, the genetically engineered Origami strain has mutations in two genes, thioredoxin reductase and glutathione reductase, which shift the reducing potential and therefore allow disulfide-bond formation in the cytosol. Thus, plasmid-encoded RNase A and Angiogenin fold and are toxic to Origami cells, allowing the identification of inactive mutants of these ribonucleases (Smith and Raines 2006).

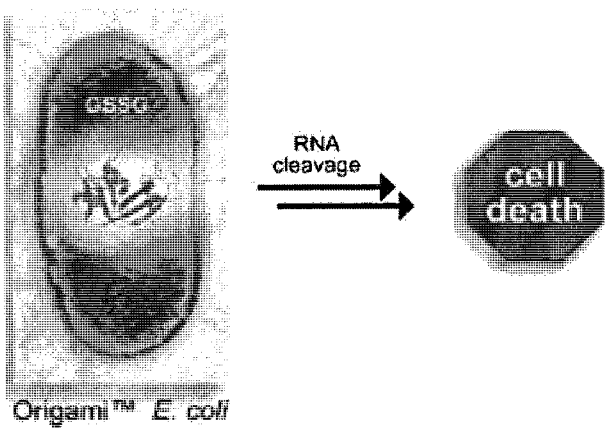

Figure 32: The genetic selection system for ribonuclease activity in Origami cells (Smith and Raines 2006). Ribonuclease activity is toxic to the cells, unless missing residues essential for its activity.

The advantage of this system is that it is fast and has successfully been demonstrated to detect biologically relevant ribonuclease activities of RNase A and Angiogenin. In chapter 3, APE1 was shown to cleave multiple RNAs *in vitro*. In turn, APE1 is expected to have an impact on Origami cells' survival by cleaving multiple RNAs. When expressed in Origami

cells, the mutant forms of APE1 missing essential residues through amino acid substitutions are expected to result in colony formation.

4.1 Methodology

4.1.1 Assessing the steady-state *c-myc* mRNA level in APE1 knocked down cells

Cell culture and reagents

HeLa cells were cultured in a tissue culture flask T75CN vent cap red (Sarstedt, Newton, NC) with 20 mL of Minimum Essential Medium (MEM) (Invitrogen, Carlsbad, CA) supplemented with 10% fetal bovine serum. The cells were incubated under 5% CO_2 and at 37°C. Maintenance of cells were done by splitting the cells in 1:10 ratio into a fresh flask approximately after two days of growth or when the cells have reached a confluency of 90%. To plate cells on experimental culture plates, cells in the T75CN flask were washed with 3 mL of PBS pH 7.4 (Invitrogen, Carlsbad, CA) and subsequently treated with 2 mL of 0.25% Trypsin-EDTA (Invitrogen, Carlsbad, CA) and incubated at 37°C and 5% CO_2 for 4 mins. Next, 8 mL of MEM was added to the cells and by pipetting, chunks of cells were separated. From 10 mL, 0.5 mL of cell sample was taken and from that, 40 µl of cells were mixed with equal volume of Trypan Blue dye (Sigma). Sample of the mixture was loaded onto the each side of the Bright Line hemacytometer (Hausser Scientific, Horsham, PA) and the number of cells in the 16-square quadrant was counted. After counting several quadrants, the numbers were averaged and the cell concentration in the T75CN flask was determined. Subsequently, cells in the flask were diluted to 2.5 x 10^4 cells/mL or 5 x 10^4 cells/mL and was plated at 2 mL (5 x 10^4 cells or 10 x 10^5) onto each wells of 6-well flat bottom plates (Sarstedt, Newton, NC). The plated cells were grown for 15 – 17 hrs at 37°C and 5% CO_2 before transfection.

Transfection

Before transfection, cells in the 6-well plates were washed with 1 mL/well PBS pH 7.4 and changed of their media with 2 mL of fresh MEM. 2 µl of Lipofectamine 2000 Reagent (Invitrogen, Carlsbad, CA) and 248 µl of OPTI-MEM (Invitrogen, Carlsbad, CA) were mixed and incubated under room temperature for 5 mins. As well, 2.5 µl of 20 µM DICER substrate RNAi against APE1 mRNA (Table 13) or DICER substrate Scrambled-Negative control (IDT, San Diego, CA) was mixed with 247.5 µl of OPTI-MEM, and incubated under room temperature of 5 mins. Next, 250 µl of OPTI-MEM and Lipofectamine 2000 Reagent mix was added to the 250 µl of siRNA or scramble OPTI-MEM mixture, shaken vigorously, and incubated under room temperature for 20 mins. This allows the association of lipofectant agent and siRNA to ensure high transfection efficiency. 500 µl of siRNA or scramble mixture in OPTI-MEM was added to the well of the 6-well plates. The cells were grown for 24 hrs at 37°C and 5% CO_2 before another transfection following the same protocol.

Table 13: Sequences of Scrambled-Negative DICER substrate double stranded RNAi (dsRNAi) and dsRNAi against APE1 mRNA.

Oligonucleotide	**Sequence**
Scrambled Negative-dsRNAi sense	r(CUUCCUCUCUUUCUCUCCCUUGU)dGA
Scrambled Negative-dsRNAi antisense	r(UCACAAGGGAGAGAAAGAGAGGAAGGA)
APE1-dsRNAi sense	r(GUCUGGUACGACUGGAGUACCGG)dCA
APE1-dsRNAi antisense	r(UGCCGGUACUCCAGUCGUACCAGACCU)

Lysis and protein extraction

After 24 hrs or 48 hrs since the first transfection, cells were washed with 1 mL of PBS pH 7.4. For each well, 200 µl of 8M Urea Lysis Buffer (8M Urea, 100 mM NH_2PO_4, 10 mM Tris-HCl) was added. The cell lysates were collected with cell scraper and the lysates were transferred to an eppendorf tube. The lysates were stored at -80°C for 15 min before

quickly thawing them at 42°C for 5 mins. Subsequently, the lysates were vortexed for 30 secs. The freeze-thaw-vortex cycle was repeated for two additional times. After the final vortex, lysates were spun at 12,000 rpm for 15 mins at 4°C. The supernatant (~ 200 µl) was transferred to a fresh eppendorf tube and 3 µl of the sample was taken for Bradford assay to determine the total extracted protein concentration. The rest of the proteins were stored at -80°C.

Bradford assay

Concentration standards were prepared to generate a linear regression equation. 10 mg/mL of Bovine Serum Albumin (BSA, New England Biolabs, Beverly, MA) was diluted 1:10 in autoclaved water. The resulting stock of 1 mg/mL BSA was subsequently aliquoted in 5, 10, 15, 20, 25, 30 µl portions to be diluted in 795, 790, 785, 780, 775, 770 µl of autoclave water, respectively. Next, the 800 µl BSA samples were mixed with 200 µl Bradford assay reagent (Biorad, Hercules, CA) and incubated at room temperature for 2 to 5 mins to have their colors change. From the total mixture of 1 mL, 200 µl aliquots placed in triplicates into the wells of the 96-well plate (Sarstedt, Newton, NC). The software for Multiskan Ascent (Thermo Fisher Scientific, Waltham, MA) was used to quantify the absorption at a wavelength of 595 nm. Subsequently, the measurements were plotted in absorption versus µg/mL and the linear equation was derived using Excel spreadsheet. 3 µl of the lysate sample was mixed with 797 µl of autoclaved water. Then, 200 µl Bradford assay reagent was added and 200 µl aliquots were placed in triplicates into the wells of the 96-well plate. Using the software MultiSkan, the absorption value of the sample at a wavelength of 595 nm was obtained. Subsequently, the concentration of the protein sample was determined using the BSA standard equation.

Acetone precipitation

To concentrate the proteins for Western Blot analysis purposes, a calculated volume of protein sample was mixed with five volumes of 100% acetone. The sample was mixed and stored in -20°C for 15 mins before spinning at 12,000 rpm for 10 mins at 4°C. The protein pellet was formed and the supernatant was removed by pouring. 200 µl of 80% acetone was added to the pellet for rinsing and the sample was spun at 10,000 rpm for 5 mins at 4°C. The supernatant was removed by pouring and the pellet was dried under fumehood for 15 mins. Subsequently, the pellet was resuspended in 10 µl of autoclaved water and stored at -20°C.

Western Blot

Prior to transfer, a nitrocellulose membrane and four pieces of filter papers were cut out in order to have the same dimension as the SDS-PAGE resolving gel. The membrane was first soaked in de-ionized water for 1 min and subsequently equilibrated in Western Transfer Buffer for 5 mins at room temperature. SDS-PAGE resolving gel was also equilibrated in Western Transfer Buffer (Table 14) for 5 mins at room temperature. The transfer sandwich was assembled in the following order starting from the bottom. A sponge mat was soaked in Western Transfer Buffer and was placed on the very bottom, followed by the two soaked filter papers, nitrocellulose membrane, SDS-PAGE resolving gel, two filter papers, and a sponge mat at the top. The transfer sandwich was placed into the transfer apparatus and the transfer was done at 90 V for 40 mins at 4°C.

Table 14: Composition of the reagents used in Western blot.

Reagents	Composition
10 x TBS	100 mM Tris-HCl pH 7.4, 1.5 M NaCl
Western Transfer Buffer	37 mM Tris-HCl, 39 mM Glycine, 20 % methanol
Western Blocking Buffer	10 mM Tris-HCl pH 7.4, 0.15 M NaCl, 5 % Skim Milk
ST	10 mM Tris-HCl pH 7.4, 0.15 M NaCl, 1 % Skim Milk, 0.1 % Tween-20
Western Stripping Buffer	62.5 mM Tris-HCl pH 6.7, 2 % SDS, 100 mM β-mercaptoethanol

Following the transfer, the membrane was blocked with Western Blocking Buffer either at 37°C for 30 mins or at 4°C overnight. Next, the membrane was rinsed twice quickly in 3 mL of ST and washed for 15 mins at room temperature under gentle shaking with 5 mL ST. Additional two washes of 5 mins in 5 mL ST was done at room temperature. The membrane was then incubated with 1° antibody diluted in 1:1500 for monoclonal anti-APE1 antibody raised in mouse (Santa Cruz Biotechnology Inc.) or 1:2500 for monoclonal anti-β-actin antibody raised in mouse (Sigma) in ST for 2 hrs at room temperature. The membrane was then, rinsed and washed as described previously. Next, the membrane was incubated with 2° antibody (anti-mouse polyclonal IgG (Promega, Wyoming, MI)) diluted in 1:4000 in ST for 1 hour at room temperature. The membrane was then, rinsed and washed as described previously. After the final wash, the membrane was developed by incubation of 1 min with SuperSignal West Pico Chemilluminescent substrate (Pierce, Rockford, IL) as per manufacturer's protocol and exposed and visualized using ChemImager (Alpha Innotech, San Leandro, CA). The membrane was stripped by incubation with Western Stripping Buffer at 50°C for 30 mins, and blocked by Western Blocking Buffer as described previously for another round of immunoblot detection when necessary.

Total RNA extraction

Twenty-four hrs or 48 hrs after the first transfection, cells were washed with 1 mL of PBS pH 7.4. Subsequently, 1 mL of Trizol Reagent (Invitrogen, Carlsbad, CA) was added and pipetted up and down to homogenize the cells. The mixture was soon transferred to a fresh eppendorf tube, to which 200 µl of chloroform : isoamyl alcohol ($CHCl_3$: IAA = 49 : 1, Fluka) was added and the mixture was inverted six times before spinning at 3,000 rpm for 10 mins at 4 °C. The top aqueous layer was transferred to a fresh eppendorf tube and 500 µl of isopropanol was added and inverted six times. The sample was spun at 11,000 rpm for 15 mins at 4 °C to form an RNA pellet. The supernatant was removed by decanting and 200 µl of cold 75% ethanol was added to rinse the pellet, and then spun at 9,000 rpm for 5 mins at 4 °C. The supernatant was removed by decanting and the pellet was dried in fumehood for 15 mins. RNA was resuspended in 100 µl of DEPC-treated water and its concentration was determined by ND-1000 UV-Spectrophotometer (NanoDrop V.3.1.0, Wilmington, Delaware). The concentration was determined by using the relationship:

RNA concentration (µg/ml) = (OD_{260}) x (dilution factor) x (40 µg RNA/ml) / (1 OD_{260} unit).

cDNA synthesis

A total reaction mix of 20 µl included 1 µg of total RNA, 4 µl of 5 x iScript Reaction Mix (Biorad, Hercules, CA), 1 µl of iScript Reverse Transcriptase (Biorad, Hercules, CA), and varying amount of nuclease-free water (Biorad, Hercules, CA) to adjust the total volume. At times, half volume of each reagent was used for the total reaction mix of 10 µl. The MiniCycler PCR machine (MJ Research Inc., Watertown, MA) was programmed for 5 min at 25°C, 30 min at 42°C, 5 min at 85°C, and hold at 4°C to generate the cDNA.

Quantitative Real Time PCR (qRT-PCR)

For one reaction per gene, a 24 µl master mix was made using 12.5 µl of iQ SYBR Green Supermix (Biorad, Hercules, CA), 1 µl of 10 µM forward primer (Table 15), 1 µl of 10 µM reverse primer (Table 15), and 9.5 µl of autoclaved water.

Table 15: Primer sequences used in qRT-PCR.

RT-qPCR Primers	**Sequence**
Human APE1 Forward	5'-TGGAATGTGGATGGGCTTCGAGCC-3'
Human APE1 Reverse	5'-AAGGAGCTGACCAGTATTGATGA-3'
Human c-Myc Forward	5'-ACGAAACTTTGCCCATAGCA-3'
Human c-Myc Reverse	5'-GCAAGGAGAGCCTTTCAGAG-3'
β-actin Forward	5'-TTGCCGACAGGATGCAGAAGGA-3'
β-actin Reverse	5'-AGGTGGACAGCGAGGCCAGGAT-3'

This master mix was aliquotted into the well of the 96-well PCR microplate (Axygen Scientific, Union City, CA) at room temperature. Next, 1 µl of cDNA sample was added to the master mix in the PCR plate and the plate was sealed using the MicroSeal B Adhesive Sealer (Biorad, Hercules, CA). For one gene, there were triplicates of each reaction. iCycler Thermal Cycler (Biorad, Hercules, CA) was programmed by using the software, iQ5 Optical System Software Version 2.0 (Biorad, Hercules, CA). The program was set up for cycle 1 at 95°C for 3 mins, cycle 2 repeated 40 times at 95°C for 10 secs and at 52°C for 30 secs, and cycle 3 repeated 87 times at 52°C for 10 secs. The C_T values obtained from each triplicates were averaged and used to calculate the relative mRNA levels of interest using the Livak method (Livak and Schmittgen, 2001). C_T value represents the cycle number at which the fluorescence generated within a reaction crosses the threshold and this value is inversely correlated to the logarithm of the initial copy number of cDNAs. A sample calculation determining the fold changes in mRNA levels using C_T values is shown on section 4.2.1.

4.1.2 Assessing *c-myc* mRNA half-life in APE1 knocked down cells

A transcriptional inhibitor, 5,6-dichloro-1-β-D-ribofuranosylbenzimidazole (DRB, Sigma) was used for this method. The DRB stock of 200 μM x 100 was prepared in 100% ethanol and stored at -20 °C until further use. The cells were plated at 10 x 10^4 or 5 x 10^4 cells/well and transfected with either siRNA against APE1 or scramble over 36 hrs as described previously in section 4.1.1. After 36 hrs since the first transfection, the cells were washed with 1 mL PBS pH 7.4. Next, DMEM containing 200 μM of DRB was applied to the cells and the cells were incubated at 37°C and 5% CO_2. At each desired time point, the cells were washed with PBS pH 7.4 and their RNA harvested using 1 mL of Trizol Reagent (Invitrogen, Carlsbad, CA). The subsequent steps in extracting RNA are identical to the described method in 4.1.1.

4.1.3 Preparation of LB-antibiotic plates for Origami cells

The solid LB-agar mixture was liquefied in microwave and appropriate antibiotics were added. One set of LB-agar plates contained the final concentration of 12.5 μg/mL Tetracycline and 15 μg/mL Kanamycin. Another set contained 100 μg/mL Ampicillin. Next, per each 100 mm plates (Fisherbrand), 15 mL of LB-agar was added and allowed to solidify in room temperature.

4.1.4 Preparation of Origami competent cells

50 μl of Origami B(DE3) cells (Novagen) were streaked on LB-kan-tet plate. The plate was wrapped on its sides with a strip of plastic plate and incubated overnight at 37°C. The next day, a single colony was picked from the plate and was grown overnight at 37°C with shaking in a 50 mL falcon tube containing 10 mL of LB-kan-tet. The next day, 500 mL LB supplemented with 12.5 μg/mL Tetracycline and 15 μg/mL Kanamycin was prepared and

5 mL of the overnight culture was added to the 500 mL LB-kan-tet. The culture was shaken (200 rpm) at 37°C until the optical density measured at wavelength of 600nm (OD_{600nm}) had reached ~0.4. The OD_{600nm} was measured using DU800 UV/visible Spectrophotometer (Beckman Coulter Inc., Palo Alto, CA). Next, the culture was split in 250 mL portions and transferred into sterile centrifuge bottles. The culture was centrifuged for 30 mins at 3500 rpm at 4°C using benchtop centrifuge Allegra X-12R Centrifuge (Beckman Coulter Inc., Palo Alto, CA). Once, most of the cells were pelleted at the bottom, the cells were resuspended in 30 mL of cold 100 mM $CaCl_2$ and transferred to a 50 mL falcon tube to be incubated on ice for 30 mins. Again, the cells were centrifuged at 3500 rpm at 4°C for 15 mins. Next, the clear supernatant was discarded and the cells were resuspended in 4 mL of cold 100 mM $CaCl_2$ with 15% glycerol. The cells were aliquotted in 100 µl stocks and stored at -80°C.

4.1.5 Transformation and induction of protein expression by IPTG

The competent Origami cells in 100 µl aliquots were thawed on ice. Next, 100 ng of plasmids containing either APE1 WT or mutant cDNA were aliquotted into 15 mL round bottom tubes on ice. The thawed cells were added to the plasmids and the cells were incubated on ice for 20 mins. The cells were transformed by heat shock at 42°C for 75 to 90 secs and subsequently cooled on ice for 2 mins. 500 µl of LB was added to the cells and they were allowed to recover at 37°C for 40 mins with shaking (200 rpm). In the meantime, LB agar plates containing 100µg/mL Ampicillin were pre-warmed at 37°C. Ampicilliln plates were used to initially screen transformed cells. For IPTG induction, 125 µl aliquots of cells were further incubated with 0 to 750 µM IPTG for additional 5 mins before being plated on to LB-ampicillin plates. The plates were incubated at 37°C for 24 hrs. It is noteworthy that, with Ampicillin alone, we can not distinguish whether the surviving colonies were truly

Origami cells. For this purpose, Tetracycline and Kanamycin supplemented plates would be used. However, in our results testing the effects of mutant APE1s, except for H309N, all of the transformed cells did not survive on LB-ampicillin plates, hence there was no need to additionally screen them under Tetracycline and Kanamycin supplemented plates.

4.2 Results and Discussion

4.2.1 APE1 knock down in HeLa cells up-regulates c-myc mRNA expression

To assess the RNA cleaving activity of APE1 and its influence on c-myc mRNA level, we knocked down the expression of APE1 in HeLa human cervical cancer cell line using DICER substrate RNAi against APE1 mRNA (APE1-dsRNAi). The sequences were based on siRNA that was successfully used to knock down APE1 (Fan *et al.* 2003; Table 13). For the control, DICER substrate Scrambled-Negative (Control-dsRNAi) was used (Table 13). The delivery of these substrates was mediated through Lipofectamine 2000, which had shown a transfection efficiency of ~80% (Bassett *et al.* 2008). The level of APE1 and c-myc mRNAs were assessed through quantitative Real-Time PCR (qRT-PCR) and normalized against mRNA for β-actin, which served as a constitutive expression control.

The reduced levels of APE1 protein and transcripts after 24 hrs and 48 hrs of transfection were assessed through Western analysis and qRT-PCR. The degree of APE1 reduction at protein levels was quantified by calculating the ratios of density of APE1 in the control versus the knock down lane using OptiQuant software (Hewlett Packard, Palo Alto, CA). The reduction was found to be ~60% after 24 hrs and ~70% after 48 hrs (Figure 33).

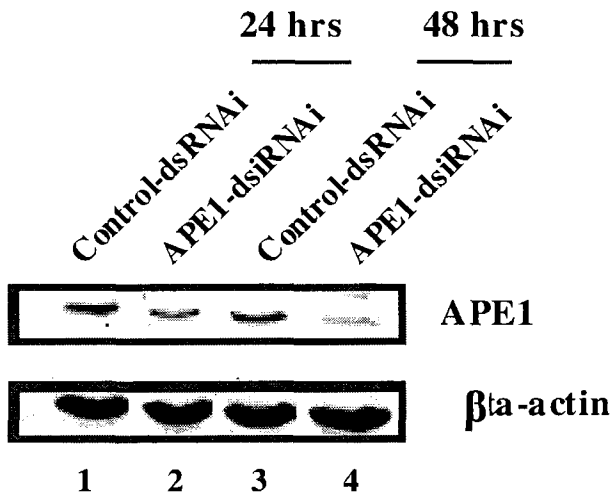

Figure 33: Western blot illustrating the reduced levels of APE1 after two time points using dsiRNAi against APE1 in HeLa cells. A total of 30 μg of proteins were loaded onto the wells and ran on SDS-PAGE gel. The gel was then blotted onto a nitrocellulose membrane. The identification of proteins was made via monoclonal antibodies against APE1 and beta-actin. Top panel shows the amount of APE1 in dsiRNA-scramble (lanes 1 and 3) versus the dsiRNA-APE1 (lanes 2 and 4) treated cells at two time points. Bottom panel shows the amount of β-actin in these cells as a control for loading the same amount.

This was correlated to APE1 reduction at mRNA levels after 24 hrs (~80%) and 48 hrs (~85%) of transfection (Figure 34A). After 24 hrs, the knock down was significant ($P < 0.001$, student t-test). Although the t-test ($P > 0.001$) for the knock down at 48 hrs did not give significance, we could speculate a significant reduction of APE1 mRNA at this time point verified by Western data (Figure 33). APE1 knock down was also associated with elevated expression of c-myc mRNA. Using the same total RNA extract, we found increased level of c-myc mRNA in both 24 hrs (~2.2-fold) and 48 hrs (~4.6-fold) upon APE1-dsiRNAi transfection (Figure 34B). At 24 hrs, the up-regulation was not significant according to the student t-test ($P > 0.001$). However, at 48 hrs, the up-regulation was significant ($P < 0.001$). This showed that APE1 was involved in the regulation of c-myc mRNA expression and warranted further studies to verify whether APE1 was involved in the control of c-myc mRNA stability.

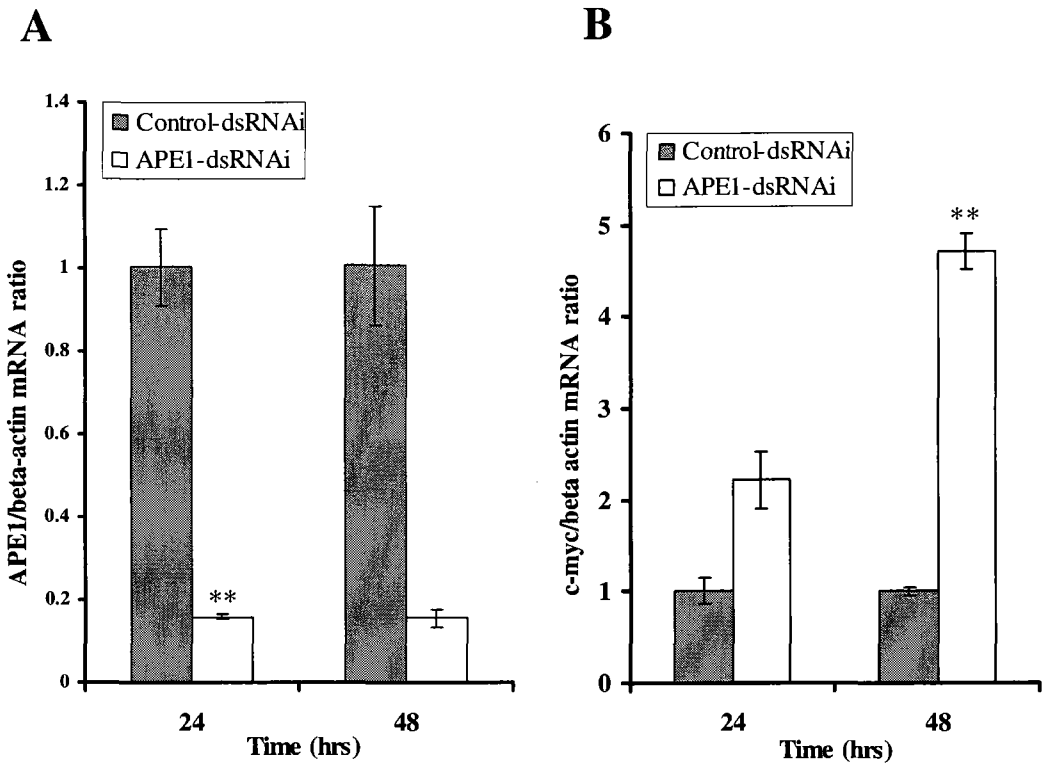

Figure 34: Steady state level of c-myc mRNA is elevated after transient knock down of APE1 using double stranded siRNA in HeLa cells. qRT-PCR was carried out on cDNA samples generated from harvested RNAs at two different time points to measure the relative levels of **(A)** APE1 mRNA or **(B)** c-myc mRNA in both Control-dsiRNAi and APE1-dsiRNAi treated HeLa cells. Asterisks indicate the student t-test value was less than 0.001.

Table 16 shows a sample calculation using C_T values obtained from qRT-PCR to assess the fold changes in *c-myc* mRNA after 24 hrs of transfection with APE1-dsRNAi as compared to the Control-dsRNAi. To begin the calculation, C_T value for ß-actin (15.13) was subtracted from c-myc (23.46) for the Control-dsRNAi 24h-1 sample to give a ΔC_T value of 8.33.

$$\Delta C_T\text{: c-myc } C_T\,(23.46) - \text{ß-actin } C_T\,(15.13) = 8.33$$

Next, similar calculations were performed for two other samples for Control-dsRNAi treated samples as well as the triplicates treated with APE1-dsRNAi to obtain the differences

in their C_T values (ΔC_T) between c-myc and ß-actin mRNAs as shown under column ΔC_T (*c-myc* C_T - β-actin C_T) (Table 16).

From these values, an average was calculated for the Control-dsRNAi (8.11) and APE1-dsRNAi (6.97) treated samples.

Average of ΔC_T for Control-dsRNAi: (8.33 + 8.02 + 7.98)/3 = 8.11

Average of ΔC_T for APE1-dsRNAi : (6.58 + 7.11 + 7.22)/3 = 6.97

Next, each ΔC_T value of the triplicate in the Control-dsRNAi were subtracted from the average values for Control-dsRNAi (8.11) and APE1-dsRNAi (6.97), respectively. For example, from an average value for Control-dsRNAi (8.11), Control-dsRNAi 24h-1 (8.33), Control-dsRNAi 24h-2 (8.02), and Control-dsRNAi 24h-3 (7.98) were all subtracted separately to give -0.22, 0.09, and 0.13, respectively.

Average of ΔC_T for Control-dsRNAi (8.11) – Control-dsRNAi 24h-1 (8.33) = -0.22

Average of ΔC_T for Control-dsRNAi (8.11) – Control-dsRNAi 24h-2 (8.02) = 0.09

Average of ΔC_T for Control-dsRNAi (8.11) – Control-dsRNAi 24h-3 (7.98) = 0.13

Similarly, from an average value for APE1-dsRNAi (6.97), values for Control-dsRNAi 24h-1 (8.33), Control-dsRNAi 24h-2 (8.02), and Control-dsRNAi 24h-3 (7.98) were also subtracted separately to give -1.36, -1.05, and -1.01, respectively.

Average of ΔC_T for APE1-dsRNAi (6.97) – Control-dsRNAi 24h-1 (8.33) = -1.36

Average of ΔC_T for APE1-dsRNAi (6.97) – Control-dsRNAi 24h-2 (8.02) = -1.05

Average of ΔC_T for APE1-dsRNAi (6.97) – Control-dsRNAi 24h-3 (7.98) = -1.01

These differences ($\Delta\Delta C_T$) were averaged for the Control-dsRNAi (0.00) and APE1-dsRNAi (-1.14) treated samples.

Average of $\Delta\Delta C_T$ of Control-dsRNAi: (-0.22 + 0.09 + 0.13)/3 = 0.00

Average of $\Delta\Delta C_T$ of APE1-dsRNAi: (-1.36 + -1.05 + -1.01)/3 = -1.14

Finally, by calculating $2^{-\Delta\Delta CT}$, normalized c-myc mRNA fold changes for the Control-dsRNAi ($2^{-(0.00)} = 1$) and APE1-dsRNAi ($2^{-(-1.14)} = 2.22$) treated samples were determined.

Table 16: Sample table of C_T values generated from qRT-PCR

	ß-actin mRNA C_T	*c-myc* mRNA C_T	ΔC_T (*c-myc* C_T - β-actin C_T)	$\Delta\Delta C_T$ (Avg. ΔC_T Control-dsRNAi – ΔC_T Control-dsRNAi) OR (Avg. ΔC_T APE1-dsRNAi – ΔC_T Control-dsRNAi)	Normalized *c-myc* mRNA in Control-dsRNAi OR APE1-dsRNAi relative to Control-dsRNAi ($2^{-\Delta\Delta CT}$)
Control-dsRNAi 24h-1	15.13	23.46	8.33	-0.22	1.17
Control-dsRNAi 24h-2	14.90	22.92	8.02	0.09	0.94
Control-dsRNAi 24h-3	14.97	22.94	7.98	0.13	0.91
Average	15.00	23.11	8.11	0.00	1.01
DEV	.12	.31	0.19	0.19	0.14
APE1-dsRNAi 24h-1	16.40	22.98	6.58	-1.36	2.58
APE1-dsRNAi 24h-2	15.92	23.02	7.11	-1.05	2.07
APE1-dsRNAi 24h-3	15.86	23.08	7.22	-1.01	2.01
Average	16.06	23.03	6.97	-1.14	2.22
DEV	.30	.05	0.34	0.19	0.31

4.2.2 Optimization of monitoring c-myc mRNA stability in HeLa cells

By using transcriptional inhibitors, c-myc mRNA decay could be monitored. c-myc mRNA has been shown decay with a half-life of about 20 to 40 mins (Dani *et al.* 1984; Herrick and Ross 1994). A few candidate chemicals were initially selected and applied in our experiments using HeLa cells. Actinomycin D and alpha-amanitin were tested at a concentration of 5 μg/mL and 15 μg/mL, respectively (Figure 35A). It was found that at tested concentrations these two drugs were not able to inhibit transcription. Under such

conditions, monitoring c-myc mRNA decay was not feasible. Later, it was found that 5,6-dichloro-1-β-D-ribofuranosylbenzimidazole (DRB) at concentrations of 100 μM and 200 μM were able to inhibit transcription (Figure 35B). Apparent decay c-myc mRNA was observable after 30 mins of DRB incubation. We therefore chose DRB as the transcriptional inhibitor for our mRNA half-life studies.

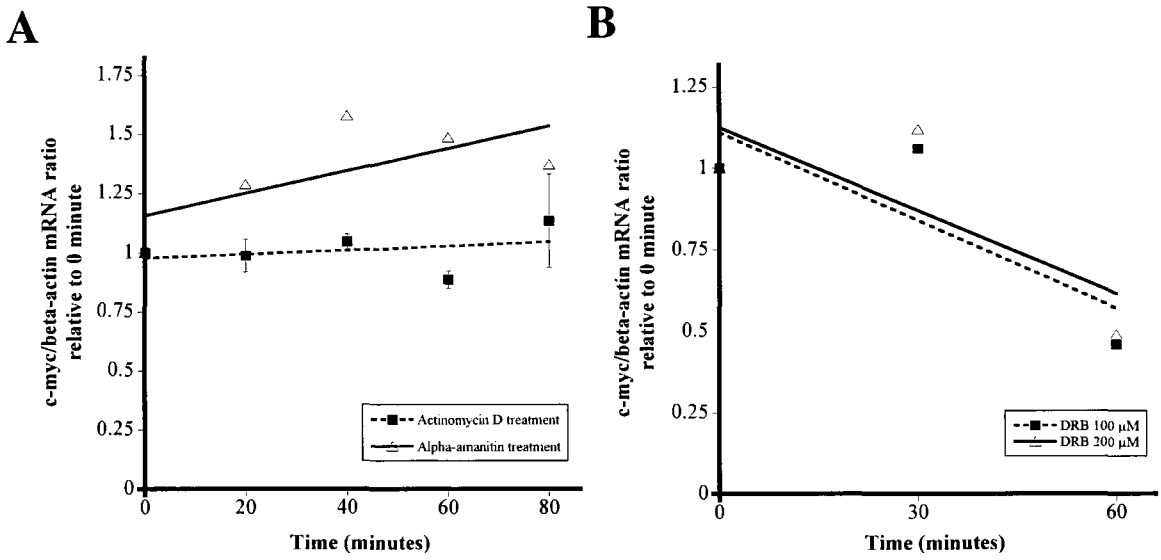

Figure 35: Level of c-myc mRNA monitored over time after treating cells with transcriptional inhibitor Actinomycin D, α-amanitin, and DRB. Cells were initially treated with Control-dsiRNAi over 24 hrs and qRT-PCR was performed on cDNA samples generated from total RNA extracted at different time points. **(A)** Data points from two experiments were pooled in treatment of cells with Actinomycin D (5 μg/mL). For Alpha-amanitin treatment (15 μg/ml), only one screening was carried out. **(B)** mRNA decay occurring at 60 mins after treatment with DRB (100 μM or 200 μM equivalent to 32 μg/ml or 64 μg/ml).

Cells were plated at a density of 5 x 10^4 cells/well and 200 μM DRB was applied after ~40 hrs of growth. At different time points, these cells were harvested and their total RNA were subjected to qRT-PCR to determine their relative levels of c-myc mRNA (Figure 36). It was found that at multiple time points, c-myc mRNA exhibited decay after treating cells with DRB. Over the course of 75 mins, 200 μM of DRB was able to inhibit transcription and c-myc mRNA decayed to about 20 % (Figure 36). The faster initiation of

mRNA decay compared to the previous observation in Figure 35B may have resulted from the higher ratio of DRB concentration to the cells. The decay plot showed after ~45 mins, c-myc mRNA decayed to ~50 % and this observation was in line to the previously reported half life of c-myc mRNA.

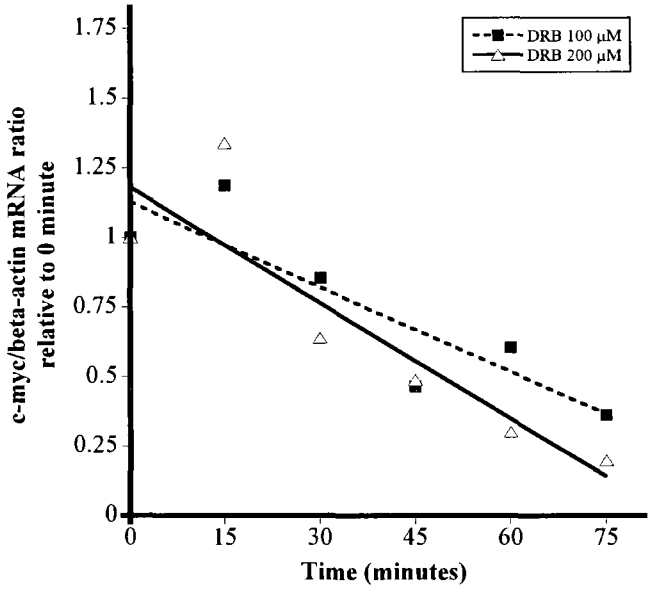

Figure 36: Decay of c-myc mRNA over time after treating cells with DRB. Cells were treated with Control-dsiRNAi over 24 hrs and then treated with DRB at two concentrations (100 μM & 200 μM). qRT-PCR was performed on cDNA samples generated from total RNA extracted at different time points.

4.2.3 Knock down of APE1 in HeLa cells stabilizes c-myc mRNA

To investigate the reason behind c-myc mRNA elevation, stability of c-myc mRNA in APE1-dsiRNAi treated samples was assessed (Figure 37). HeLa cells were plated at a density of 5 x 10^4 cells/well and transfected with either APE1-dsRNAi or Control-dsRNAi for 30 hrs before they were treated with 200 μM of DRB. It was found that the stability of c-myc mRNA in APE1-dsRNAi treated samples were enhanced up to 60 mins compared to the control which exhibited mRNA half-life of ~30 mins which is consistent with the previously

reported value (Dani *et al.* 1984; Herrick and Ross 1994). This experiment suggested that the increased expression of c-myc mRNA in APE1-knock down cells is in part due to increased transcript stability.

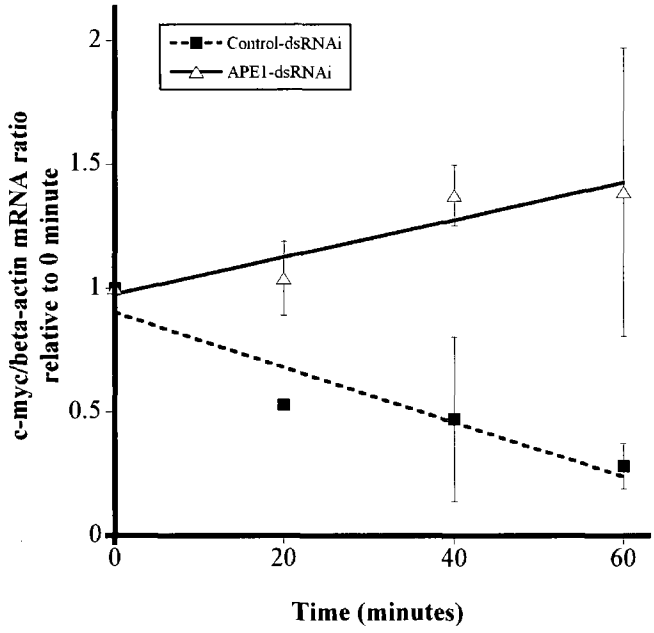

Figure 37: c-myc mRNA is stabilized after transient knock down of APE1 in HeLa cells. qRT-PCR was carried out on cDNA samples generated from harvested RNAs at three different time points to measure the relative levels of c-myc mRNA in both scramble dsiRNA and dsiRNA-APE1 treated HeLa cells. The difference in the slopes were determined to be significant by regression analysis ($p < 0.05$).

4.2.4 Origami cell transformation with pGEX4T3-Thioredoxin A and RNase A

The pGEX4T3 based vector carrying cDNAs for Thioredoxin A and RNase A were kindly provided as a gift from Dr. Ronald Raines, University of Wisconsin-Madison. When pGEX4T3-Thioredoxin A was transformed into Origami cells in an increasing amount of plasmids (10ng - 750ng), an increase in the numbers of colonies was observed (Figure 38).

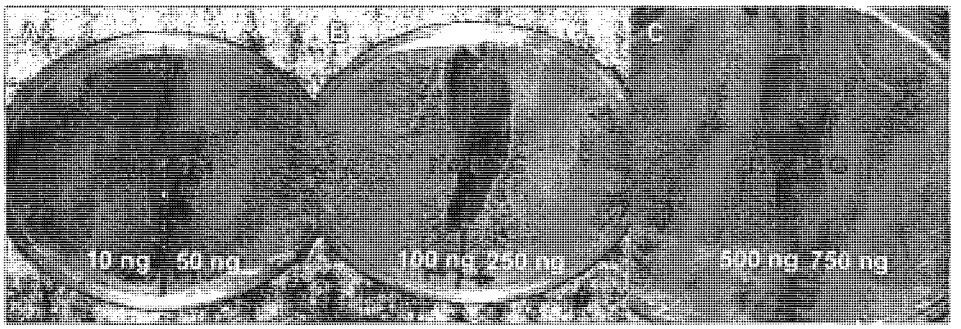

Figure 38: Transformation of Origami cells with increasing amounts of pGEX4T3-Thioredoxin A. (A) 10 ng and 50 ng of plasmids were used for transformation. **(B)** 100 ng and 250 ng of plasmids were used for transformation **(C)** 500 ng and 750 ng of plasmids were used for transformation.

Indeed, Thioredoxin A did not exert any ribonuclease activity in these cells and colonies were able to form. Also, this data gave us an idea on what amount of plasmids to use to observe an optimal level of cell growth. In contrast, when pGEX4T3-RNase A was transformed into Origami cells (Figure 39), no colonies were observed indicating cell death imposed by expressed RNase A. This is consistent with a previously reported study (Smith and Raines 2006). This gave us confidence to proceed with our investigation in assessing the WT APE1 and its mutants on the growth of Origami cells which would serve as a model to rapidly assess the endoribonuclease activity of APE1 in cells.

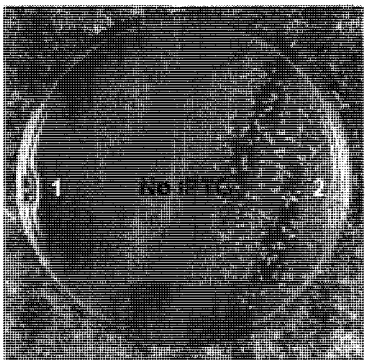

Figure 39: Transformation of Origami cells with pGEX4T3 plasmids carrying cDNAs for Thioredoxin A and Ribonuclease A. 10ng of pGEX4T3-RNase A (1) and pGEX4T3-Thioredoxin A (2) were used to transform 100 µl of Origami cells. The cells were heat shocked, recovered, and plated on LB-agar-Ampicillin plate as described in 4.1.5.

4.2.5 Induction of pET15b-WT-APE1 in Origami cells is toxic

The validity of this genetic selection was evaluated by observing the correlation between the *in vitro* activities of APE1 mutants (Table 9) and the death/survival of Origami cells after expressing these mutants. To test the effects of expressing APE1 WT and its mutants, we used pET15b based plasmids that carried cDNA sequences for His_{6x} tagged to the N-terminal end of the APE1 WT or mutants (Figure 40A). We also tested the effects of IPTG induction (Figure 40B). pET15b-Acetate Kinase, kindly provided by Dr. Andrea Gorrell, UNBC, was used as an inert control and was expected to allow cell growth.

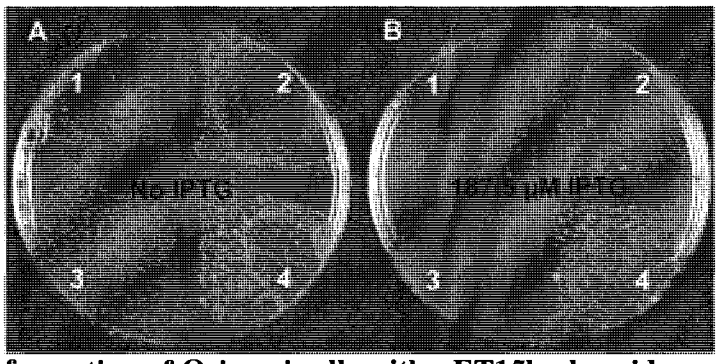

Figure 40: Transformation of Origami cells with pET15b plasmids carrying cDNAs for WT-APE1 and recombinant enzymes. 100ng of plasmids were used carrying cDNAs for WT APE1 (1), D148E (2), H255A (3), Acetate Kinase (AK) (4) in transforming 100 µl of Origami cells as described previously. IPTG were applied to Origami cells after their heat shock recovery of 40 mins at 37 °C. Two concentrations of IPTG are shown in the figure. **(A)** 0 µM **(B)** 187.5 µM.

Without IPTG, the WT APE1 allowed cell survival (region 1, Figure 40A), but inducing its expression instigated cell death as shown in region 1 of Figure 40B. Acetate kinase showed that this enzyme is not able to induce cell death both at 0 and 187.5 µM IPTG induction (region 4 in Figure 40A and 40B), which was in line with our expected results. However, we observed a discrepancy between the *in vitro* RNA cleavage activities of APE1 mutants and their expected effects in Origami cells. D148E was shown to have a reduced RNA cleaving activity *in vitro*, and was expected to have a non-toxic effect in Origami cells.

However, we found decreased/retarded growth in Origami cells upon transformation with D148E and induction with IPTG (Region 2, Figure 40A and B). In addition, H255A, later found to have reduced RNA cleaving activity *in vitro* (Kim S.E. *et al.*, unpublished results) also exerted toxic effects on Origami cells (Region 3, Figure 40A and 40B), raising the questions on the validity of this system in assessing the endoribonuclease activity of APE1.

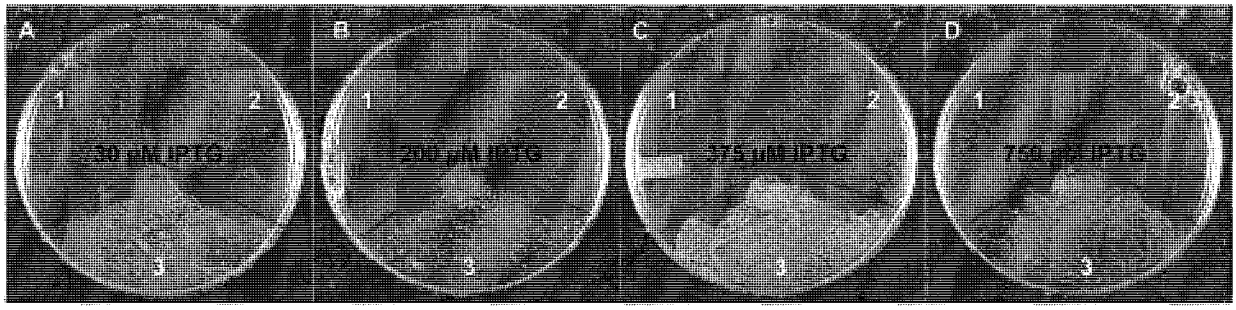

Figure 41: IPTG induces expression of APE1 WT, D283A, and H309N which exerts toxic/non-toxic effects in Origami cells. Increasing concentration of IPTG (**A**) 30 μM, (**B**) 200 μM, (**C**) 375 μM, (**D**) 750 μM were applied to Origami cells after their recovery of 40 mins at 37 °C. The regions of colonies transformed with pET15b-His6x based vectors carrying cDNA genes for D283A (1), WT APE1 (2), and H309N (3) are noted.

To further test the validity of this system, we tested the effects of pET15b based vectors carrying cDNAs for D283A and H309N (Figure 41). It was also found that as the amount of IPTG increased, fewer colonies were visible for the WT and D283A (Region 1 and 2, Figure 41A to D). This indicated that their increased expression was toxic to Origami cells, possibly via their functional ribonuclease activity. In addition, the number of colonies for H309N did not vary as much through out different IPTG concentrations tested (Region 3, Figure 41A to D). This indicated the increased expression of H309N is tolerant for cell growth, suggesting its ribonuclease activity is reduced or abrogated. Hence, the results of expressing these two mutants (D283A and H309N) in Origami cells agreed with the expected results from *in vitro* endonuclease assays showing D283N having similar activity as the WT

(Figure 9 and 10, section 2.2.2) and H309N having a severe reduction in RNA cleavage (Barnes *et al.* 2009).

Table 17: Summary of the results of Origami cell transformations using pET15b based plasmids coding for APE1 mutants and their RNA cleaving activities *in vitro*.

APE1 Mutants	Results after expression in Origami cells	Fold reduction in RNA incision (Table 9 and Table 10)
WT	Death	1
N68A	Death	Abolished
D70A	Death	55.6
E96A	Death	Not tested
D148E	Death	6.8
Y171F	Death	17.7
D210N	Death	8312.6
H255A	Death	Reduction (Kim S.E. *et al.*, unpublished results)
F266A	Death	Abolished
D283N	Death	4.0
H309N	Growth	Not tested

Therefore, to rigorously investigate the validity of this system, other mutants of APE1 were tested in Origami cells (Table 17). It was found that pET15b based vectors coding for N68A, E96A, Y171F, D210N, and F266A, all of which have shown severe reduction in RNA cleaving activity *in vitro*, were found to have toxic effects on Origami cells (data not shown). This suggested that the death/growth of Origami cells upon transformation with APE1 mutants to assess their endoribonuclease activities was not a reliable indicator since the results from the genetic screening did not correspond to what is expected from the *in vitro* assessment of enzymatic activities. Also, cell deaths induced by expressing most of these APE1 mutants meant that the distinction among these mutants were impossible.

The unknown effects of His_{6x} tag in the N-terminus of APE1 as well as the different plasmid (pET15b) system used by us may possibly explain the discrepancies seen in our system using APE1 and the previous report using pGEX-RNase A (Smith and Raines 2006).

Apart from the His_{6x} tag in our pET-APE1 vector systems, another difference between our pET-APE1 and their pGEX vector system (pGEX-RNase A) was that their pGEX-RNase A was designed to expresss RNase A without a GST tag. From our observations, pGEX system also gave similar transformation success comparable to our pET system when used at lower plasmid amount. Hence, pGEX4T3-WT APE1 and pGEX4T3-E96A were transformed into Origami cells. We found that Origami cells transformed with these plasmids showed no signs of cell death even at higher concentrations of IPTG used (Figure 42B and 42C). WT expression in these cells can not induce cell death, but allows visible growth. This indicated that the method can not be an effective way to compare the growth of cells expressing APE1 mutants. Our results showed that the growth of cells expressing E96A was less than that of the WT indicating notable a contrast to what is expected from their *in vitro* RNA-incision activities. Conclusively, this showed that genetic selection by plating Origami cells after transformation with pGEX4T3 based vector (Smith and Raines 2006) is not an optimal biological system to assess the effects of APE1 RNA cleaving activity.

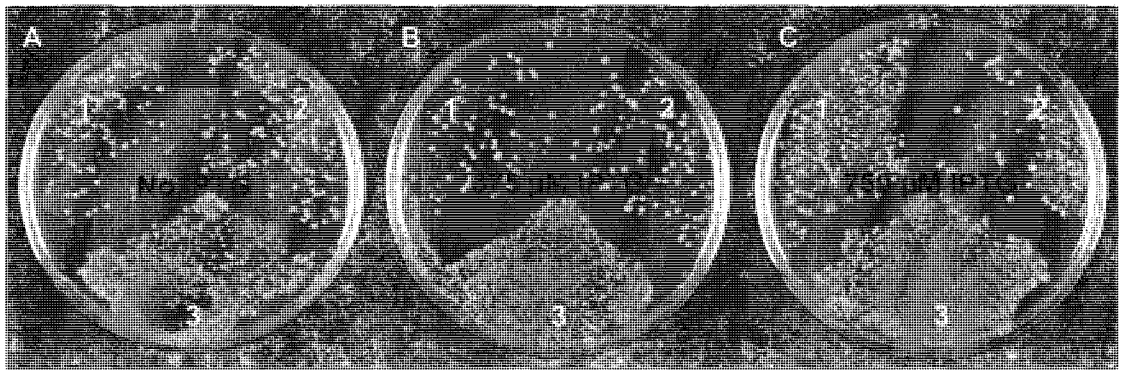

Figure 42: Transformation of Origami cells with pGEX4T3 plasmids carrying cDNAs for Thioredoxin A, WT-APE1, and E96A-APE1. Increasing concentration of IPTG (**A**) 0 μM, (**B**) 375 μM, (**C**) 750 μM were applied to Origami cells after their recovery of 40 mins at 37 °C. The areas of colonies transformed with pET-His6x based vectors carrying cDNA genes for WT APE1 (1), E96A (2), and Thioredoxin A (3) are noted.

CHAPTER 5

General discussion

5.1 Role of post-transcriptional control in cancer

A variety of trans-acting factors come into effect in the regulation of gene expression at the mRNA level. These factors include ncRNAs, RBPs, and RNases which can influence the degradation of transcripts, and thus the production of proteins (Kim and Lee 2009). Alterations in this process are caused by aberrant levels or activities of these factors which are also associated with tumorigenesis and cancer progression. Whether it is due to rapid degradation or prolonged half-life, several studies have provided the evidence which suggest that disrupted elements involved in mRNA turnover can give rise to abnormal levels of gene products as well as sustaining their effects (Kim and Lee 2009). Different trans-acting factors play their part in regulating the stability of oncogenic and tumor suppressive mRNAs (Figure 43), and alterations have been associated with the attenuation or the enhancement of mRNA degradation. For instance, HuR can stabilize a diverse population of mRNAs including oncogenic mRNAs like that of Bcl-2, Mcl-2, ERBB2, and VEGF-A that can elicit an anti-apoptotic effect as well as several matrix-metalloproteinases that have been associated with advance stage tumors (Abdelmohsen *et al.* 2007; Mook *et al.* 2004; Björklund and Koivunen 2005; Yan and Boyd 2007; Scott *et al.* 2008; Ido *et al.* 2008). Similar effects are reported with destabilizing RNA Binding Proteins as well as miRNAs and RNases. Decreased level of AUF1 was reported in proliferating lymphoma cells with increased levels of DENR/DRP mRNA that gives enhanced translation of several oncogenes (Reinert *et al.* 2006; Mazan-Mamczarz *et al.* 2007). In addition, miRNA let-7 in early stages of cancer was implicated in

the overexpression of oncogenes CRD-BP and HMGA2 (Boyerinas *et al.* 2008) as well as in integrin-beta-3 (Muller and Bosserhoff 2008).

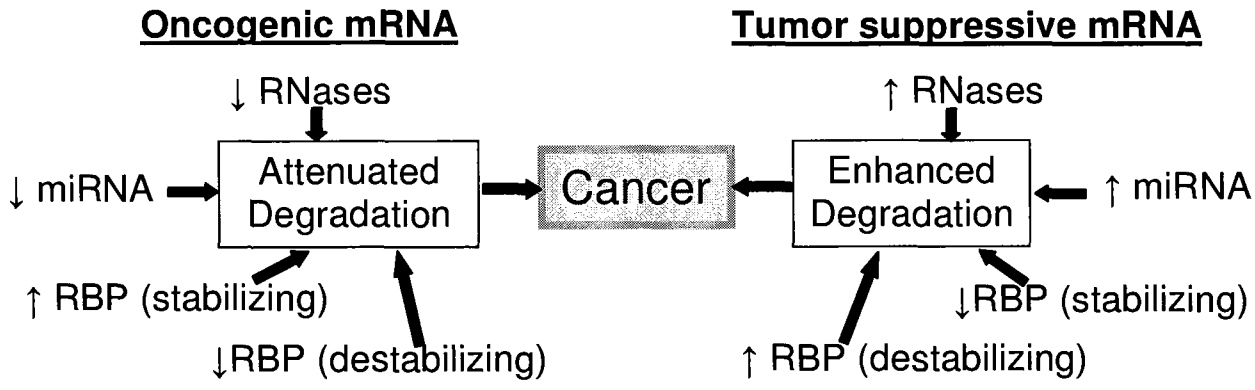

Figure 43: Altered post-transcriptional control in cancer (Kim and Lee 2009). Attenuated degradation of oncogenic mRNAs can lead to the development of cancer. This can be caused by the following factors on the left side. Decrease in the activity of ribonuclease (RNase) targeting such mRNAs as well as miRNAs that inhibit their translation and promoting mRNA decay can attenuate their degradation. Decrease in the activity of destabilizing RNA binding protein (RBP) while up-regulation in that of the stabilizing RBP can also have similar effects. Vice versa, enhanced degradation of tumor suppressive mRNAs can also lead to the development of cancer (Right side).

Overexpression of miR-135a and miR-135b is implicated in the down regulation of APC mRNA and its reduction implicated in colorectal cancer (Nagel *et al.* 2008). Similarly, miR-29c has been found to down-regulate oncogenic mRNAs implicated in tumor cell invasiveness and metastatic potential (Sengupta *et al.* 2008). In contrast, miR-106b family has been found to degrade p21/CDKN1A mRNA and promote cell cycle progression in immortalized cell lines (Ivanovska *et al.* 2008). Also, over-expression of miRNA-373 in a cancer cell line was shown to contribute to the down-regulation of CD44 mRNA which had implications in raising cells' metastatic potential (Huang *et al.* 2008).

5.2 Significance of identifying and studying RNases

RNases not only play a critical role in the turn over of various transcripts, but they also process RNAs that are required for translational control of gene expression. In eukaryotic mRNA degradation, a number of endonucleolytic cleavage intermediates have been reported. For example, decay intermediates have been detected for the transferrin receptor (Binder *et al.* 1989), albumin (Tharun and Sirdeshmukh 1995), urokinase (Timofeeva *et al.* 2000), insulin-like growth factor II (Van Dijk *et al.* 1998), α-globin (Wang and Kiledjian 2000), β-globin (Stevens *et al.* 2002), c-myc (Ioannidis *et al.* 1996), MDR1 (Lee *et al.* 2005), hepatitis B virus (Heise *et al.* 2001), and mRNAs with premature termination codons (PTC) (Gatfield and Izaurralde 2004).

In the past, only a handful of the responsible endoribonucleases have been identified presumably due to their specificities to limited number of substrates and having no sequence homology to known nucleases (Dodson and Shapiro 2002). Selected endoribonucleases have been described in section 1.1.1 of this thesis. Apart from these, there are also ErEN that was shown to cleave α-globin (Wang and Kiledjian 2000) and ARD-1 which was proposed to cleave 3' UTR of c-myc mRNA (Claverie-Martin *et al.* 1997). The limited numbers of identified mammalian endoribonucleases therefore warrant further studies to identify and study these groups of enzymes. In addition, in order to assess their influence on the mRNA decay and abundance, the mechanism of their catalysis and the significance their activities need to be studied.

Also, recent reports have highlighted the emerging roles of endoribonucleolytic mRNA decay in eukaryotic gene expression. For instance, Rrp44, previously found to possess an 3'-5' exonuclease activity in yeast exosome complex have also been found to

possess an endoribonuclease activity (Schaeffer *et al.* 2009). This finding is expected to remodel the conventional exonucleolytic mRNA decay revealing another layer of mRNA abundance control mechanism mediated through endoribonuclease. Another report demonstrated that SMG6, an enzyme associated in metazoan nonsense-mediated decay (NMD) pathway, can cleave at or near the site of the PTC endonucleolytically (Eberle *et al.* 2009). This indicated that for metazoan NMD, endonucleolytic decay can efficiently initiate this process and bypass the requirements for deadenylating/decapping of the transcript. In addition, discoveries of novel endoribonucleases, for instance, the DYW domain of the pentatricopeptide repeat protein (Nakamura and Sugita 2008) and tumor marker human placental protein 11 (Laneve *et al.* 2009) are being reported from recent studies. In contrast to the past where the role of endoribonucleases has been un-recognized, these reports have highlighted their major potential in mediating the post-transcriptional regulation of gene expression.

5.3 Benefits of studying RNases in health and therapeutics

The obvious benefit of discovering and studying RNases is in translational research where these enzymes and/or their properties can be used for the treatment of human diseases such as cancer. Particularly, exploiting their ability to control gene expression at the RNA level has been incorporated into similar oncogene inactivation strategies such as antisense oligonucleotides (ASOs), small interfering RNAs (siRNAs), ribozymes, and DNazymes. For example, ASOs and DNazyme have been used to specifically target *c-myc* mRNAs (Tafech *et al.* 2007) and inhibit tumorigenesis (Ponzielli *et al.* 2005; Tack *et al.* 2008). siRNAs targeting the mRNA of reverse transcriptase of human telomerase also have demonstrated their ability to decrease c-Myc levels in nasopharyngeal carcinoma (Wang *et al.* 2007).

Similarly, as a first of its class of anti-cancer agent, an RNase from Rana pipiens oocyte, Ranpirnase, has been extensively studied as a novel class of cancer chemotherapeutic. It is a homolog of bovine ribonuclease A that exhibits anti-tumor activity specific for cancer cells (Lee and Raines 2008). In combination with other agents such as doxorubicin, it is now being evaluated in treating breast cancers and non-small cell lung cancers, despite its shortcomings in recent phase IIIb trial. Another example is bovine seminal RNase (BS-RNase). The mechanism of its specificity toward cancer cells is not known yet (Benito *et al.* 2005), but against tumours induced in rats and mice, this RNase inhibits the tumours without any appearance of adverse side effects. Their potential and success thus far have encouraged development of such RNases to treat cancers. In addition, potencies and specificities of these RNases are expected to be improved through protein engineering and as the translational research progresses further, some of the known properties of other RNases may be applied towards therapeutic purposes. It is with these reasons, we chose to observe and document some of the important aspects of the novel RNA cleaving activity of APE1.

5.4 Identification of active site residues critical for RNA-cleaving activity of APE1

The first objective of this research was to identify the active site residues of APE1 in RNA cleavage. Previous studies on APE1 mutants tested against abasic DNA had given us the rationale to test whether these residues were also involved in RNA catalysis. Results from DNA incision assays on APE1 mutants revealed varying degrees of reduction in AP-DNA endonuclease activities amongst different mutants (refer to section 2.2.2). This had provided us with the basis for assessing these mutants for endoribonuclease activity. Results from APE1 against c-myc 1705-1792 CRD RNA and Oligo IB revealed moderate to severe reduction in RNA incision activity exhibited by these mutants. It is noteworthy that moderate

reductions observed in D70A and D308A agreed with previous suggestions that these two residues were involved in the coordination of metals during abasic DNA incision (Erzberger and Wilson 1999). It can be speculated that the absence of one of these residues may be relieved by the presence of the other and the mutant APE1 would be able to retain its RNA incision activity. In addition, the most severe reductions were observed from N68A and D210N, which were also in agreement with the previous reports. Both of these residues were previously suggested to have a critical role in the catalysis of abasic DNA incision activity, with N68 hydrogen bonding to D210 and H309 to allow optimal active site environment, while D210 participating in the generation of a nucleophile (Nguyen *et al.* 2000; Erzberger and Wilson 1999). Hence, the results showed that APE1 shares its active site residues in cleaving both abasic DNA and RNA. One particular result different from that of abasic DNA incision assays was the comparable RNA cleaving activity of D283N to that of the WT. Considering the role of D283 in the maintenance of the D283-H309 dyad (Hadi *et al.* 2000), our results indicated the alteration in this dyad may not be critical for RNA incision. However, it is still a critical component for abasic DNA incision (Hadi *et al.* 2000). To further confirm the dispensability of the dyad, we can test the RNA binding and cleavage ability of D283A, which will have no ability to hydrogen bond to H309, and compare these results with the data on its effect on abasic DNA.

Previously, H309N was shown to have a 2-fold reduction in its affinity towards abasic DNA (Masuda *et al.* 1998). This is in line with our preliminary data that showed its limited binding ability to RNA compared to the WT enzyme. Also, this indicated that H309 may be involved in the RNA-binding process and its mutation leads to reduced incision activity. Our results indicated that the residues (N68, E96A, Y171, and D210) from the active

site are not directly involved in RNA-binding, but are important in the catalytic step of RNA incision. D283N mutation may have affected the binding abilities to a certain extent (lanes 18 and 19), but at a higher concentration of the protein (lane 20), it displayed better binding than the WT (Figure 12B). This was consistent to the previous report testing its binding ability to abasic DNA where it showed less affinity than the WT at lower concentrations, but at higher concentrations, it showed better affinity than the WT (Masuda *et al.* 1998). Hence, the role of D283 in RNA-binding may not be as critical as H309. The binding abilities of E96A and D210N to abasic DNA were all comparable to that of the WT (Barzilay *et al.* 1995; Marenstein *et al.* 2004). Although the study on abasic DNA-binding abilities of N68A and Y171F has not been conducted yet, none of these active site mutants, except H309N, are expected to show alterations in the binding of DNA. It is because these residues are not part of the DNA-binding domains that are predicted to interact with abasic DNA (Mol *et al.* 2000). Similarly, our EMSA and endoribonuclease assays revealed that APE1 uses residues, N68, E96, Y171, D210, and D283, mainly for RNA incision. Hence, this similarity supports that APE1 shares these residues to incise abasic DNA as well as RNA.

During the progress of this research, we noticed that APE1 displayed similar RNA cleavage pattern to that of the RNase A. Hence, we attempted to test whether APE1 also utilized the two histidine residues to cleave RNA in a manner analogous to RNase A (Kim S.E. *et al.*, unpublished results). The candidate histidine pair (H255-H289) was chosen based on the three dimensional structure of APE1 generated by X-ray crystallography (Mol *et al.* 2000). We generated Ala mutants of these residues as well as generating Ala mutants for three other histidines (H116, H151, and H215) found in the sequence of APE1. It was found on endoribonuclease assays that the mutant H255A had reduction in its RNA-cleavage

activity, however, other mutants (H116A, H151A, H215A, H309N) also displayed moderate to severe reduction in RNA cleavage. This indicated that the effect of Ala mutations were not specific to H255-H289 pair, but altering histidines, in general, may have affected the overall conformation of APE1 that had altered its RNA cleaving activity. This would require further experimentation to confirm. Hence, results from screening our structural mutants revealed that APE1 shared its active site residues for abasic DNA incision as well as RNA incision.

In addition, we have screened the RNA cleaving activities of APE1 population variants. L104R and E126D retained their ability to cleave RNA but reduced activity against abasic DNA. Interestingly, in RNA cleavage, they also exhibited alterations in their cleavage sites compared to those of the WT. L104 is located in the loop region close to the DNA binding domain (Hadi *et al.* 2002). It is also speculated to be a part of hydrophobic packing constituted by L72, L108 and W119. Arg substitution may alter this packing which results in reduced DNA cleaving activity of APE1. It is also speculated that the DNA binding region may be altered by this substitution which can result in alternative RNA interaction that may render its activity to be RNasin-resistant. Alteration in the cleavage site may also result from this perturbation. This can arise from having Arg that has basicity instead of hydrophobicity. To further test the role of basicity in giving cleavage site alteration, mutants retaining this basicity can be generated such as L104N, L104Q. A mutant with a bulkier base, L104K, could also be tested. Also, the effects of hydrophobic packaging and the requirement of optimal side chain size similar to Leu could be tested. L104I which has a similar size but a different conformation and L104V which has one less -CH2- group can be tested of their RNA cleaving activities and binding.

E126 is located on one of the DNA binding domains and is near the AP-DNA phosphate backbone during AP-DNA binding (Mol *et al.* 2000). E126 is speculated to provide an important repulsive interaction, during this binding (Hadi *et al.* 2002). However, with E126D, it can be speculated that though it retains its negative charge, its effect may not be as great since it has been cut short of its side chain by one $-CH_2-$. This may in turn affect how different secondary structures of RNA may interact with APE1 and lead to alteration in cleavage specificities. To investigate the role of the negative charge, mutants of E126 may be generated and tested of their cleavage specificity. Mutants with basicities (E126Q or E126N) or mutants with no charge (E126L or E126I) may be tested. Also, variants of such mutations bearing smaller groups with no charge (E126G or E126A) or a bulkier group (E126F or E126W) with no charge may also be tested.

R237A was abrogated of its abasic DNA and RNA incision activities. R237 is located in α-helix number 9 (Hadi *et al.* 2002) that is near the DNA binding domain (Figure 4). It is speculated that R237A substitution imparts structural instability by disrupting the hydrogen-bonding network between R237-E216 and R237-E217 (Figure 4 & Hadi *et al.* 2002). To confirm the role of this network, mutants E216Q, E216D, E216N, E216A could also be generated and tested for their RNA and abasic DNA binding and cleavage activities. Similarly, mutations for E217 that disrupts its electrostatic state or the length of the side chain arm may also be tested.

The three variants, D148E, G241R, and G306A, all exhibited severe reductions in their RNA cleaving activities. This was in contrast to their functional abasic DNA incision activities (Figure 13, section 2.2.4 and Hadi *et al.* 2002), and to date no study has been done

extensively on these residues since their mutations had minimal effects on AP-DNA endonuclease activity.

D148 is located on the outer surface of APE1 and is likely to contribute in the interaction with RNA and/or in the maintenance of APE1 structure. The effect of its mutation to Glu, can further be investigated by generating mutants that can provide useful information. We can first test the requirement of acidity of D148 with D148N. We know the effect of gaining -CH2- from D148E showing loss of RNA cleaving activity. But, an additional effect of losing its acidity can be tested by D148Q. Also, the effect of gain in basicity and side chain bulk can be tested with D148H D148R, D148K. Further, the steric effects of D148 can be tested with having a constant hydrophobicity with an increase in side chain bulk (D148G < D148A < D148L < D148W).

G241 is located on α-helix number 9. Its mutation to Arg is expected to affect the local helical structure driven by the increase in side chain bulk and basicity. To test the effects of increase in side chain bulk and RNA catalysis, we can test the mutants with a gradual increase in side chain size (G241A < G241V < G241L < G241F). Also, the effects of basicity can be tested by testing mutants with (G241K or G241H) and compared to acidic residues (G241D or G241E).

G306 is closely located to a critical residue H309 and its Gly to Ala mutation may perturb the local structure sterically through a gain of -CH3 group. The effect of G306A has not been described thus far, and by testing the presence charge (acidic and basic) and the increase in side chain bulk, we could gain more knowledge into its role in maintaining the local structure. To test the effects of charge, one can generate G306D, G306E, G306H,

G306R, and G306K. To test the effects of side chain size, one can generate mutants of increasing side chain size (G306V < G306L < G306F < G306W).

In the future, assessing the effects of D148E, G241R, or G306A versus R237A in cultured cells would produce interesting results since the first group showed reductions in RNA cleavage but functional DNA repair activity and the R237A showed abrogation in both of these activities. The implications drawn from these biological studies may reveal a novel link between reductions in APE1 RNA cleavage activity and human diseases.

5.5 Role of metal ions in APE1 RNA-cleaving activity

Many nucleases that cleave DNA or RNA utilize metal ions for their catalysis (Wang 2008). Against a standard abasic DNA substrate, APE1 requires divalent metal ions for its optimal activity (Erzberger and Wilson 1999; Wilson 2005). It is reported that these metal ions occupy the active site to stabilize the transition state during DNA incision, and facilitate the release of the incised product. Previously, it was found that Mg^{2+}, Mn^{2+}, Ni^{2+}, and Zn^{2+} was able to rescue an EDTA-inactivated APE1 incision activity on an abasic DNA substrate, but Ca^{2+} could not (Barzilay *et al.* 1995). Another study found Ni^{2+} and Zn^{2+} ions permitted the DNA incision activity up to concentrations of 100 μM (Ni^{2+}) and 50 μM (Zn^{2+}) (Wang *et al.* 2006). These reports suggest that APE1 RNA-cleaving activity may also require divalent metal ions for its catalysis.

In comparison with these reports, our results showed a similar trend (refer to section 2.2.7). APE1 was able to cleave RNA without the presence of divalent metal ions and showed a range of [Mg^{2+}] for its optimal activity in our experimental setting. The results indicated that APE1 RNA cleaving activity is best enhanced at 5 mM of Mg^{2+}, but other concentrations also allowed incision to take place. The observable RNA cleaving activity of

APE1 at 0 mM Mg^{2+} is in agreement with previous reports. APE1 has previously been found to weakly cleave abasic DNA in the presence of EDTA (Masuda *et al.* 1998), and particularly has exhibited EDTA-resistant activity towards acyclic substrates that are considered to have better flexibility (Erzberger *et al.* 1999). Single stranded RNA structures (e.g. hairpin loops) are particularly more flexible than those of RNA stems and abasic DNAs, which could allow APE1 to cleave such RNA substrates without their divalent metal cofactors.

APE1 was inhibited by 2 mM of Ni^{2+}, and Zn^{2+} which was in contrast to the reports on abasic DNA incision that was active even under 100 μM (Ni^{2+}) and 50 μM (Zn^{2+}) (Wang *et al.* 2006). These two metal ions have been shown to interact with amino acid histidine in other proteins to inhibit their enzymatic activities (Okamura *et al.* 2003; Kang *et al.* 2007). Presence of these metal ions may therefore affect the amino acid residues that are specifically critical for RNA catalysis of APE1. Alternatively, these metal ions can affect the secondary structure of RNA substrates and interfere with APE1 binding to these RNAs or interfere with their release after incision. Further testing by EMSA in the presence of these metal ions may clarify such questions.

5.6 Role of N-terminus in APE1

Although no experimentation was done in this research on elucidating the role of N-terminus in APE1, it may be still noteworthy to mention some of the previous findings in better understanding the APE1-RNA interaction. Recently, co-immunoprecipitation of WT APE1 had shown APE1 binding to the endogenous rRNAs (47S, 28S, and 18S) in HeLa cells. Interestingly, the NΔ33 APE1 deletion mutant had lower ability to bind to rRNAs, indicating the important role of N-terminus in APE1 RNA binding to rRNAs (Vascotto *et al.*

2009). *In vitro* EMSA study showed that NΔ33 APE1 had significantly less ability to bind to single stranded 34nt RNA compared to the WT at tested enzyme amounts of 0.9 and 1.8 μg. In addition, endonuclease assays showed the abasic RNA incision activity of NΔ33 APE1 was weaker than that of the WT. Interestingly, abasic DNA incision activity of NΔ33 APE1 was stronger than that of the WT. This indicated that N-terminus is important in RNA binding ability of APE1. However, it is still unknown, how much is contributed from these N-terminal residues and the residues from the five APE1 DNA-binding regions (Mol *et al.* 2000) in RNA-APE1 interaction. Upon assessing their contributions *in vitro*, the role of these residues can be further pursued in cells for their effects in RNA decay.

In regards to APE1-protein interaction, it was found that the first 33 N-terminal amino acids of APE1 are essential for stabilizing the interaction of APE1 with ribosomal and RNA processing factors such as, NPM1, pre-mRNA-processing factor 19 (PRP19), and 60S acidic ribosomal protein P0 (Vascotto *et al.* 2009). In nuclear localization, APE1 was shown to interact with nuclear importins as demonstrated by co-immunoprecipitation with karyopherin α1 and α2. This interaction was found to require the first 20 residues of APE1 (Jackson *et al.* 2005).

It was found that NΔ20 APE1 was re-distributed to the cytoplasm (Jackson *et al.* 2005). This indicated a presence of nuclear localization signal (NLS) within the 20 residues. Further, it was found that APE1 possessed two independent NLS with first signal present at residues 1 to 7 and the second at 8-13. For a significant cytosolic re-distribution, both of these signals need to be deleted/mutated as demonstrated by visualizing NΔ7-E12A/D13A APE1 in the cytoplasm. In addition, treating cells with leptomycin B inhibited the nuclear export of NΔ7-E12A/D13A APE1. Leptomycin B is a common inhibitor for nuclear export

protein, CRM1 which was shown to interact with APE1, indicating that APE1 may possess a nuclear export signal. However, further investigation is required to confirm this hypothesis.

One study reported significant re-distribution of APE1 to the cytoplasm upon RNase treatment of permeable cells pre-treated with Triton X-100 (Vascotto *et al.* 2009). This suggested that the RNA binding was in part a mechanistic factor in APE1 nuclear localization. This hypothesis may explain NΔ33 APE1, with presumably less RNA binding ability, to be predominantly redistributed to the cytoplasm (Chattopadhyay *et al.* 2006). This indicated that the RNA binding ability of APE1 is important for its localization in the cytoplasm and the role of N-terminus may act as an important functional determinant in different cell compartments. However, it is unclear the mechanistic detail of how this RNA binding ability of APE1 becomes utilized in nuclear localization of APE1.

In vitro assay showed that APE1 was preferentially ubiquitinated at residues K24 and K25, and somewhat less at K27. In addition, nuclear export was observed with a fusion protein, APE1(1–23)-ubiquitin (G76A)-APE1(24–318). Also, independent of CRM1, a nuclear exportin, APE1 can be exported out of the nucleus by nitrosylation at residues C93 and C310 (Qu et al. 2007).

Hence, the role of the first 33 amino acids constituting the N-terminus is still unclear. APE1 has been shown to be redistributed across nucleus and cytoplasm depending on the cellular conditions and cell types (Tell *et al.* 2005). In contrast to the aforementioned results on NΔ33 APE1, a similar truncated mutant NΔ34 APE1 was found to have increased 3'-5' DNA exonuclease activities that carries out chromatin fragmentation in apoptotic HL-60 cells which also showed predominant nuclear localization (Yoshida *et al.* 2003). Hence,

further characterization on the role of N-terminal residues in RNA binding/cleaving activities and how it relates to the subcellular localization need to be investigated.

5.7 RNA secondary structure and sequences preferentially cleaved by APE1

The second objective of this research was to establish the RNA structure and sequences cleaved by APE1. We found that APE1 can cleave multiple RNAs when presented *in vitro* (refer to section 3.2.2). APE1 cleavage sites were predominantly located in the single stranded regions of the RNA substrate with dinucleotide sequences of UA, UG, and CA. In addition, new cleavage sites were found though very weak compared to the aforementioned sequences and they were UC, CU, AC, and AU.

To account for the preferred cleavages of single stranded regions or weak stems of RNA, we have to consider how APE1 recognizes its main substrate, the abasic DNA. In abasic DNA cleavage, APE1 interacts strongly with an abasic deoxyribose flipped out of the DNA helix and tightly binds to this moiety facilitated by a hydrophobic pocket composed of Phe 266, Trp 280, and Leu 282. Such tight packing expels the binding of regular nucleotides and gives specificity towards the abasic sites (Mol *et al.* 2000). Similarly in RNA cleavage, we speculate that APE1 can recognize some of these extra helical bases found in the single stranded regions or in the weak stems of RNA. It is because the individual RNA nucleotides in these 'flexible' regions may act similarly in conformational or chemical context to the abasic nucleotide. It was found that single stranded regions of RNA as in the case of RNA hairpin loops have their bases flipping outwards from the centre of the loop which allow RNA binding proteins to easily interact (De Guzman *et al.* 1998). Such similarity may account for the preferential activity of APE1 for RNA structures that have weak stems or single stranded regions. However, RNA nucleotides with normal bases retain polarities, and

we expect their interactions with the hydrophobic pocket to be weak and, hence, should explain the strong preference of APE1 for abasic DNAs over RNAs. It is noteworthy that F266A was shown to have severe reduction in endoribonuclease activity only (Figure 10A, section 2.2.2), but not its phosphodiesterase activity (Hadi *et al.* 2002). This also supported the proposal that F266 being in the hydrophobic pocket is a critical component in endoribonuclease activity of APE1 by recognizing RNA bases and accounts for its preference to cleave in the single stranded regions or weak stems of RNA. Future studies can confirm the role of this hydrophobic pocket in RNA binding and cleavage by generating Ala mutants of Trp 280 and Leu 282.

The residues of APE1 responsible for conferring specificity for pyrimidines still need to be identified. But, some insights can be drawn from the example of RNase A. In recognition of its substrate, RNase A uses residue Thr 45 for recognition to cleave poly Cs and poly Us. Such specificity is facilitated by specific hydrogen bonds between the side chain -OH with –NH (pyrimidine) and the main chain –NH and =O (pyrimidine) (Raines 1998). In APE1 RNA cleavage specificity, Thr 268 could serve a similar purpose, which is located near the hydrophobic pocket of APE1 (Phe 266-Trp 280-Leu 282) for recognizing the extra helical abasic deoxyribose (Mol *et al.* 2000) and it also may require further mutagenesis studies to validate its role. Testing T268G or T268A may show indications of how this residue plays its role in giving RNA cleavage specificities.

However, we should bear in mind the results from L104R and E126D giving altered cleavage specificity. The positions of these two residues are also close or on the domain that is known to interact with DNA (Mol *et al.* 2000). This indicates that the alteration in the cleavage site can result from the perturbation of local APE1 structure that can also likely

affect the RNA binding ability of APE1 and can not be attributed solely to a specific putative residue like Thr 268.

Pre-treatment of pre-miRNAs with APE1 significantly reduced the ability of DICER to process these substrates *in vitro* (refer to section 3.2.4). This implies that APE1 could potentially influence the level of mature miRNA in cells. Such speculation could be tested by looking at the changes in mature miRNA levels after knocking down or over-expressing APE1. Identification of interaction partners especially with the components of micro RNA ribonucleoprotein complex or pri- or pre-miRNA processing machineries could reveal a novel role of APE1 in miRNA maturation pathway.

5.8 Assessment of biological significance of RNA-cleaving activity of APE1

There were a number of reports from the past that had speculation as to the identity of the enzyme responsible for the endonucleolytic decay of c-myc mRNA (Swartwout and Kinniburgh 1989; Wisdom and Lee 1991; Morello *et al.* 1993; Herrick and Ross 1994; Ioannidis *et al.* 1996; Yeilding and Lee 1997; Hanson and Schoenberg 2001). Indeed, APE1 has been found to be present in the nucleus, cytoplasm, and mitochondria of the cell (Tell *et al.* 2005; Chattopadhyay *et al.* 2006). However, for certain cell types such as macrophages, spermatocytes, hippocampal cells, hepatocytes, hypoglossal motor neurons, and breast cells, APE1 has been found to be prevalently localized in the cytoplasm (Evans *et al.* 2000). Indeed, redistribution of APE1 into the cytoplasm raised further questions in elucidating its role in that compartment. Previously in our lab, APE1 had been purified from rat liver polysomal fraction that gave a hint to its role in RNA metabolism (Bergstrom *et al.* 2006). In addition, recent report showed that APE1 could cleave abasic RNA (Berquist *et al.* 2008) *in vitro* and this was followed by a report on abasic RNA cleavage in cells (Vascotto *et al.*

2009). These evidence further support the role of APE1 in RNA metabolism. Hence, the third objective of this research was to assess the endoribonuclease activity of APE1 in biological systems.

To investigate this matter, we observed the c-myc mRNA expression after APE1 has been transiently knocked down by siRNA technology in HeLa cells (refer to section 4.2.1).

Our results revealed that there was an increase in the expression levels of c-myc mRNA when APE1 was transiently knocked down. On one note, this result contradicted with an earlier report that in HeLa cell line, a conditional APE1 expression knockdown by RNAi leads to a modest reduction in the levels of c-myc mRNA (Vascotto *et al.* 2009). However, we speculate that the experimental condition in this particular study had APE1 knocked down for 10 days, and in this setting, unidentified compensatory mechanisms could reverse the elevation of c-myc mRNA levels.

Hence, it was intriguing to speculate the causes behind the elevation in c-myc mRNA. First, reduction in APE1 may have resulted in the attenuation of c-myc mRNA decay. Second, reduction in APE1 may have led to a decrease in the transcriptional repressor of c-myc mRNA. In agreement with the first possibility, our results showed that APE1 knock down in HeLa cells can enhance the stability of c-myc mRNA, indicating its direct involvement in c-myc mRNA turnover (refer to section 4.2.3). The mechanistic pathway for the second possibility is still unknown and requires further investigations. This was the first report in cells that APE1 can act as a regulator of RNA stability. Microarray studies that can provide information on the global changes of mRNA abundance for tens of thousands of genes (Lockhart and Winzeler 2000) can reveal potential APE1 targeted mRNAs. These

mRNAs can be further looked at for their turnover in APE1 knocked down cells. Such studies are expected to provide further insights into the role of APE1 in mRNA decay.

Nonetheless, the role of APE1 should not be limited to RNA decay. Its activity may have other biological implications that require further studies. There was evidence that suggested the likeliness of APE1 being involved in RNA processing. One of the initial findings showed that APE1 can associate with hnRNP-L in cells (Kuninger *et al.* 2002), a master regulator in pre-mRNA splicing which was also shown to control the stability of human VEGF mRNA during hypoxia (Shih and Claffey 1999). Later, APE1 was also shown to interact with YB-1, an RNA binding protein and a splicing factor (Stickeler *et al.* 2001; Chattopadhyay *et al.* 2008), giving further support to the possibility of APE1 involved in RNA processing.

Also, APE1 was also found to stably interact with NPM1, an RNA binding protein involved in the RNA maturation and processing (Vascotto *et al.* 2009). From this study, APE1 was found to strongly associate with rRNAs in HeLa cells and had the ability to cleave abasic RNAs. Presence of NPM1 was inhibitory to this activity and was thought to instigate a fine tuning of APE1 in the process of rRNA quality control.

Testing the effects of APE1 and its mutants in Origami cells revealed significant deviations from our *in vitro* data (refer to section 4.2.4 & 4.2.5). This indicated that observing the colony formation to assess the RNA-cleaving function of APE1 was not feasible. The method was adopted from a study that had successfully tested the activities of the WT versus the active site mutants of RNase A and Angiogenin (Smith and Raines 2006). RNase A and Angiogenin are both part of a ribonuclease A superfamily that have protein sizes < 20kDa. Their function is solely dedicated for hydrolyzing RNA and this is in contrast

to APE1 which is a larger protein capable of exerting multiple activities in cells including DNA repair activities, redox activation of transcription factors, 3'-5' exonuclease, phosphodiesterase, RNase H, and endoribonuclease activities (Tell *et al.* 2005; Barnes *et al.* 2009). Hence, APE1 may exert any of these functions in Origami cells making it uncertain whether the effect on cell growth is solely attributed to its endoribonuclease activity. In addition, the method of observing colony formation after transforming cells heavily depends on the transformation efficiency, compromising the evaluation of the effect of protein expression less clear. A possible way to overcome this problem would be to assess the growth of these cells in solution supplemented by medium and IPTG. This way we could monitor the growth of cells not depending on transformation efficiency but on the level of protein production and its activity.

5.9 Concluding remarks

This research was designed to understand the three main aspects of the endoribonuclease activity of APE1. First, we have confirmed the importance of catalytic residues that are required for this activity. APE1 mutants having one of these essential residues substituted with another amino acid displayed moderate to severe reductions in RNA catalysis. From these results, it is likely that APE1 shares these residues for cleaving abasic DNA as well as RNA, however, certain residues may play different roles during each reaction. We have also documented the RNA cleaving activities of the APE1 variants found in human populations. Interestingly, a few of these variants displayed severe reductions in RNA incision in contrast to their functional abasic DNA endonuclease activities. Hypothetically, an APE1 variant with functional DNA repair activity, but dysfunctional RNA cleaving activity has implications for aberrant RNA processing and turnover. Biological

work in understanding the role of these variants in RNA catalysis may generate valuable insights into understanding a few of their associations with cancers. We have also discovered important biochemical properties of APE1 in its RNA catalysis. APE1 is active in RNA cleaving without the presence of divalent metal ions and leaves RNA products with 3' phosphate as well as suggested to implement an acid-base catalysis mechanism in cleaving RNA. Second, APE1 is able to cleave multiple RNAs when presented *in vitro* and has the preference to cleave in the single stranded regions or weak stems. It prefers to cleave after pyrimidines and shows its strongest activity towards dinucleotides of UA, UG, and CA. Further studies are required to identify the residue(s) in giving pyrimidine specificity. Third, we have assessed the role of APE1 as the regulator of mRNA stability. Our results have shown that the knock down of APE1 resulted in the elevation of c-myc mRNA and is directly responsible for its enhanced stability. This finding warrants further studies on the regulation of its ribonuclease activities in cells. The sub-cellular localization and expression levels of APE1 were found to be altered by external stimuli (Tell 2005). These include cellular signals initiated by oxidative stress, hypoxia, and ischemia. The relationship between the changes in such stimuli and the ribonuclease activity of APE1 has not been investigated. In addition, more studies are required to reveal how APE1 interacts with RNA binding proteins or processing enzymes involved in pre-mRNA maturation and processing pathway. The contribution of ribonuclease activity of APE1 in these interactions and how such activity affects the mRNA processing or degradation still awaits further experimentation. Future studies focused on the identification of APE1-associated cellular RNAs and APE1-interacting proteins involved in the post transcriptional controls or translation are expected to generate further insights.

References

Abdelmohsen, K. Lal, A. Kim, H.H. and Gorospe, M. (2007) Posttranscriptional orchestration of an anti-apoptotic program by HuR. *Cell Cycle*, **6**, 1288-1292.

Adams, S.A. and Subramanian, V. (1999) The angiogenins: an emerging family of ribonuclease related proteins with diverse cellular functions. *Angiogenesis*, **3**, 189-199.

Adams, B.D., Claffey, K.P., White, B.A. (2009) Argonaute-2 expression is regulated by epidermal growth factor receptor and mitogen-activated protein kinase signaling and correlates with a transformed phenotype in breast cancer cells. *Endocrinology*, **150**, 14-23.

Asangani, I.A., Rasheed, S.A., Nikolova, D.A., Leupold, J.H., Colburn, N.H., Post, S. and Allgayer, H. (2008) MicroRNA-21 (miR-21) post-transcriptionally downregulates tumor suppressor Pdcd4 and stimulates invasion, intravasation and metastasis in colorectal cancer. *Oncogene*, **27**, 2128-2136.

Audic, Y. and Hartley, R.S. (2004) Post-transcriptional regulation in cancer. *Biol Cell*, **96**, 479-498.

Bandyopadhyay, S., Sengupta, T.K. and Spicer, E.K. (2008) PMA induces stabilization of oncostatin M mRNA in human lymphoma U937 cells. *Biochem J*, **410**, 177-186.

Barnes, T., Kim, W-C., Mantha, A., Kim, S-E., Izumi, T., Sankar, M. and Lee, C. H. (2009) Identification of apurinic/apyrimidinic endonuclease (APE1) as the endoribonuclease that cleaves c-*myc* mRNA. *Nucleic Acids Res,* doi: 10.1093/nar/gkp275.

Barreau, C., Paillard, L. and Osborne, H.B. (2006) AU-rich elements and associated factors: are there unifying principles?. *Nucleic Acids Res*, **33**, 7138-7150.

Bartsch, D.K., Fendrich, V., Slater, E.P., Sina-Frey, M., Rieder, H., Greenhalf, W., Chaloupka, B., Hahn, S.A., Neoptolemos, J.P. and Kress, R. (2005) RNASEL germline variants are associated with pancreatic cancer. *Int J Cancer*, **117**, 718-722.

Barzilay, G., Mol, C.D., Robson, C.N., Walker, L.J., Cunningham, R.P., Tainer, J.A. and Hickson, I.D. (1995) Identification of critical active-site residues in the multifunctional human DNA repair enzyme HAP1. *Nat Struct Biol*, **2**, 561-568.

Barzilay, G., Walker, L.J., Robson, C.N. and Hickson, I.D. (1995) Site-directed mutagenesis of the human DNA repair enzyme HAP1: identification of residues important for AP endonuclease and RNase H activity. *Nucleic Acids Res*, **23**, 1544-1550.

Beernink, P.T., Segelke, B.W., Hadi, M.Z., Erzberger, J.P., Wilson, D.M.3rd. and Rupp, B. (2001) Two divalent metal ions in the active site of a new crystal form of human apurinic/apyrimidinic endonuclease, APE1: implications for the catalytic mechanism. *J Mol Biol.* **307**, 1023-1034.

Benito, A. Ribó, M. and Vilanova, M. (2005) On the track of antitumour ribonucleases. *Mol Biosyst*, **1**, 294-302.

Bergstrom, K., Urquhart, J.C., Tafech, A., Doyle, E. and Lee, C.H. (2006) Purification and characterization of a novel mammalian endoribonuclease. *J Cell Biochem*, **98**, 519-537.

Bernales, S., Papa, F.R. and Walter, P. (2006) Intracellular signaling by the unfolded protein response. *Annu Rev Cell Dev Biol*, **22**, 487-508.

Bernstein, P.L., Herrick, D.J., Prokipcak, R.D. and Ross, J. (1992) Control of c-*myc* mRNA half-life *in vitro* by a protein capable of binding to a coding region determinant. *Genes Dev*, **6**, 642-654

Berquist, B.R., McNeill, D.R. and Wilson, D.M.3rd. (2008) Characterization of abasic endonuclease activity of human Ape1 on alternative substrates, as well as effects of ATP and sequence context on AP site incision. *J Mol Biol*, **379**, 17-27.

Bettoun, D.J., Scafonas, A., Rutledge, S.J., Hodor, P., Chen, O., Gambone, C., Vogel, R., McElwee-Witmer, S., Bai, C., Freedman, L. and Schmidt A. (2005) Interaction between the androgen receptor and RNase L mediates a cross-talk between the interferon and androgen signaling pathways. *J Biol Chem*, **280**, 38898-38901.

Binder,R., Hwang,S.P., Basilion,J.P., Koeller,D.M., Klausner,R.D., and Harford,J.B. (1994) Degradation of apolipoprotein II mRNA occurs via endonucleolytic cleavage at 5'-AAU-3'/5'-UAA-3' elements in single-stranded loop domains of the 3'-noncoding region. *EMBO J*, **13**, 1969-1980.

Bisbal, C., Silhol, M., Laubenthal, H., Kaluza, T., Carnac, G., Milligan, L., Le Roy, F. and Salehzada, T. (2000) The 2'-5' oligoadenylate/RNase L/RNase L inhibitor pathway regulates both MyoD mRNA stability and muscle cell differentiation. *Mol Cell Biol*, **20**, 4959-4969.

Bisbal, C. and Silverman, R.H. (2007) Diverse functions of RNase L and implications in pathology. *Biochimie*, **89**, 789-798.

Björklund, M. and Koivunen, E. (2005) Gelatinase-mediated migration and invasion of cancer cells. *Biochim Biophy Acta*, **1755**, 37-69.

Blenkiron, C., Goldstein, L.D., Thorne, N.P., Spiteri, I., Chin, S.F., Dunning, M.J., Barbosa-Morais, N.L., Teschendorff, A.E., Green, A.R., Ellis, I.O., Tavare, S., Caldas, C. and Miska, F.A. (2007) MicroRNA expression profiling of human breast cancer identifies new markers of tumour subtype. *Genome Biol*, **8**, R214.

Boyerinas, B., Park, S.M., Shomron, N., Hedegaard, M.M., Vinther, J., Andersen, J.S., Feig, C., Xu, J., Burge, C.B., Peter, M.E. (2008) Identification of let-7-regulated oncofetal genes. *Cancer Res*, **68**, 2587-2591.

Cai, X. and Cullen, B.R. (2007) The imprinted H19 noncoding RNA is a primary microRNA precursor. *RNA*, **13**, 313-316.

Calderwood, S.K., Khaleque, M.A., Sawyer, D.B. and Ciocca D.R. (2006) Heat shock proteins in cancer: chaperones of tumorigenesis. *Trends Biochem Sci*, **31**, 164-172.

Chandrasekaran, K., Mehrabian, Z., Li, X.L. and Hassel, B. (2004) RNase-L regulates the stability of mitochondrial DNA-encoded mRNAs in mouse embryo fibroblasts. *Biochem Biophys Res Commun*, **325**, 18-23.

Chattopadhyay, R., Das, S., Maiti, A.K., Boldogh, I., Xie, J., Hazra, T.K., Kohno, K., Mitra, S. and Bhakat, K.K. (2008) Regulatory role of human AP-endonuclease (APE1/Ref-1) in YB-1-mediated activation of the multidrug resistance gene MDR1. *Mol Cell Biol*, **28**, 7066-7080.

Chattopadhyay, R., Wiederhold, L., Szczesny, B., Boldogh, I., Hazra, T.K., Izumi, T. and Mitra, S. (2006) Identification and characterization of mitochondrial abasic (AP)-endonuclease in mammalian cells. *Nucleic Acids Res*, **34**, 2067-2076.

Chen, C.Y. and Shyu, A.B. (1995) AU-rich elements: characterization and importance in mRNA degradation. *Trends Biochem Sci*, **20**, 465-470.

Chen, D.S., Herman, T. and Demple, B. (1991) Two distinct human DNA diesterases that hydrolyze 3'-blocking deoxyribose fragments from oxidized DNA. *Nucleic Acids Res*, **19**, 5907-5914.

Chen, Y., Zhang, S., Chen, Y.P. and Lin, J.Y. (2006) Increased expression of angiogenin in gastric carcinoma in correlation with tumor angiogenesis and proliferation. *World J Gastroenterol*, **12**, 5135-5139.

Chernokalskaya, E., Dompenciel, R. and Schoenberg, D.R. (1997) Cleavage properties of an estrogen-regulated polysomal ribonuclease involved in the destabilization of albumin mRNA. *Nucleic Acids Res*, **25**, 735–742.

Chiosea, S.I., Barnes, E.L., Lai, S.Y., Egloff, A.M., Sargent, R.L., Hunt, J.L., and Seethala, R.R. (2008) Mucoepidermoid carcinoma of upper aerodigestive tract: clinicopathologic study of 78 cases with immunohistochemical analysis of Dicer expression. *Virchows Arch*, **452**, 629-635.

Chiosea, S., Jelezcova, E., Chandran, U., Acquafondata, M., McHale, T., Sobol, R.W. and Dhir, R. (2006) Up-regulation of dicer, a component of the MicroRNA machinery, in prostate adenocarcinoma. *Am J Pathol*, **169**, 1812-1820.

Chiosea, S., Jelezcova, E., Chandran, U., Luo, J., Mantha, G., Sobol, R.W. and Dacic, S. (2007) Overexpression of Dicer in precursor lesions of lung adenocarcinoma. *Cancer Res*, **67**, 2345-2350.

Chou, C.F., Mulky, A., Maitra, S., Lin, W.J., Gherzi, R., Kappes, J. and Chen, C.Y. (2006) Tethering KSRP, a decay-promoting AU-rich element-binding protein, to mRNAs elicits mRNA decay. *Mol Cell Biol*, **26**, 3695-3706.

Chou, K.M. and Cheng, Y.C. (2002) An exonucleolytic activity of human apurinic /apyrimidinic endonuclease on 3' mispaired DNA. *Nature*, **415**, 655-659.

Chou, K.M. and Cheng, Y.C. (2003) The exonuclease activity of human apurinic/apyrimidinic endonuclease (APE1). Biochemical properties and inhibition by the natural dinucleotide Gp4G. *J Biol Chem*, **278**, 18289-18296.

Chou, K. M., Kukhanova, M. and Cheng, Y. C. (2000) A novel action of human apurinic/apyrimidinic endonuclease. Excision of L-configuration deoxyribonucleoside analogs from the 3' termini of DNA. *J Biol Chem*, **275**, 31009-31015.

Claverie-Martin,F., Wang,M. and Cohen,S.N. (1997) ARD-1 cDNA from human cells encodes a site specific single-stranded endoribonuclease that functionally resembles *Escherichia coli* RNase E. *J Biol Chem*, **272,** 13823-13828.

Connolly, E., Melegari, M., Landgraf, P., Tchaikovskaya, T., Tennant, B.C., Slagle, B.L., Rogler, L.E., Zavolan, M., Tuschl, T. and Rogler, C.E. (2008) Elevated expression of the miR-17-92 polycistron and miR-21 in hepadnavirus-associated hepatocellular carcinoma contributes to the malignant phenotype. *Am J Pathol*, **173**, 856-864.

Crabtree, B., Holloway, D.E., Baker, M.D., Acharya, K.R. and Subramanian, V. (2007) Biological and structural features of murine angiogenin-4, an angiogenic protein. *Biochemistry*, **46**, 2431-2443.

Crabtree, B., Thiyagarajan, N., Prior, S.H., Wilson, P., Iyer, S., Ferns, T., Shapiro, R., Brew, K., Subramanian, V. and Acharya, A.R. (2007) Characterization of human angiogenin variants implicated in amyotrophic lateral sclerosis. *Biochemistry*, **46**, 11810-11818.

Cunningham, K.S., Dodson, R.E., Nagel, M.A., Shapiro, D.J. and Schoenberg, D.R. (2000) Vigilin binding selectively inhibits cleavage of the vitellogenin mRNA 3'-untranslated region by the mRNA endonuclease polysomal ribonuclease 1. *Proc Natl Acad Sci USA*, **97**, 12498-12502.

Cunningham, K.S., Hanson, M.N. and Schoenberg, D.R. (2001) Polysomal ribonuclease 1 exists in a latent form on polysomes prior to estrogen activation of mRNA decay. *Nucleic Acids Res*, **29**, 1156-1162.

Curran, T.P., Shapiro, R. and Riordan, T.F. (1993) Alteration of the enzymatic specificity of human angiogenin by site-directed mutagenesis. *Biochemistry*, **32**, 2307-2313.

Dani, C., Blanchard, J.M., Piechaczyk, M., El Sabouty, S., Marty, L., Jeanteur, P. (1984) Extreme instability of myc mRNA in normal and transformed human cells. *Proc Natl Acad Sci USA*, **81**, 7046-7050.

Dang, C.V., O'donnell, K.A. and Juopperi, T. (2005) "The great MYC escape in tumorigenesis.". *Cancer Cell,* **8,** 177–178.

Daugherty, S.E., Hayes, R.B., Yeager, M., Andriole, G.L., Chatterjee, N., Huang, W.Y., Isaacs, W.B. and Platz, E.A. (2007) RNASEL Arg462Gln polymorphism and prostate cancer in PLCO. *Prostate*, **67**, 849-854.

Davenport, E.L., Moore, H.E., Dunlop, A.S., Sharp, S.Y., Workman, P., Morgan, G.J. and Davies, F.E. (2007) Heat shock protein inhibition is associated with activation of the unfolded protein response pathway in myeloma plasma cells. *Blood*, **110**, 2641-2649.

Davies, M.P., Barraclough, D.L., Stewart, C., Joyce, K.A., Eccles, R.M., Barraclough, R., Rudland, P.S. and Sibson, D.R. (2008) Expression and splicing of the unfolded protein response gene XBP-1 are significantly associated with clinical outcome of endocrine-treated breast cancer. *Int J Cancer*, **123**, 85-88.

Davis, B.N., Hilyard, A.C., Lagna, G. and Hata, A. (2008) SMAD proteins control DROSHA-mediated microRNA maturation. *Nature*, **454**, 56-61.

De Guzman, R.N., Turner, R.B. and Summers, M.F. (1998) Protein-RNA recognition. *Biopolymers,* **48**, 181-195.

De Ruyck, K., Szaumkessel, M., De Rudder, I., Dehoorne, A., Vral, A., Claes, K., Velghe, A., Van Meerbeeck, J. and Thierens, H. (2007) Polymorphisms in base-excision repair and nucleotide-excision repair genes in relation to lung cancer risk. *Mutat Res*, **631**, 101-110.

Demple, B. and Harrison, L. (1994) Repair of oxidative damage to DNA: enzymology and biology. *Annu Rev Biochem*, 63, 915-948.

Demple, B., Herman, T. and Chen, D.S. (1991) Cloning and expression of APE, the cDNA encoding the major human apurinic endonuclease: definition of a family of DNA repair enzymes. *Proc Natl Acad Sci USA*, **88**, 11450-11454.

Dillhoff, M., Liu, J., Frankel, W., Croce, C. and Bloomston, M. (2008) MicroRNA-21 is Overexpressed in Pancreatic Cancer and a Potential Predictor of Survival. *J Gastrointest Surg*, **12**, 2171-2176.

Di Maso, V., Avellini, C., Crocè, L.S., Rosso, N., Quadrifoglio, F., Cesaratto, L., Codarin, E., Bedogni, G., Beltrami, C.A., Tell, G. and Tiribelli, C. (2007) Subcellular localization of APE1/Ref-1 in human hepatocellular carcinoma: possible prognostic significance. *Mol Med*, **13**, 89-96.

Dimitriadis, E., Trangas, T., Milatos, S., Foukas, P.G., Gioulbasanis, I., Courtis, N., Nielsen, F.C., Pandis, N., Dafni, U., Bardi, G. and Ioannidis, P. (2007) Expression of oncofetal RNA-binding protein CRD-BP/IMP1 predicts clinical outcome in colon cancer. *Int J Cancer*, **121**, 486-494.

Dodson,R.E. and Shapiro,D.J. (2002) Regulation of pathways of mRNA destabilization and stabilization. *Prog Nucleic Acid Res Mol Biol*, **72**, 129-164.

Doetsch, P.W. and Cunningham, R.P. (1990) The enzymology of apurinic/apyrimidinic endonucleases. *Mutat Res*, **236**, 173-201.

Doyle, G.A., Bourdeau-Heller, J.M., Coulthard, S., Meisner, L.F. and Ross, J. (2000) Amplification in human breast cancer of a gene encoding a c-myc mRNA-binding protein. *Cancer Res*, **60**, 2756–2759.

Drogat, B., Auguste, P., Nguyen, D.T., Bouchecareilh, M., Pineau, R., Nalbantoglu, J., Kaufman, R.J., Chevet, E., Bikfalvi, A. and Moenner, M. (2007) IRE1 signaling is essential for ischemia-induced vascular endothelial growth factor-A expression and contributes to angiogenesis and tumor growth in vivo. *Cancer Res*, 67, 6700-6707.

Duguid, J.R., Eble, J.N., Wilson, T.M. and Kelley, M.R. (1995) Differential cellular and subcellular expression of the human multifunctional apurinic/ apyrimidinic endonuclease (APE/ref-1) DNA repair enzyme. *Cancer Res*, **55**, 6097-6102.

Eberle, A.B., Lykke-Andersen, S., Mühlemann, O. and Jensen, T.H. (2009) SMG6 promotes endonucleolytic cleavage of nonsense mRNA in human cells. *Nat Struct Mol Biol*, **16**, 49-55.

Elcheva, I., Tarapore, R.S., Bhatia, N. and Spiegelman, V.S. (2008) Overexpression of mRNA-binding protein CRD-BP in malignant melanomas. *Oncogene*, **27**, 5069-5074.

Erzberger, J.P., Barsky, D., Schärer, O.D., Colvin, M.E. and Wilson, D.M. 3rd. (1998) Elements in abasic site recognition by the major human and Escherichia coli apurinic/apyrimidinic endonucleases. *Nucleic Acids Res*, **26**, 2771-2778.

Erzberger, J.P. and Wilson, D.M.3rd. (1999) The role of Mg2+ and specific amino acid residues in the catalytic reaction of the major human abasic endonuclease: new insights from EDTA-resistant incision of acyclic abasic site analogs and site-directed mutagenesis. *J Mol Biol* **290**, 447-457.

Evans, A.R., Limp-Foster, M. and Kelley, M.R. (2000) Going APE over ref-1. *Mutat Res.* **461**, 83-108.

Fan, Z., Beresford, P.J., Zhang, D., Xu, Z., Novina, C.D., Yoshida, A., Pommier, Y. and Lieberman, J. (2003) Cleaving the oxidative repair protein Ape1 enhances cell death mediated by granzyme A. *Nat Immunol*, **4**, 145-153.

Fernández-Salas, E., Peracaula, R., Frazier, M.L. and de Llorens, R. (2000) Ribonucleases expressed by human pancreatic adenocarcinoma cell lines. *Eur J Biochem*, **267**, 1484-1494.

Flavin, R.J., Smyth, P.J., Finn, S.P., Laios, A., O'Toole, S.A., Barrett, C., Ring, M., Denning, K.M., Li, J., Aherne, S.T., Aziz, N.A., Alhadi, A., Sheppard, B.L., Loda, M., Martin, C., Sheils, O.M. and O'Leary, J.J. (2008) Altered eIF6 and Dicer expression is associated with clinicopathological features in ovarian serous carcinoma patients. *Mod Pathol*, **21**, 676-684.

Friedberg, E. C., Walker, G. C. and Siede, W. (1995) *DNA Repair and Mutagenesis*, 135-190.

Fu, P., Chen, J., Tian, Y., Watkins, T., Cui, X., Zhao, B. (2005) Anti-tumor effect of hematopoietic cells carrying the gene of ribonuclease inhibitor. *Cancer Gene Ther*, **12**, 268-275.

Gallouzi, I.-E., Parker, F., Chebli, K., Maurier, F., Labourier, E., Barlat, I., Capony, I.-P., Tocque, B. and Tazi, J. (1998) A Novel Phosphorylation-Dependent RNase Activity of GAP-SH3 Binding Protein: a Potential Link between Signal Transduction and RNA Stability. *Mol Cell Biol*, **18**, 3956-3965.

Gao, B., Lee, S.M., Chen, A., Zhang, J., Zhang, D.D., Kannan, K., Ortmann, R.A. and Fang, D. (2008) Synoviolin promotes IRE1 ubiquitination and degradation in synovial fibroblasts from mice with collagen-induced arthritis. *EMBO Rep*, **9**, 480-485.

Gao, X., Hu, H., Zhu, J. and Xu, Z. (2007) Identification and characterization of follistatin as a novel angiogenin-binding protein. *FEBS Lett*, **581**, 5505-5510.

Garneau, N.L., Wilusz, J. and Wilusz, C. J. (2007) The highways and byways of mRNA decay. *Nat Rev Mol Cell Biol*, ***8***,113-126.

Gatfield,D. and Izaurralde,E. (2004) Nonsense-mediated messenger RNA decay is initiated by endonucleolytic cleavage in *Drosophila*. *Nature,* **429,** 575-578.

Gherzi, R., Lee, K.Y., Briata, P., Wegmüller, D., Moroni, C., Karin, M. and Chen, C.Y. (2004) A KH domain RNA binding protein, KSRP, promotes ARE-directed mRNA turnover by recruiting the degradation machinery. *Mol Cell*, **14**, 571-583.

Goldstrohm, A.C. and Wickens, M. (2008) Multifunctional deadenylase complexes diversify mRNA control. *Nat Rev Mol Cell Biol*, **9**, 337-344.

Gomez, B.P., Riggins, R.B., Shajahan, A.N., Klimach, U., Wang, A., Crawford, A.C., Zhu, Y., Zwart, A., Wang, M and Clarke ,R. (2007) Human X-box binding protein-1 confers both estrogen independence and antiestrogen resistance in breast cancer cell lines. *FASEB J*, **21**, 4013-4027.

Gorman, M.A., Morera, S., Rothwell, D.G., de La Fortelle, E., Mol, C.D., Tainer, J.A., Hickson, I.D. and Freemont, P.S. (1997) The crystal structure of the human DNA repair endonuclease HAP1 suggests the recognition of extra-helical deoxyribose at DNA abasic sites. *EMBO J,* **16**: 6548-6558.

Gramantieri, L., Fornari, F., Callegari, E., Sabbioni, S., Lanza, G., Croce, C.M., Bolondi, L. and Negrini, M. (2008) MicroRNA involvement in hepatocellular carcinoma. *J Cell Mol Med*, **12**, 2189-2204.

Grosshans, H. and Filipowicz, W. (2008) Molecular biology: the expanding world of small RNAs. *Nature*, **451**, 414-416.

Grove, K.L., Guo, X., Liu, S.H., Gao, Z., Chu, C.K. and Cheng, Y.C. (1995) Anticancer activity of beta-L-dioxolane-cytidine, a novel nucleoside analogue with the unnatural L configuration. *Cancer Res*, **55**, 3008-3011.

Guichard, C., Pedruzzi, E., Fay, M., Marie, J.C., Braut-Boucher, F., Daniel, F., Grodet, A., Gougerot-Pocidalo, M.A., Chastre, E., Kotelevets, L., Lizard, G., Vandewalle, A., Driss, F. and Ogier-Denis, E. (2006) Dihydroxyphenylethanol induces apoptosis by activating serine/threonine protein phosphatase PP2A and promotes the endoplasmic reticulum stress response in human colon carcinoma cells. *Carcinogenesis,* **27**, 1812-1827.

Guo, X. and Hartley, R.S. (2006) HuR Contributes to Cyclin E1 Deregulation in MCF-7 Breast Cancer Cells. *Cancer Res*, **66**, 7948-7956.

Hadi, M.Z., Coleman, M.A., Fidelis, K., Mohrenweiser, H.W. and Wilson, D.M.3rd. (2000) Functional characterization of APE1 variants identified in the human population. *Nucleic Acids Res*, **28**, 3871-3879.

Hadi, M.Z., Ginalski, K., Nguyen, L.H. and Wilson, D.M.3rd. (2002) Determinants in nuclease specificity of APE1 and Ape2, human homologues of Escherichia coli exonuclease III. *J Mol Biol*, **316**, 853–866.

Hagan, J. P. and Croce, C. M. (2007) MicroRNAs in carcinogenesis. *Cytogenet Genome Res*, **118**, 252-259.

Hanson, M.N. and Schoenberg, D.R. (2001) Identification of *in vivo* mRNA decay intermediates corresponding to sites of *in vitro* cleavage by polysomal ribonuclease 1. *J. Biol. Chem.*, **276,** 12331-12337.

Harrigan, J.A., Fan, J., Momand, J., Perrino, F.W., Bohr, V.A. and Wilson, D.M. 3rd. (2007) WRN exonuclease activity is blocked by DNA termini harboring 3' obstructive groups. *Mech Ageing Dev*, **128**, 259-66.

Heinonen, M., Bono, P., Narko, K., Chang, S.H., Lundin, J., Joensuu, H., Furneaux, H., Hla, T., Haglund, C. and Ristimäki, A. (2005) Cytoplasmic HuR expression is a prognostic factor in invasive ductal breast carcinoma. *Cancer Res*, **65**, 2157–2161.

Heise, T., Guidotti, L.G. and Chisari, F.V. (2001) Characterization of nuclear RNases that cleave hepatitis B virus RNA near the La protein binding site. *J Virol,* **75,** 6874-6883.

Henneke, G., Koundrioukoff, S. and Hübscher, U. (2003) Phosphorylation of human Fen1 by cyclin-dependent kinase modulates its role in replication fork regulation. *Oncogene*, **22**, 4301-4313.

Herrick, D.J. and Ross, J. (1994) The half-life of c-*myc* mRNA in growing and serum-stimulated cells: influence of the coding and 3' untranslated regions and role of ribosome translocation. *Mol. Cell. Biol.,* **14,** 2119-2128.

Hetz, C., Bernasconi, P., Fisher, J., Lee, A.H., Bassik, M.C., Antonsson, B., Brandt, G.S., Iwakoshi, N.N., Schinzel, A., Glimcher, L.H. and Korsmeyer, S.J. (2006) Proapoptotic BAX and BAK modulate the unfolded protein response by a direct interaction with IRE1alpha. *Science*, **312**, 572-576.

Hiyoshi, Y., Kamohara, H., Karashima, R., Sato, N., Imamura, Y., Nagai, Y., Yoshida, N., Toyama, E., Hayashi, N., Watanabe, M. and Baba, H. (2009) MicroRNA-21 regulates the proliferation and invasion in esophageal squamous cell carcinoma. *Clin Cancer Res*, **15**, 1915-1922.

Houseley, J., LaCava, J. and Tollervey, D. (2006) RNA-quality control by the exosome. *Nat Rev Mol Cell Biol*, **7**, 529-539.

Huang, Q., Gumireddy, K., Schrier, M., le Sage, C., Nagel, R., Nair, S., Egan, D.A., Li, A., Huang, G., Klein-Szanto, A.J., Gimotty, P.A., Katsaros, D., Coukos, G., Zhang, L., Puré, E. and Agami, R. (2008) The microRNAs miR-373 and miR-520c promote tumour invasion and metastasis. *Nat Cell Biol*, **10**, 202-210.

Ido, K., Nakagawa, T., Sakuma, T., Takeuchi, H., Sato, K. and Kubota, T. (2008) Expression of vascular endothelial growth factor-A and mRNA stability factor HuR in human astrocytic tumors. *Neuropathology*, **28**, 604-611.

Ioannidis, P., Havredaki, M., Courtis, N. and Trangas, T. (1996) *In vivo* generation of 3' and 5'truncated species in the process of c-*myc* mRNA decay. *Nucleic Acids Res,* **24**, 4969-4977.

Ioannidis, P., Kottaridi, C., Dimitriadis, E., Courtis, N., Mahaira, L., Talieri, M., Giannopoulos, A., Iliadis, K., Papaioannou, D., Nasioulas, G. and Trangas, T. (2004) Expression of the RNA-binding protein CRD-BP in brain and non-small cell lung tumors. *Cancer Lett*, **209**, 245-250.

Ioannidis, P., Mahaira, L., Papadopoulou, A., Teixeira, M.R., Heim, S., Andersen, J.A., Evangelou, E., Dafni, U., Pandis, N. and Trangas, T. (2003) 8q24 Copy number gains and expression of the c-myc mRNA stabilizing protein CRD-BP in primary breast carcinomas. *Int J Cancer*, **104**, 54-59.

Ioannidis, P., Trangas, T., Dimitriadis, E., Samiotaki, M., Kyriazoglou, I., Tsiapalis, C.M., Kittas, C., Agnantis, N., Nielsen, F.C., Nielsen, J., Christiansen, J. and Pandis, N. (2001) C-MYC and IGF-II mRNA-binding protein (CRD-BP/IMP-1) in benign and malignant mesenchymal tumors. *Int J Cancer*, **94**, 480-484.

Iorio, M.V., Ferracin, M., Liu, C.G., Veronese, A., Spizzo, R., Sabbioni, S., Magri, E., Pedriali, M., Fabbri, M., Campiglio, M., Ménard, S., Palazzo, J.P., Rosenberg, A., Musiani, P., Volinia, S., Nenci, I., Calin, G.A., Querzoli, P., Negrini, M. and Croce, C.M. (2005) MicroRNA gene expression deregulation in human breast cancer. *Cancer Res*, **65**, 7065-7070.

Irby, R.B. and Yeatman, T.J. (2000) Role of Src expression and activation in human cancer. *Oncogene*, **19**, 5636-5642.

Irvine, K., Stirling, R., Hume, D. and Kennedy, D. (2004) Rasputin, more promiscuous than ever: a review of G3BP. *Int J Dev Biol*, **48**, 1065-1077.

Ivanovska, I., Ball, A.S., Diaz, R.L., Magnus, J.F., Kibukawa, M., Schelter, J.M., Kobayashi, S.V., Lim, L., Burchard, J., Jackson, A.L., Linsley, P.S. and Cleary, M.A. (2008) MicroRNAs in the miR-106b family regulate p21/CDKN1A and promote cell cycle progression. Mol Cell Biol, **28**, 2167-2174.

Jackson, R.J. and Standart, N. (2007) How do microRNAs regulate gene expression? *Sci STKE*, **367**, re1.

Jackson, E.B., Theriot, C.A., Chattopadhyay, R., Mitra, S. and Izumi, T. (2005) Analysis of nuclear transport signals in the human apurinic/apyrimidinic endonuclease (APE1/Ref1). *Nucleic Acids Res*, **33**, 3303-3312.

Jin, Z., May, W.S., Gao, F., Flagg, T. and Deng, X. (2006) Bcl2 suppresses DNA repair by enhancing c-Myc transcriptional activity. *J Biol Chem*, **281**, 14446-14456.

Jing, Q., Huang, S., Guth, S., Zarubin, T., Motoyama, A., Chen, J., Di Padova, F., Lin, S.C., Gram, H. and Han, J. (2005) Involvement of microRNA in AU-rich element-mediated mRNA instability. *Cell*, **120**, 623-634.

Kane, C.M. and Linn, S. (1981) Purification and characterization of an apurinic/apyridiminic endonuclease from HeLa cells. *J Biol Chem* **256**, 3405-3414.

Kang, H.W., Moon, H.J., Joo, S.H. and Lee, J.H. (2007) Histidine residues in the IS3-IS4 loop are critical for nickel-sensitive inhibition of the Cav2.3 calcium channel. *FEBS Lett*, **581**, 5774-5780.

Kao, R.Y., Jenkins, J.L., Olson, K.A., Key, M.E., Fett, J.W. and Shapiro, R. (2002) A small-molecule inhibitor of the ribonucleolytic activity of human angiogenin that possesses antitumor activity. *Proc Natl Acad Sci USA*, **99**, 10066-10071.

Karube, Y., Tanaka, H., Osada, H., Tomida, S., Tatematsu, Y., Yanagisawa, K., Yatabe, Y., Takamizawa, J., Miyoshi, S., Mitsudomi, T. and Takahashi, T. (2005) Reduced expression of Dicer associated with poor prognosis in lung cancer patients. *Cancer Sci*, **96**, 111-115.

Katona, T.M., Neubauer, B.L., Iversen, P.W., Zhang, S., Baldridge, L.A. and Cheng, L. (2005) Elevated expression of angiogenin in prostate cancer and its precursors. *Clin Cancer Res*, **11**, 8358-8363.

Kaul, D. and Sikand, K. (2004) Defective RNA-mediated c-myc gene silencing pathway in Burkitt's lymphoma. *Biochem Biophys Res Commun*, **313**, 552-554.

Kawada, M., Inoue, H., Arakawa, M., Takamoto, K., Masuda, T. and Ikeda, D. (2007) Highly tumorigenic human androgen receptor-positive prostate cancer cells overexpress angiogenin. *Cancer Sci*, **98**, 350-356.

Kedersha, N., Stoecklin, G., Ayodele, M., Yacono, P., Lykke-Andersen, J., Fritzler, M.J., Scheuner, D., Kaufman, R.J., Golan, D.E. and Anderson, P. (2005) Stress granules and processing bodies are dynamically linked sites of mRNP remodeling. *J Cell Biol*, **169**, 871-884.

Kim, W-C. and Lee, C.H. (2009) The role of mammalian ribonucleases in cancer. *Biochim Biophys Acta. - Reviews on Cancer,* doi:10.1016/j.bbcan.2009.05.002.

Kumar, M.S., Lu, J., Mercer, K.L., Golub, T.R. and Jacks, T. (2007) Impaired microRNA processing enhances cellular transformation and tumorigenesis. *Nat Genet*, **39**, 673-677.

Kobe, B. and Deisenhofer J. (1996) Mechanism of ribonuclease inhibition by ribonuclease inhibitor protein based on the crystal structure of its complex with ribonuclease A. *J Mol Biol*, **264**, 1028-1043.

Koong, A.C., Chauhan, V. and Romero-Ramirez, L. (2006) Targeting XBP-1 as a novel anti-cancer strategy. *Cancer Biol Ther*, **5**, 756-759.

Kovalchuk, O., Filkowski, J., Meservy, J., Ilnytskyy, Y., Tryndyak, V.P., Chekhun, V.F. and Pogribny, I.P. (2008) Involvement of microRNA-451 in resistance of the MCF-7 breast cancer cells to chemotherapeutic drug doxorubicin. *Mol Cancer Ther*, **7**, 2152-2159.

Krüger, S., Silber, A.S., Engel, C., Görgens, H., Mangold, E., Pagenstecher, C., Holinski-Feder, E., von Knebel Doeberitz, M., Moeslein, G., Dietmaier, W., Stemmler, S., Friedl, W., Rüschoff, J., Schackert, H.K. and German Hereditary Non-Polyposis Colorectal Cancer Consortium. (2005) Arg462Gln sequence variation in the prostate-cancer-susceptibility gene RNASEL and age of onset of hereditary non-polyposis colorectal cancer: a case-control study. *Lancet Oncol*, **6**, 566-572.

Kucherlapati, M., Nguyen, A., Kuraguchi, M., Yang, K., Fan, K., Bronson, R., Wei, K., Lipkin, M., Edelmann, W. and Kucherlapati, R. (2007) Tumor progression in Apc(1638N) mice with Exo1 and Fen1 deficiencies. *Oncogene*, **26**, 6297-6306.

Kucherlapati, M., Yang, K., Kuraguchi, M., Zhao, J., Lia, M., Heyer, J., Kane, M.F., Fan, K., Russell, R., Brown, A.M., Kneitz, B., Edelmann, W., Kolodner, R.D., Lipkin, M. and Kucherlapati, R. (2002) Haploinsufficiency of Flap endonuclease (Fen1) leads to rapid tumor progression. *Proc Natl Acad Sci USA*, **99**, 9924-9929.

Kuehbacher, A., Urbich, C., Zeiher, A.M. and Dimmeler, S. (2007) Role of Dicer and Drosha for endothelial microRNA expression and angiogenesis. *Circ Res*, **101**, 59-68.

Kuninger, D.T., Izumi, T., Papaconstantinou, J. and Mitra, S. (2002) Human AP-endonuclease 1 and hnRNP-L interact with a nCaRE-like repressor element in the AP-endonuclease 1 promoter. *Nucleic Acids Res.* **30**, 823-829.

Lai, W.S., Kennington, E.A. and Blackshea, P.J. (2003) Tristetraprolin and Its Family Members Can Promote the Cell-Free Deadenylation of AU-Rich Element-Containing mRNAs by Poly(A) Ribonuclease. *Mol Cell Biol*, **23**, 3798-3812.

Lam, J.S., Seligson, D.B., Yu, H., Li, A., Eeva, M., Pantuck, A.J., Zeng, G., Horvath, S. and Belldegrun, A.S. (2006) Flap endonuclease 1 is overexpressed in prostate cancer and is associated with a high Gleason score. *BJU Int*, **98**, 445-451.

Laneve, P., Gioia, U., Ragno, R., Altieri, F., Di Franco, C., Santini, T., Arceci, M., Bozzoni, I. and Caffarelli, E. (2008) The tumor marker human placental protein 11 is an endoribonuclease. *J Biol Chem*, **283**, 34712-34719.

Lebreton, A., Tomecki, R., Dziembowski, A. and Seraphin, B. (2008) Endonucleolytic RNA cleavage by a eukaryotic exosome. *Nature,* **456,** 993-997.

Lee, C.H., Bradley, G. and Ling, V. (1998) Increased P-glycoprotein messenger RNA stability in rat liver tumors in vivo. *J Cell Physiol*, **177**, 1-12.

Lee, C.H., Rehaume, V.E. and Shandro, J. (2005) Identification of in vivo P-glycoprotein mRNA decay intermediates in normal liver but not in liver tumors. *J Cell Physiol*, **204**, 638-645.

Lee, D.Y. and Sugden, B. (2008) The LMP1 oncogene of EBV activates PERK and the unfolded protein response to drive its own synthesis. *Blood*, **111**, 2280-2289.

Lee, H.H., Kim, Y.S., Kim, K.H., Heo, I., Kim, S.K., Kim, O., Kim, H.K., Yoon, J.Y, Kim, H.S., Kim, D.J., Lee, S.J., Yoon, H.J., Kim, S.J., Lee, B.G., Song, H.K., Kim, V.N., Park, C.M. and Suh, A.W. (2007) Structural and functional insights into Dom34, a key component of no-go mRNA decay. *Mol Cell*, **27**, 938-950.

Lee, K.P., Dey, M., Neculai, D., Cao, C., Dever, T.E. and Sicheri, F. (2008) Structure of the dual enzyme Ire1 reveals the basis for catalysis and regulation in nonconventional RNA splicing. *Cell*, **132**, 89-100.

Lemm, I., and Ross, J. (2002) Regulation of c-*myc* mRNA decay by translational pausing in a coding region instability determinant. *Mol. Cell. Biol.,* **22**, 3959-3969.

Le Roy, F., Bisbal, C., Silhol, M., Martinand, C., Lebleu, B. and Salehzada, T. (2001) The 2-5A/RNase L/RNase L inhibitor (RLI) [correction of (RNI)] pathway regulates mitochondrial mRNAs stability in interferon alpha-treated H9 cells. *J Biol Chem*, **276**, 48473-48482.

Le Roy, F., Silhol, M., Salehzada, T. and Bisbal, C. (2007) Regulation of mitochondrial mRNA stability by RNase L is translation-dependent and controls IFNalpha-induced apoptosis. *Cell Death Differ*, **14**, 1406-1413.

Levens, D. (2003) Reconstructing MYC. *Genes Dev.*, **17**, 1071-1077.

Levin, J.D., Johnson, A.W. and Demple, B. (1988) Homogeneous Escherichia coli endonuclease IV. Characterization of an enzyme that recognizes oxidative damage in DNA. *J Biol Chem*, **263**, 8066-8071.

Li, X.L., Andersen, J.B., Ezelle, H.J., Wilson, G.M. and Hassel, B.A. (2007) Post-transcriptional regulation of RNase-L expression is mediated by the 3'-untranslated region of its mRNA. *J Biol Chem*, **282**, 7950-7960.

Li, X.L., Blackford, J.A., Judge, C.S., Liu, M., Xiao, W., Kalvakolanu, D.V. and Hassel, B.A. (2000) RNase-L-dependent destabilization of interferon-induced mRNAs. A role for the 2-5A system in attenuation of the interferon response. *J Biol Chem*, **275**, 8880-8888.

Liang, S.L., Quirk, D. and Zhou, A. (2006) RNase L: its biological roles and regulation. *IUBMB. Life*, **58**, 508-514.

Lin, J.H., Li, H., Yasumura, D., Cohen, H.R., Zhang, C., Panning, B., Shokat, K.M., Lavail, M.M., and Walter, P. (2007) IRE1 signaling affects cell fate during the unfolded protein response. *Science*, **318**, 944-949.

Little, J.L., Wheeler, F.B., Fels, D.R., Koumenis, C. and Kridel, S.J. (2007) Inhibition of fatty acid synthase induces endoplasmic reticulum stress in tumor cells. *Cancer Res*, **67**, 1262-1269.

Liu, J., Carmell, M.A., Rivas, F.V., Marsden, C.G., Thomson, J.M., Song, J.J., Hammond, S.M., Joshua-Tor, L. and Hannon, G.J. (2004) Argonaute2 is the catalytic engine of mammalian RNAi. *Science*, **305**, 1437-1441.

Liu, W., Liang, S.L., Liu, H., Silverman, R. and Zhou, A. (2007) Tumour suppressor function of RNase L in a mouse model. *Eur J Cancer*, **43**, 202-209.

Liu, X., Schumacher, F.R., Plummer, S.J., Jorgenson, E., Casey, G. and Witte, J.S. (2007) Trans-fatty acid intake and increased risk of advanced prostate cancer: modification by RNASEL R462Q variant. *Carcinogenesis*, **28**, 1232-1236.

Liu, Y., Zheng, J., Fang, W., You, J., Wang, J., Cui, X. and Wu, B. (2001) Identification of metastasis associated gene G3BP by differential display in human cancer cell sublines with different metastatic potentials G3BP as highly expressed in non-metastatic. *Chin Med J*, **114**, 35-38.

Livak, K.J. and Schmittgen, T.D. (2001) Analysis of relative gene expression data using real-time quantitative PCR and the 2(-Delta Delta C(T)) Method. *Methods*, **25**, 402-408

Lockhart, D.J. and Winzeler, E.A. (2000) Genomics, gene expression and DNA arrays. *Nature*, **405**, 827-836.

Lui, W.O., Pourmand, N., Patterson, B.K. and Fire A. (2007) Patterns of known and novel small RNAs in human cervical cancer. *Cancer Res*, **67**, 6031-6043.

Ma, L. and Weinberg, R.A. (2008) MicroRNAs in malignant progression. *Cell Cycle*, **7**, 570-572.

Malathi, K., Dong, B., Gale Jr, M. and Silverman, R.H. (2007) Small self-RNA generated by RNase L amplifies antiviral innate immunity. *Nature*, **448**, 816-819.

Malathi, K., Paranjape, J.M., Bulanova, E., Shim, M., Guenther-Johnson, J.M., Faber, P.W., Eling, T.E., Williams, B.R. and Silverman, R.H. (2005) A transcriptional signaling pathway in the IFN system mediated by 2'-5'-oligoadenylate activation of RNase L. *Proc Natl Acad Sci USA*, **102**, 14533-14538.

Mantha, A.K., Oezguen, N., Bhakat, K.K., Izumi, T., Braun, W. and Mitra, S. (2008) Unusual role of a cysteine residue in substrate binding and activity of human AP-endonuclease 1. *J Mol Biol*, **379**, 28-37.

Marenstein, D.R. and Wilson, D.M.3rd., Teebor, G.W. (2004) Human AP endonuclease (APE1) demonstrates endonucleolytic activity against AP sites in single-stranded DNA. *DNA Repair (Amst)*, **3**, 527-533.

Markou, A., Tsaroucha, E.G., Kaklamanis, L., Fotinou, M., Georgoulias, V. and Lianidou, E.S. (2008) Prognostic Value of Mature MicroRNA-21 and MicroRNA-205 Overexpression in Non-Small Cell Lung Cancer by Quantitative Real-Time RT-PCR. *Clin Chem*, **54**, 1696-1704.

Masuda, Y., Bennett, R.A.O. and Demple, B. (1998) Rapid dissociation of human apurinic endonuclease (APE1) from incised DNA induced by magnesium. *J Biol Chem* **273**, 30360-30365.

Mazan-Mamczarz, K. and Gartenhaus, R.B. (2007) Post-transcriptional control of the MCT-1-associated protein DENR/DRP by RNA-binding protein AUF1. *Cancer Genomics Proteomics*, **4**, 233-239.

McNeill, D.R., Narayana, A., Wong, H.K. and Wilson, D.M.3rd. (2004) Inhibition of APE1 nuclease activity by lead, iron and cadmium. *Toxigenomics*, **112**, 799–804.

Meister, G., Landthaler, M., Patkaniowska, A., Dorsett, Y., Teng, G. and Tuschl, T. (2004) Human Argonaute2 Mediates RNA Cleavage Targeted by miRNAs and siRNAs. *Mol Cell*, **15**, 185-197.

Miyasaka, T., Morita, M., Ito, K., Suzuki, T., Fukuda, H., Takeda, S., Inoue, J., Semba, K. and Yamamoto, T. (2008) Interaction of antiproliferative protein Tob with the CCR4-NOT deadenylase complex. *Cancer Sci*, **99**, 755-761.

Mol, C.D., Izumi, T., Mitra, S. and Tainer, J.A. (2000) DNA-bound structures and mutants reveal abasic DNA binding by APE1 and DNA repair coordination. *Nature*, **403**, 451-456.

Mook, O.R. Frederiks, W.M. and Van Noorden, C.J. (2004) The role of gelatinases in colorectal cancer progression and metastasis. *Biochim Biophys Acta*, **1705**, 69-89.

Moraes, K.C., Wilusz, C.J. and Wilusz, J. (2006) CUG-BP binds to RNA substrates and recruits PARN deadenylase. *RNA*, **12**, 1084-1091.

Morello, D., Lavenu, A., Pournin, S. and Babinet, C. (1993) The 5' and 3' non-coding sequences of the c-myc gene, required in vitro for its post-transcriptional regulation, are dispensable in vivo. *Oncogene*, **8**, 1921-1929.

Morita, M., Suzuki, T., Nakamura, T., Yokoyama, K., Miyasaka, T. and Yamamoto, T. (2007) Depletion of mammalian CCR4b deadenylase triggers elevation of the p27Kip1 mRNA level and impairs cell growth. *Mol Cell Biol*, **27**, 4980-4890.

Mullan, P.B., Hosey, A.M., Buckley, N.E., Quinn, J.E., Kennedy, R.D., Johnston, P.G. and Harkin, D.P. (2005) The 2,5 oligoadenylate synthetase/RNaseL pathway is a novel effector of BRCA1- and interferon-gamma-mediated apoptosis. *Oncogene*, **24**, 5492-5501.

Müller, D.W. and Bosserhoff, A.K. (2008) Integrin beta(3) expression is regulated by let-7a miRNA in malignant melanoma. *Oncogene*, **27**, 6698-6706.

Muralidhar, B., Goldstein, L.D., Ng, G., Winder, D.M., Palmer, R.D., Gooding, E.L., Barbosa-Morais, N.L., Mukherjee, G., Thorne, N.P., Roberts, I., Pett, M.R. and Coleman, N. (2007) Global microRNA profiles in cervical squamous cell carcinoma depend on Drosha expression levels. *J Pathol*, **212**, 368-377.

Nagel, R., le Sage, C., Diosdado, B., van der Waal, M., Oude Vrielink, J.A., Bolijn, A., Meijer, G.A. and Agami, R. Regulation of the adenomatous polyposis coli gene by the miR-135 family in colorectal cancer. *Cancer Res*, **68**, 5795-5802.

Naito, T., Yokogawa, T., Kim, H.S., Matsuda, A., Sasaki, T., Fukushima, M., Kitade, Y. and Wataya, Y. (2006) An apoptotic pathway of 3'-Ethynylcytidine(ECyd) involving the inhibition of RNA synthesis mediated by RNase L. *Nucleic Acids Symp Ser (Oxf)*, **50**, 103-104.

Nakamura, T., Canaani, E. and Croce, C.M. (2007) Oncogenic All1 fusion proteins target Drosha-mediated microRNA processing. *Proc Natl Acad Sci USA*, **104**, 10980-10985.

Nakamura, T. and Sugita, M. (2008) A conserved DYW domain of the pentatricopeptide repeat protein possesses a novel endoribonuclease activity. *FEBS Lett*, **582**, 4163-4168.

Nguyen, L.H., Barsky, D., Erzberger, J.P. and Wilson, D.M.3rd. (2000) Mapping the protein-DNA interface and the metal-binding site of the major human apurinic/apyrimidinic endonuclease. *J Mol Biol*, **298**, 447-459.

Noonan-Wheeler, F.C., Wu, W., Roehl, K.A., Klim, A., Haugen, J., Suarez, B.K. and Kibel, A.S. (2006) Association of hereditary prostate cancer gene polymorphic variants with sporadic aggressive prostate carcinoma. *Prostate*, **66**, 49-56.

O'Carroll, D., Mecklenbrauker, I., Das, P.P., Santana, A., Koenig, U., Enright, A.J., Miska, E.A. and Tarakhovsky, A. (2007) A Slicer-independent role for Argonaute 2 in hematopoiesis and the microRNA pathway. *Genes Dev*, **21**, 1999-2004.

Oezguen, N., Schein, C.H., Peddi, S.R., Power, T.D., Izumi, T. and Braun, W. (2007) A 'moving metal mechanism for substrate cleavage by the DNA repair endonuclease APE-1. *Proteins,* **68**, 313-323.

Oikawa, D., Tokuda, M. and Iwawaki, T. (2007) Site-specific cleavage of CD59 mRNA by endoplasmic reticulum-localized ribonuclease, IRE1. *Biochem Biophys Res Commun*, **360**, 122-127.

Okamura, M., Terada, T., Katsura, T., Saito, H. and Inui, K. (2003) Inhibitory effect of zinc on PEPT1-mediated transport of glycylsarcosine and beta-lactam antibiotics in human intestinal cell line Caco-2. *Pharm Res*, **20**, 1389-1393.

Orii, A., Masutani, H., Nikaido, T., Zhai, Y.L., Kato, K., Kariya, M., Konishi, I., Yodoi, J. and Fujii, S. (2002) Altered post-translational modification of redox factor 1 protein in human uterine smooth muscle tumors. *J Clin Endocrinol Metab*, **87**, 3754-3759.

Pardini, B., Naccarati, A., Novotny, J., Smerhovsky, Z., Vodickova, K., Polakova, V., Hanova, M., Slyskova, J., Tulupova, E., Kumar, R., Bortlik, M., Barale, R., Hemminki, K. and Vodicka, P. (2008) DNA repair genetic polymorphisms and risk of colorectal cancer in the Czech Republic. *Mutat Res*, **638**, 146-153.

Park, C.M. and Suh, S.W. (2007) Structural and functional insights into Dom34, a key component of no-go mRNA decay. *Mol Cell*, **27**, 938-950.

Parker, R. and Song, H. (2004) The enzymes and control of eukaryotic mRNA turnover. *Nat Struct Mol Biol,* **11**, 121-127.

Paschoud, S., Dogar, A.M., Kuntz, C., Grisoni-Neupert, B., Richman, L. and Kühn, L.C. (2006) Destabilization of interleukin-6 mRNA requires a putative RNA stem-loop structure, an AU-rich element, and the RNA-binding protein AUF1. *Mol Cell Biol*, **26**, 8228-8241.

Peng, Y., Liu, X. and Schoenberg, D.R. (2008) Hsp90 Stabilizes the PMR1 mRNA Endonuclease to Degradation by the 26S Proteasome. *Mol Biol Cell*, **19**, 546-552.

Peng, Y. and Schoenberg, D.R. (2007) c-Src activates endonuclease-mediated mRNA decay. *Mol Cell*, **25**, 779-787.

Peracaula, R., Royle, L., Tabares, G., Mallorqui-Fernández, G.S., Barrabés, S., Harvey, D.J., Dwek, R.A., Rudd, P.M. and de Llorens, R. (2003) Glycosylation of human pancreatic ribonuclease: differences between normal and tumor states. *Glycobiology*, **13**, 227-244.

Ponzielli, R., Katz, S., Barsyte-Lovejoy, D. and Penn, L.Z. (2005) Cancer therapeutics: targeting the dark side of Myc. *Eur J Cancer*, **41**, 2485-2501.

Pulcrano, G., Leonardo, R., Piscopo, M., Nargi, E., Locascio, A., Aniello, F., Branno, M. and Fucci, L. (2007) PLAUF binding to the 3'UTR of the H3.3 histone transcript affects mRNA stability. *Gene*, **406**, 124-133.

Qian, B., Katsaros, D., Lu, L., Preti, M., Durando, A., Arisio, R., Mu, L., Yu, H. (2008) High miR-21 expression in breast cancer associated with poor disease-free survival in early stage disease and high TGF-beta1. *Breast Cancer Res Treat*, doi:10.1007/s10549-008-0219-7

Qiu, J., Li, X., Frank, G. and Shen, B. (2001) Cell cycle-dependent and DNA damage-inducible nuclear localization of FEN-1 nuclease is consistent with its dual functions in DNA replication and repair. *J Biol Chem*, **276**, 4901-4908.

Qu, J., Liu, G.H., Huang, B. and Chen, C. (2007) Nitric oxide controls nuclear export of APE1/Ref-1 through S-nitrosation of cysteines 93 and 310. *Nucleic Acids Res*, **35**, 2522-2532.

Quann, E.J., Khwaja, F. and Djakiew, D. (2007) The p38 MAPK pathway mediates aryl propionic acid induced messenger rna stability of p75 NTR in prostate cancer cells. *Cancer Res*, **67**, 11402-11410.

Raines, R.T. (1998) Ribonuclease A. *Chem Rev*, **98**, 1045-1066.

Reinert, L.S., Shi, B., Nandi, S., Mazan-Mamczarz, K., Vitolo, M., Bachman, K.E., He, H. and Gartenhaus, R.B. (2006) MCT-1 protein interacts with the cap complex and modulates messenger RNA translational profiles. *Cancer Res*, **66**, 8994-9001.

Rennert, H., Zeigler-Johnson, C.M., Addya, K., Finley, M.J., Walker, A.H., Spangler, E., Leonard, D.G., Wein, A., Malkowicz, S.B. and Rebbeck, T.R. (2005) Association of susceptibility alleles in ELAC2/HPC2, RNASEL/HPC1, and MSR1 with prostate cancer severity in European American and African American men. *Cancer Epidemiol Biomarkers Prev*, **14**, 949-957.

Rivas, F.V., Tolia, N.H., Song, J.J., Aragon, J.P., Liu, J., Hannon, G.J. and Joshua-Tor, L. (2005) Purified Argonaute2 and an siRNA form recombinant human RISC. *Nat Struct Mol Biol*, **12**, 340-349.

Robins, P., Pappin, D.J., Wood, R.D. and Lindahl, T. (1994) Structural and functional homology between mammalian DNase IV and the 5'-nuclease domain of Escherichia coli DNA polymerase I. *J Biol Chem*, **269**, 28535-28538.

Robson, C.N., Milne, A.M., Pappin, D.J. and Hickson, I.D. (1991) Isolation of cDNA clones encoding an enzyme from bovine cells that repairs oxidative DNA damage *in vitro*: homology with bacterial repair enzymes. *Nucleic Acids Res*, **19**, 1087-1092.

Rökman, A., Ikonen, T., Seppälä, E.H., Nupponen, N., Autio, V., Mononen, N., Bailey-Wilson, J., Trent, J., Carpten, J., Matikainen, M.P., Koivisto, P.A., Tammela, T.L., Kallioniemi, O.P. and Schleutker J. (2002) Germline alterations of the RNASEL gene, a candidate HPC1 gene at 1q25, in patients and families with prostate cancer. *Am J Hum Genet*, **70**, 1299-1304.

Roldo, C., Missiaglia, E., Hagan, J.P., Falconi, M., Capelli, P., Bersani, S., Calin, G.A., Volinia, S., Liu, C.G., Scarpa, A. and Croce, C.M. (2006) MicroRNA expression abnormalities in pancreatic endocrine and acinar tumors are associated with distinctive pathologic features and clinical behavior. *J Clin Oncol*, **24**, 4677-4684.

Rothwell, D.G., Hang, B., Gorman, M.A., Freemont, P.S., Singer, B. and Hickson, I.D. (2000) Substitution of Asp-210 in HAP1 (APE/Ref-1) eliminates endonuclease activity but stabilises substrate binding. *Nucleic Acids Res*, **28**, 2207-2213.

Rothwell, D.G. and Hickson, I.D. (1996) Asparagine 212 is essential for abasic site recognition by the human DNA repair endonuclease HAP1. *Nucleic Acids Res*, **24**, 4217-21

Rosell, R., Cuello, M., Cecere, F., Santarpia, M., Reguart, N., Felip, E. and Taron, M. (2006) Usefulness of predictive tests for cancer treatment. *Bull Cancer*, **93**, E101-E108.

Ross, J. (1995) mRNA stability in mammalian cells. *Microbiol Rev*, **59**, 423-450.

Ross, J., Lemm, I. and Berberet, B. (2001) Overexpression of an mRNA-binding protein in human colorectal cancer. *Oncogene*, **20**, 6544-6550.

Roth, J.S. (1963) Ribonuclease activity and cancer: a review. *Cancer Res*, **23**, 657-666.

Sato, M., Girard, L., Sekine, I., Sunaga, N., Ramirez, R.D., Kamibayashi, C. and Minna, J.D. (2003) Increased expression and no mutation of the Flap endonuclease (FEN1) gene in human lung cancer. *Oncogene*, **22**, 7243-7246.

Schaeffer, D., Tsanova, B., Barbas, A., Reis, F.P., Dastidar, E.G., Sanchez-Rotunno, M., Arraiano, C.M. and van Hoof, A. (2009) The exosome contains domains with specific endoribonuclease, exoribonuclease and cytoplasmic mRNA decay activities. *Nat Struct Mol Biol*, **16**, 56-62.

Schwede, A., Ellis, L., Luther, J., Carrington, M., Stoecklin, G. and Clayton, C. (2008) A role for Caf1 in mRNA deadenylation and decay in trypanosomes and human cells. *Nucleic Acids Res*, **36**, 3374-3388.

Scott, G.K., Marx, C., Berger, C.E., Saunders, L.R., Verdin, E., Schäfer, S., Jung, M., Benz, C.C. (2008) Destabilization of ERBB2 transcripts by targeting 3' untranslated region messenger RNA associated HuR and histone deacetylase-6. *Mol Cancer Res*, **6**, 1250-1258.

Scotto, L., Narayan, G., Nandula, S.V., Subramaniyam, V., Kaufmann, A.M., Wright, J.D., Pothuri, B., Mansukhani, M., Schneider, A., Arias-Pulido, H. and Murty, V.V. (2008) Integrative genomics analysis of chromosome 5p gain in cervical cancer reveals target over-expressed genes including Drosha. *Mol Cancer*, **17**, 58.

Selaru, F.M., Olaru, A.V., Kan, T., David, S., Cheng, Y., Mori, Y., Yang, J., Paun, B., Jin, Z., Agarwal, R., Hamilton, J.P., Abraham, J., Georgiades, C., Alvarez, H., Vivekanandan, P., Yu, W., Maitra, A., Torbenson, M., Thuluvath, P.J., Gores, G.J., Larusso, N.F., Hruban, R. and Meltzer SJ. (2009) MicroRNA-21 is overexpressed in human cholangiocarcinoma and regulates programmed cell death 4 and tissue inhibitor of metalloproteinase 3. *Hepatology*, doi: 10.1002/hep.22838.

Sen, G.L. and Blau, H.M. (2005) Argonaute 2/RISC resides in sites of mammalian mRNA decay known as cytoplasmic bodies. *Nat Cell Biol*, **7**, 633-636.

Sengupta, S., den Boon, J.A., Chen, I.H., Newton, M.A., Stanhope, S.A., Cheng, Y.J., Chen, C.J., Hildesheim, A., Sugden, B., Ahlquist, P. (2008) MicroRNA 29c is down-regulated in nasopharyngeal carcinomas, up-regulating mRNAs encoding extracellular matrix proteins. *Proc Natl Acad Sci USA*, **105**, 5874-5878.

Shen, B., Singh, P., Liu, R., Qiu, J., Zheng, L., Finger, L.D. and Alas, S. (2005) Multiple but dissectible functions of FEN-1 nucleases in nucleic acid processing, genome stability and diseases. *Bioessays*, **27**, 717-729.

Shen, J.C. and Loeb, L.A. (2003) Mutations in the alpha8 loop of human APE1 alter binding and cleavage of DNA containing an abasic site. *J Biol Chem*, **278**, 46994-47001.

Shih, S.C. and Claffey, K.P. (1999) Regulation of human vascular endothelial growth factor mRNA stability in hypoxia by heterogeneous nuclear ribonucleoprotein L. *J Biol Chem*, **274**, 1359-1365.

Shook, S.J., Beuten, J., Torkko, K.C., Johnson-Pais, T.L., Troyer, D.A., Thompson, I.M. and Leach, R.J. (2007) Association of RNASEL variants with prostate cancer risk in Hispanic Caucasians and African Americans. *Clin Cancer Res*, **13**, 5959-5964.

Shuda, M., Kondoh, N., Imazeki, N., Tanaka, K., Okada, T., Mori, K., Hada, A., Arai, M., Wakatsuki, T., Matsubara, O., Yamamoto, N., Yamamoto, M. (2003) Activation of the ATF6, XBP1 and grp78 genes in human hepatocellular carcinoma: a possible involvement of the ER stress pathway in hepatocarcinogenesis. *J Hepatol*, **38**, 605-614.

Sidransky, H., Murty, C.N. and Verney, E. (1978) Turnover of messenger RNA in transplantable hepatomas and host liver of rats. *Cancer Res*, **38**, 1645-1653.

Slaby, O., Svoboda, M., Fabian, P., Smerdova, T., Knoflickova, D., Bednarikova, M., Nenutil, R. and Vyzula, R. (2007) Altered expression of miR-21, miR-31, miR-143 and miR-145 is related to clinicopathologic features of colorectal cancer. *Oncology*, **72**, 397-402.

Smith, B.D. and Raines, R.T. (2006) Genetic selection for critical residues in ribonucleases. *J Mol Biol*, **362**, 459-478.

Smith, B.D. and Raines, R.T. (2008) Genetic selection for peptide inhibitors of angiogenin. *Protein Eng Des Sel*, **21**, 289-294.

Sobue, S., Murakami, M., Banno, Y., Ito, H., Kimura, A., Gao, S., Furuhata, A., Takagi, A., Kojima, T., Suzuki, M., Nozawa, Y. and Murate, T. (2008) v-Src oncogene product increases sphingosine kinase 1 expression through mRNA stabilization: alteration of AU-rich element-binding proteins. *Oncogene*, **27**, 6023-6033.

Sokhansanj, B.A., Rodrigue, G.R., Fitch, J.P. and Wilson, D.M.3rd. (2002) A quantitative model of human DNA base excision repair. I. Mechanistic insights. *Nucl. Acids Res.* **30**, 1817–1825.

Song, J., Wang, J., Yang, J., Jiang, S., Shen, W. and Wang, L. (2006) Influence of angiogenin on the growth of A375 human melanoma cells and the expression of basic fibroblast growth factor. *Melanoma Res*, **16**, 119-126.Song, J.-J., Smith, S.K., Hannon, G.J. and Joshua-Tor, L. (2004) Crystal Structure of Argonaute and Its Implications for RISC Slicer Activity. *Science*, **305**, 1434-1437.

Steinman, R.A. (2007) mRNA stability control: a clandestine force in normal and malignant hematopoiesis. *Leukemia*, **21**, 1158-1171.

Stevens, A. (1998) Endonucleolytic cleavage of RNA at 5' endogenous stem structures by human flap endonuclease 1. *Biochem Biophys Res Commun*, **251**, 501-508.

Stevens,A., Wang,Y., Bremer,K., Zhang,J., Hoepfner,R., Antoniou,M., Schoenberg,D.R. and Maquat,L.E. (2002) β-globin mRNA decay in erythroid cells: UG site-preferred endonucleolytic cleavage that is augmented by a premature termination codon. *Proc Natl Acad Sci USA,* **99**, 12741-12746.

Stickeler, E., Fraser, S.D., Honig, A., Chen, A.L., Berget, S.M., Cooper, T.A. (2001) The RNA binding protein YB-1 binds A/C-rich exon enhancers and stimulates splicing of the CD44 alternative exon v4. *EMBO J*, **20**, 3821-3830.

Sugito, N., Ishiguro, H., Kuwabara, Y., Kimura, M., Mitsui, A., Kurehara, H., Ando, T., Mori, R., Takashima, N., Ogawa, R. and Fujii, Y. (2006) RNASEN regulates cell proliferation and affects survival in esophageal cancer patients. *Clin Cancer Res*, **12**, 7322-7328.

Suh, D. and Wilson, D.M.3rd. (1997) Povirk LF 3'-phosphodiesterase activity of human apurinic/apyrimidinic endonuclease at DNA double-strand break ends. *Nucleic Acids Res,* **25**, 2495-2500.

Sun, J., Turner, A., Xu, J., Grönberg, H. and Isaacs, W. (2007) Genetic variability in inflammation pathways and prostate cancer risk. *Urol Oncol*, **25**, 250-259.

Suswam, E., Li, Y., Zhang, X., Gillespie, G.Y., Li, X., Shacka, J.J., Lu, L., Zheng, L. and King, P.H. (2008) Tristetraprolin down-regulates interleukin-8 and vascular endothelial growth factor in malignant glioma cells. *Cancer Res*, **68**, 674-82.

Swartwout, S.G. and Kinniburgh, A.J. (1989) c-myc RNA degradation in growing and differentiating cells: possible alternate pathways. *Mol Cell Biol*, **9**, 288-295.

Tack, F., Noppe, M., Van Dijck, A., Dekeyzer, N., Van Der Leede, B.J., Bakker, A., Wouters, W., Janicot, M. and Brewster, M.E. (2008) Delivery of a DNAzyme targeting c-myc to HT29 colon carcinoma cells using a gold nanoparticulate approach. *Pharmazie*, **63**, 221-225.

Tafech, A., Bennett, W.R., Mills, F. and Lee, C.H. (2007) Identification of c-myc coding region determinant RNA sequences and structures cleaved by an RNase1-like endoribonuclease. *Biochim Biophys Acta*, **1769**, 49-60.

Takahashi, H., Maeda, M., Sawa, H., Hasegawa, H., Moriyama, M., Sata, T., Hall, W.W. and Kurata, T. (2006) Dicer and positive charge of proteins decrease the stability of RNA containing the AU-rich element of GM-CSF. *Biochem Biophys Res Commun*, **340**, 807-814.

Tan, Y-T., Lim, S.G. and Hong, W. (2005) Characterization of viral proteins encoded by the SARS-coronavirus genome. *Antiviral Res*, **65**, 69-78.

Tell, G., Damante, G., Caldwell, D. and Kelley, M.R. (2005) The intracellular localization of APE1/Ref-1: more than a passive phenomenon? *Antioxid Redox Signal*, **7**, 367-384.

Tell, G., Quadrifoglio, F., Tiribelli, C. and Kelley, M.R. (2009) The many functions of APE1/Ref-1: not only a DNA repair enzyme. *Antioxid Redox Signal*, **11**, doi:10.1089/ars.2008.2194.

Tello-Montoliu, A., Patel, J.V. and Lip, G.Y. (2006) Angiogenin: a review of the pathophysiology and potential clinical applications. *J Thromb Haemost*, **4**, 1864-1874.

Tessier, C.R., Doyle, G.A., Clark, B.A., Pitot, H.C. and Ross, J. (2004) Mammary tumor induction in transgenic mice expressing an RNA-binding protein. *Cancer Res*, **64**, 209–214.

Tharun, S., and Sirdeshmukh, R. (1995) Specific endonucleolytic cleavages of mouse albumin mRNA and their modulation during liver development. *Nucleic Acids Res*, **23**, 641-646.

Timofeeva, A.V., Skrypina, N.A., Savochkina, L.P., Beabealashvilli, R.S. (2000) Size distribution of the urokinase mRNA decay intermediates in different tissues and cell lines. *Biochim Biophys Acta*, **1517**, 33-45.

Tirasophon, W. Lee, K. Callaghan, B. Welihinda, A. Kaufman, R. J. (2000) The endoribonuclease activity of mammalian IRE1 autoregulates its mRNA and is required for the unfolded protein response. *Genes Dev*, 14, 2725-2736.

To, K.K., Zhan, Z., Litman, T. and Bates, S.E. (2008) Regulation of ABCG2 expression at 3'-untranslated region of its mRNA through modulation of transcript stability and protein translation by a putative microRNA in S1 colon cancer cell line. *Mol Cell Biol* **28**, 5147-5161.

Tokumaru, S., Suzuki, M., Yamada, H., Nagino, M. and Takahashi, T. (2008) let-7 regulates Dicer expression and constitutes a negative feedback loop. *Carcinogenesis*, **29**, 2073-2077.

Tollervey, D. (2006) Molecular biology: RNA lost in translation. *Nature*, **440**, 425-426.

Tourrière, H., Gallouzi, I.E., Chebli, K., Capony, J.P., Mouaikel, J., van der Geer, P. and Tazi, J. (2001) RasGAP-associated endoribonuclease G3Bp: selective RNA degradation and phosphorylation-dependent localization. *Mol Cell Biol*, **21**, 7747-7760.

Tourrière, H., Chebli, K., Zekri, L., Courselaud, B., Blanchard, J.M., Bertrand, E. and Tazi, J. (2003) The RasGAP-associated endoribonuclease G3BP assembles stress granules. *J Cell Biol*, **160**, 823-831.

Tran, H., Maurer, F. and Nagamine, Y. (2003) Stabilization of urokinase and urokinase receptor mRNAs by HuR is linked to its cytoplasmic accumulation induced by activated mitogen-activated protein kinase-activated protein kinase 2. *Mol Cell Biol*, **23**, 7177-7188.

Tsuji, T., Sun, Y., Kishimoto, K., Olson, K.A., Liu, S., Hirukawa, S. and Hu, G.F. (2005) Angiogenin is translocated to the nucleus of HeLa cells and is involved in ribosomal RNA transcription and cell proliferation. *Cancer Res*, **65**, 1352–1360.

Valencia-Sanchez, M.A., Liu, J., Hannon, G.J. and Parker, R. (2006) Control of translation and mRNA degradation by miRNAs and siRNAs. *Genes Dev*, **20**, 515-524.

Van Dijk, E.L., Sussenbach, J.S. and Holythuizen, P.E. (1998) Identification of RNA sequences and structures involved in site-specific cleavage of IGF-II mRNAs. *RNA*, **4**, 1623-1635.

Vascotto,C., Fantini,D., Romanello,M., Casaratto,L., Deganuto,M., Leonardi,A., Radicella,J.P., Kelley,M.R., D'Ambrosio,C.D., Scaloni,A., Quadrifoglio,F. and Tell,G. (2009) APE1/Ref-1 interacts with NPM1 within nucleoli and plays a role in the rRNA quality control process. *Mol Cell Biol*, doi:10.1128/MCB.01337-08.

Vickers, T.A., Lima, W.F., Nichols, J.G. and Crooke, S.T. (2007) Reduced levels of Ago2 expression result in increased siRNA competition in mammalian cells. *Nucleic Acids Res*, **35**, 6598-610.

Vihinen, P., Kallioinen, M., Vuoristo, M.S., Ivaska, J., Syrjänen, K.J., Hahka-Kemppinen, M., Kellokumpu-Lehtinen, P.L. and Pyrhönen, S.O. (2007) Serum angiogenin levels predict treatment response in patients with stage IV melanoma. *Clin Exp Metastasis*, **24**, 567-574.

Volinia, S., Calin, G.A., Liu, C.G., Ambs, S., Cimmino, A., Petrocca, F., Visone, R., Iorio, M., Roldo, C., Ferracin, M., Prueitt, R.L., Yanaihara, N., Lanza, G., Scarpa, A., Vecchione, A., Negrini, M., Harris, C.C. and Croce, C.M. (2006) A microRNA expression signature of human solid tumors defines cancer gene targets. *Proc Natl Acad Sci USA*, **103**, 2257-2261.

Wang, D., Luo, M. and Kelley, M.R. (2004) Human apurinic endonuclease 1 (APE1) expression and prognostic significance in osteosarcoma: enhanced sensitivity of osteosarcoma to DNA damaging agents using silencing RNA APE1 expression inhibition. *Mol Cancer Ther*, **3**, 679-686.

Wang, P., Guliaev, A.B. and Hang, B. (2006) Metal inhibition of human N-methylpurine-DNA glycosylase activity in base excision repair. *Toxicol Lett*, **166**, 237-247.

Wang, T., Yang, M., Chen, J., Watkins, T. and Xiuyun, C. (2005) Inhibition of B16 melanoma growth in vivo by retroviral vector-mediated human ribonuclease inhibitor. *Angiogenesis*, **8**, 73-81.

Wang, W. (2008) An equivalent metal ion in one- and two-metal-ion catalysis. *Nat Struct Mol Biol,* **15,** 1228-1231.

Wang, Y., Duan, H.G., Chen, S.M., Xiao, B.K., Cheng, J. and Tao, Z.Z. (2007) J Effect of RNA interference targeting human telomerase reverse transcriptase on telomerase and its related protein expression in nasopharyngeal carcinoma cells. *Laryngol Otol*, **121**, 476-482.

Wang, Z. and Kiledjian, M. (2000) Identification of an erythroid-enriched endonuclease activity involved in specific mRNA cleavage. *EMBO J,* **19**, 295-305.

Wilson, D.M.3rd. (2003) Properties of and substrate determinants for the exonuclease activity of human apurinic endonuclease APE1. *J Mol Biol,* **330,** 1027-1037.

Wilson, D.M.3rd. (2005) APE1 abasic endonuclease activity is regulated by magnesium and potassium concentrations and is robust on alternative DNA structures. *J Mol Biol*, **345**, 1003-1014.

Wilson, D.M.3rd. and Barsky, D. (2001) The major human abasic endonuclease: formation, consequences and repair of abasic lesions in DNA. *Mutat Res*, **485:** 283-307.

Wilson, D.M.3rd., Engelward, B.P. and Samson, L. (1998) Prokaryotic base excision repair. *DNA Damage and Repair*, 29-64, Humana Press, Totowa, NJ.

Wilson, D.M.3rd., Takeshita, M., Grollman, A.P. and Demple, B. (1995) Incision activity of human apurinic endonuclease (Ape) at abasic site analogs in DNA. *J Biol Chem*, **270**, 16002–16007.

Wilusz, C.J. and Wilusz, J. (2004) Bringing the role of mRNA decay in the control of gene expression into focus. *Trends Genet*, **20**, 491-497.

Wisdom, R. and Lee W. (1991) The protein-coding region of c-myc mRNA contains a sequence that specifies rapid mRNA turnover and induction by protein synthesis inhibitors. *Genes Dev*, **5**, 232-243.

Yan, C. and Boyd, D.D. (2007) Regulation of matrix metalloproteinase gene expression. *J Cell Physiol*, **211**, 19-26.

Yan, L.X., Huang, X.F., Shao, Q., Huang, M.Y., Deng, L., Wu, Q.L., Zeng, Y.X. and Shao, J.Y. (2008) MicroRNA miR-21 overexpression in human breast cancer is associated with advanced clinical stage, lymph node metastasis and patient poor prognosis. *RNA*, **14**, 2348-2360.

Yang, F., Peng, Y. and Schoenberg, D.R. (2004) Endonuclease-mediated mRNA decay requires tyrosine phosphorylation of polysomal ribonuclease 1 (PMR1) for the targeting and degradation of polyribosome-bound substrate mRNA. *J Biol Chem*, **279**, 48993-49002.

Yang, Z.Z., Chen, X.H. and Wang, D. (2007) Experimental study enhancing the chemosensitivity of multiple myeloma to melphalan by using a tissue-specific APE1-silencing RNA expression vector. *Clin Lymphoma Myeloma*, **7**, 296-304.

Yeilding, N.M. and Lee, W.M.F. (1997) Coding elements in exons 2 and 3 target c-*myc* mRNA downregulation during myogenic differentiation. *Mol Cell Biol* **17**, 2698-2707.

Yoshida, A., Urasaki, Y., Waltham, M., Bergman, A.C., Pourquier, P., Rothwell, D.G., Inuzuka, M., Weinstein, J.N., Ueda, T., Appella, E., Hickson, I.D. and Pommier, Y. (2003) Human apurinic/apyrimidinic endonuclease (Apel) and its N-terminal truncated form (AN34) are involved in DNA fragmentation during apoptosis. *J Biol Chem*, **278**, 37768-37776.

Yoshioka, N., Wang, L., Kishimoto, K., Tsuji, T. and Hu, G.F. (2006) A therapeutic target for prostate cancer based on angiogenin-stimulated angiogenesis and cancer cell proliferation. *Proc Natl Acad Sci USA*, **103**, 14519-14524.

Zekri, L., Chebli, K., Tourrière, J., Nielsen, F.C., Hansen, T.V., Rami, A. and Tazi, A. (2005) Control of fetal growth and neonatal survival by the RasGAP-associated endoribonuclease G3BP. *Mol Cell Biol*, **25**, 8703-8716.

Zeng, Y., Sankala, H., Zhang, X. and Graves, P.R. (2008) Phosphorylation of Argonaute 2 at serine-387 facilitates its localization to processing bodies. *Biochem J*, **413**, 429-436.

Zhang, B., Pan, X., Cobb, G.P. and Anderson, T.A. (2007) microRNAs as oncogenes and tumor suppressors. *Dev Biol*, **302**, 1-12.

Zhang, H.Z., Liu, J.G., Wei, Y.P., Wu, C., Cao, Y.K. and Wang, M. (2007) Expression of G3BP and RhoC in esophageal squamous carcinoma and their effect on prognosis. *World J Gastroenterol*, **13**, 4126-4130.

Zhang, K., Dion, N., Fuchs, B., Damron, T., Gitelis, S., Irwin, R., O'Connor, M., Schwartz, H., Scully, S.P., Rock, M.G., Bolander, M.E. and Sarkar G. (2002) The human homolog of yeast SEP1 is a novel candidate tumor suppressor gene in osteogenic sarcoma. *Gene*, **298**, 121-127.

Zheng, D., Ezzeddine, N., Chen, C.Y., Zhu, W., He, X. and Shyu, A.B. (2008) Deadenylation is prerequisite for P-body formation and mRNA decay in mammalian cells. *J Cell Biol*, **182**, 89-101.

Zhou, A., Molinaro, R. J., Malathi, K. and Silverman, R.H. (2005) Mapping of the human RNASEL promoter and expression in cancer and normal cells. *J Interferon Cytokine Res*, **25**, 595-603.

Zuker, M. (2003) Mfold web server for nucleic acid folding and hybridization prediction. *Nucleic Acids Res*, **15**, 3406-3415.